INVESTIGATING THE EFFECTS OF OPERATIONAL PARAMETERS ON PHOTOFERMENTATION IN BATCH AND SEMI-BATCH REACTORS AND THE APPLICATIONS OF PHOTOFERMENTATION IN MULTI-STAGE ENERGY SYSTEMS

A THESIS SUBMITTED TO

THE GRADUATE SCHOOL OF NATURAL AND APPLIED SCIENCES

OF

MIDDLE EAST TECHNICAL UNIVERSITY

BY

MELİH CAN AKMAN

IN PARTIAL FULFILLMENT OF THE REQUIREMENTS

FOR

THE DEGREE OF MASTER OF SCIENCE

IN

ENVIRONMENTAL ENGINEERING

MAY 2018

Approval of the thesis:

INVESTIGATING THE EFFECTS OF OPERATIONAL PARAMETERS ON PHOTOFERMENTATION IN BATCH AND SEMI-BATCH REACTORS AND THE APPLICATIONS OF PHOTOFERMENTATION IN MULTI-STAGE ENERGY SYSTEMS

Submitted by **MELİH CAN AKMAN** in partial fulfillment of the requirements for the degree of **Master of Science in Environmental Engineering Department, Middle East Technical University** by,

Prof. Dr. Halil Kalıpçılar
Dean, Graduate School of **Natural and Applied Sciences** _____

Prof. Dr. Kahraman Ünlü
Head of Department, **Environmental Engineering,** _____

Assoc. Prof. Dr. Tuba Hande Bayramoğlu
Supervisor, **Environmental Engineering Dept., METU** _____

Prof. Dr. Ufuk Gündüz
Co-Supervisor, **Department of Biological Sciences, METU** _____

Examining Committee Members:

Prof. Dr. İpek İmamoğlu
Environmental Engineering Dept., METU _____

Assoc. Prof. Dr. Tuba Hande Bayramoğlu
Supervisor, Environmental Engineering Dept., METU _____

Prof. Dr. Ufuk Gündüz
Co-Supervisor, Biology Dept., METU _____

Asst. Prof. Dr. Harun Koku
Chemical Engineering Dept., METU _____

Assoc. Prof. Dr. Selim L. Sanin
Environmental Engineering Dept., Hacettepe University _____

Date: 28.05.2018

I hereby declare that all information in this document has been obtained and presented in accordance with academic rules and ethical conduct. I also declare that, as required by these rules and conduct, I have fully cited and referenced all material and results that are not original to this work.

Name, Last Name: MELİH CAN AKMAN

Signature:

ABSTRACT

INVESTIGATING THE EFFECTS OF OPERATIONAL PARAMETERS ON PHOTOFERMENTATION IN BATCH AND SEMI-BATCH REACTORS AND THE APPLICATIONS OF PHOTOFERMENTATION IN MULTI-STAGE ENERGY SYSTEMS

Akman, Melih Can

M.S., Department of Environmental Engineering

Supervisor: Assoc. Prof. Dr. Tuba Hande Bayramoğlu

Co-Supervisor: Prof. Dr. Ufuk Gündüz

May 2018, 142 Pages

The aim of this master thesis study was to investigate the effects of operational parameters on photofermentation in batch and semi-batch reactors, and to research the application of photofermentation in multi-stage energy systems, the latter as an attempt to increase the total energy obtained from the whole system.

Four sets were conducted, namely, Set-1, Set-2, Set-3 and Set-4. Three operational parameters, namely, initial substrate (S) concentration, initial volatile suspended solids (VSS) concentration (X_o, biomass) and the light intensity leading to the maximization of hydrogen production in a single stage were optimized by Response Surface Methodology (RSM) in Set-1. Results revealed that the highest (optimized) hydrogen production rate of 1.04 mmol H_2/L.h was achieved at the initial optimum values of 35.35 mM acetic acid concentration, 0.27 g VSS/L (*Rhodobacter*

capsulatus) concentration and 3955 lux (263.6 W/m^2) light intensity. The substrate to biomass (S/X_o) ratio providing the highest hydrogen production rate was 8.3 g COD_{HAc}/g VSS (7.7 g acetate/g VSS). Experimentally highest hydrogen yield obtained was 0.11 g H_2/g acetate (3.3 mol H_2/mol acetate). Set-2, where photofermentation was studied as the second-stage of a two-stage dark fermentation and photofermentation system, revealed that the hydrogen production rate and yield obtained were 0.48±0.08 mmol H_2/L.h and 1.61±0.24 mol H_2/mol acetate (0.054 g H_2/g acetate), respectively. Set-3, where photofermentation was investigated as the third-stage of a three-stage system composed of dark fermentation, methanogenesis and photofermentation processes, revealed that the highest hydrogen production rate and yield were 0.10±0.005 mmol H_2/L.h and 0.032±0.001 g H_2/g acetate (0.95±0.03 mol H_2/mol acetate), respectively. Set-4, where the optimum hydraulic retention time (HRT) leading to the highest photofermentative hydrogen production rate in semi-batch reactors in a three-stage system was investigated, revealed that the highest hydrogen production rate (0.041 mmol H_2/L.h) was observed at 4 day-HRT.

The results of this thesis study might be beneficial in photobioreactor designs and operation with greater photofermentative hydrogen production rates. The hydrogen production rates and yields obtained in the optimization study were considerably high. Both the third-stage photofermentation studied in this thesis and three-stage systems, which are not studied so far, are believed to be promising in increasing the energy yield per unit substrate and will provide a preliminary knowledge for future studies.

Keywords: Biohydrogen, Photofermentation, Hydrogen Production Rate, Hydraulic Retention Time, *Rhodobacter capsulatus*, Substrate to Biomass (S/X_o) Ratio

ÖZ

KESİKLİ VE YARI KESİKLİ REAKTÖRLERDE İŞLETME PARAMETRELERİNİN FOTOFERMANTASYON ÜZERİNDEKİ ETKİLERİNİN VE ÇOK AŞAMALI ENERJİ SİSTEMLERİNDE FOTOFERMANTASYON UYGULAMALARININ ARAŞTIRILMASI

Akman, Melih Can

Yüksek Lisans, Çevre Mühendisliği Bölümü

Tez Yöneticisi: Doç Dr. Tuba Hande Bayramoğlu

Ortak Tez Yöneticisi: Prof. Dr. Ufuk Gündüz

Mayıs 2018, 142 Sayfa

Bu yüksek lisans tezinin amacı, kesikli ve yarı kesikli reaktörlerde işletme parametrelerinin fotofermantasyon üzerindeki etkilerinin araştılması ve tüm sistemden elde edilen toplam enerjiyi artırma girişimi olarak çok aşamalı enerji sistemlerinde fotofermantasyon uygulamasının incelenmesidir.

Set-1, Set-2, Set-3 ve Set-4 olmak üzere dört set kurulmuştur. Set-1'de, başlangıç substrat derişimi (S), başlangıç uçucu askıda katı madde (UAKM) derişimi ve ışık şiddeti olmak üzere hidrojen üretimini tek aşamalı sistemde maksimum seviyeye getirecek üç işletme parametresi Tepki Yüzey Metodu (TYM) ile optimize edilmiştir. Sonuçlar, 1,04 mmol H_2 / L.saat değerindeki en yüksek hidrojen üretim hızının, 35,35 mM HAc (asetik asit) başlangıç substrat derişimi, 0,27 g UAKM/L başlangıç biyokütle (*Rhodobacter capsulatus*) derişimi ve 3955 lux (263,6 W) ışık

şiddetindeki optimum değerlerde elde edildiğini ortaya koymuştur. En yüksek hidrojen üretim hızını sağlayacak S/X_o oranı 8,3 g $KOİ_{HAc}$/g UAKM (7,7 g asetat/g UAKM) olmaktadır. Deneysel olarak elde edilen en yüksek hidrojen verimi 0.11 g H_2/g asetat (3.3 mol H_2/mol asetat)'tır. İki aşamalı karanlık fermantasyon ve fotofermantasyon sisteminin ikinci aşaması olarak fotofermantasyonun incelendiği Set-2, hidrojen üretim hızı ve veriminin sırasıyla 0,48±08 mmol H_2/L ve 1,61 ± 0,24 mol H_2/mol asetat (0,054 g H_2/g asetat) olarak elde edildiğini göstermiştir. Sonuçlar, fotofermentasyon reaktörlerinin, karanlık fermantatif ardışık kesikli reaktörün (AKR) işletme modundan önemli ölçüde etkilendiğini gösterdi. Karanlık fermantasyon, metanojenez ve fotofermentasyon işlemlerinden oluşan üç aşamalı bir sistemin üçüncü aşaması olarak fotofermentasyonu araştıran Set-3, en yüksek hidrojen üretim hızının ve hidrojen veriminin, sırasıyla 0,10±0,005 mmol H_2/L.saat ve 0,032±0,001 g H_2/g asetat (0.95±0.03 mol H_2/mol asetat)olarak gözlendiğini gösterdi. Üç aşamalı sistemde yarı-kesikli reaktörlerde en yüksek fotofermantatif hidrojen üretim hızına yol açan optimum hidrolik bekletme süresini (HBS) araştırıldığı Set-4, en yüksek hidrojen üretim hızının (0.041 mmol H_2/L.h) HBS değerinin 4 günde gözlendiğini ortaya koymuştur.

Bu tez çalışmasının sonuçlarının, daha yüksek hızlarda fotofermantatif hidrojen üretimi için fotobiyoreaktör tasarımları ve çalışma koşulları açısından yararlı olacağına inanılmaktadır. Optimizasyon çalışmasında elde edilen hidrojen üretim hızları ve verimleri oldukça yüksektir. Bu tezde çalışılan üçüncü aşama fotofermantasyon ve üç aşamalı sistemlerin her ikisi de, literatürde bugüne kadar incelenmemiş olup, birim substrat başına enerji verimini artırmada umut verici olduğuna inanılmaktadır ve gelecekteki çalışmalar için ön bilgi sağlayacaktır.

Anahtar Kelimeler: Biyohidrojen, Fotofermantasyon, Hidrojen Üretim Hızı, Hidrolik Bekletme Süresi, *Rhodobacter capsulatus*, Substrat Biyokütle (S/X_o) Oranı

To my family and my endless love

ACKNOWLEDGEMENTS

I would like to express my sincere gratitude to my supervisor Assoc. Prof. Dr. Tuba Hande Ergüder Bayramoğlu for her guidance, patience, advice, encouragements and support throughout my study. The numerous discussions and criticisms gave me good insight on the research study. I also thank to my co-supervisor Prof. Dr. Ufuk Gündüz for her guidance, suggestions and recommendations. The contributions of Prof. Dr. İnci Eroğlu is greatly acknowledged.

I would like to thank the members of judging committee, Prof. Dr. İpek İmamoğlu, Assoc. Prof. Dr. Harun Koku and Assoc. Prof. Dr. Selim Sanin for their contributions.

I would like to express my special thanks to my dear project members, Engin Koç and Ekin Güneş Tuncay. I thank you for always being there for me, whether it was work or personnel and I am so glad that through our project partnership came along the precious friends that you are.

I also gratefully acknowledge the financial support by the Scientific and Technological Research Council of Turkey (TÜBİTAK) to the project (112M252) which this thesis has emerged from.

I am grateful to my lab mates and friends, Muazzez Gürgan, Dominic Deo Androga, Emrehan Berkay Çelebi, Emine Kayhan, Mehmet Gazaloğlu for their friendship, collaboration and assistance. I would like to thank to my friends who are as close as my family, Emin Calbay, Yiğit Özşen, Şükrü Burak Çakırlar, and everyone else that I could not mention here.

Most of all, I would like to thank to my family, my father, my mother and my brother for their support and love. I especially thank my parents for their love, engouragement and trust. Finally, I would like to thank my dearest Eser Büyükaşık for his love, engouragement and trust.

TABLE OF CONTENTS

LIST OF FIGURES

LIST OF TABLES

ABBREVIATIONS

ANOVA : Analysis of Variance

COD : Chemical Oxygen Demand

C/N : Carbon to Nitrogen

GC : Gas Chromatograph

HAc : Acetic Acid

HBu : Butyric Acid

HPLC : High Performance Liquid Chromatography

HPR : Hydrogen Production Rate

HPr : Propionic Acid

HRT : Hydraulic Retention Time

I : Light Intensity

OD : Optical Density

S : Substrate

PHB : Polyhydroxybutyrate

PNS : Purple Non-Sulphur

RSM : Response Surface Methodology

SBR : Sequencing Batch Reactor

SRT : Solid Retention Time

S/X_o : Substrate to Biomass

TAN : Total Ammonia Nitrogen (NH_4^+-N+NH_3-N)

VFA : Volatile Fatty Acids

VSS : Volatile Suspended Solids

X_0 : Volatile Suspended Solids, Biomass

CHAPTER 1

INTRODUCTION

Energy is a major requirement and a key consideration for the development of the world. In the past century, global warming and energy crisis, which are the two of the most important issues that threaten the world peace, have clearly shown their faces and no tangible solution come up with result to curb their contagion on the planet. In this respect, various approaches are under research and being applied (Mazloomi and Gomes, 2012).

The terms of alternative and renewable energies come to prominence for sustainable development because of the depletion of fossil fuels and increase in energy demand. As well as energy crisis and global warming, environmental policies to reduce CO_2 emissions stimulate finding new clean energy resources (Abd-Alla et al., 2011). Energy sources for long term sustainable solutions such as winds, waves, tides and solar radiation are renewable and environmental friendly options. Waste and biomass are also viewed as sustainable energy sources. By way of waste-to-energy technologies, it can be possible to convert waste materials to useful energy forms like hydrogen (biohydrogen), biogas, bioalcohol, etc. (Kothari et al.,2010).

The idea of using hydrogen as an energy carrier has gained strength significantly in the last half century. Especially, hydrogen fuel recently gains high importance because it is an alternative source to fossil fuels. Hydrogen is a potential non-carbon energy source that does not produce any harmful oxides of carbon, sulphur, nitrogen, etc. Although it is not ready-to-use and available, remarkable features and properties of hydrogen make it an up-and-coming energy carrier and fuel (Mazloomi and

Gomes, 2012). Possible scenarios for renewable and sustainable biohydrogen production are under investigation (Abo-Hashesh et al., 2011). Because of carbon free and environmental friendly quality, hydrogen is considered as an attractive clean and green fuel and energy carrier, and it is expected to play an essential role in future energy systems (Dutta, 2014).

Hydrogen is the most elementary and abundant substance of the universe. It is an odorless, colourless and tasteless element. Contrary to fossil fuels such as natural gas derivatives and petroleum based fuels, hydrogen has a light and small molecular structure. Hydrogen has an upper heating value of 142 MJ/kg and a lower heating value of 122 MJ/kg that are almost three times larger than those of liquid hydrocarbon based fuels on the average. Hydrogen is generally bonded with other materials such as carbon and oxygen, so, it is not available as a separated material naturally (Mazloomi and Gomes, 2012).

Different technologies and methods are being used for hydrogen production. Hydrogen is mainly produced from fossil fuels by way of gasification of coal and steam reforming of natural gas. These thermochemical processes are the most common hydrogen production methods at present. Around 49% of the hydrogen production is based on natural gas, 29% is based on liquid hydrocarbons such as naphtha and heavy oil, 18% on coal. Just 4% of hydrogen is produced from other alternative resources such as water, biomass and waste materials. The electrolysis of water is also an option to produce hydrogen (Bicakova and Straka, 2012). Among the different technologies employed, biological hydrogen production process, which is the production of hydrogen via microorganisms, offers an opportunity to utilize renewable resources. Moreover, as compared to electrochemical and thermochemical prosesses, biological hydrogen production processes provide more environmental friendly and less energy intensive solutions (Uyar et al., 2009).

Biohydrogen can be obtained by light-dependent processes, namely, biophotolysis and photofermentation, and light-independent process, namely, dark fermentation

(Öztürk and Gökçe, 2012). These processes are mainly controlled by bacteria such as photosynthetic and fermentative species. In biophotolysis of water, green algae and blue-green algae (cyanobacteria) split water into hydrogen and oxygen using carbon dioxide and sunlight as carbon source and energy, respectively. The other light-dependent process, namely, photofermentation occurs under anaerobic and nitrogen-limited conditions. This process is based on photodecomposition of organic compounds by photosynthetic bacteria. Photosynthetic bacteria such as purple non-sulfur (PNS) bacteria utilize organic acids using light energy to produce hydrogen and water. This process is catalyzed by the nitrogenase enzyme. In the dark fermentation process, organic compounds are degraded by anaerobic bacteria to produce hydrogen and organic substrates under anaerobic conditions (Das and Veziroglu, 2008).

Photofermentation is a favorable option amongst the biological hydrogen production processes to produce hydrogen from renewable resources such as sunlight, water and biomass. It has high substrate conversion efficiency. Photofermentation by PNS bacteria offers some advantages in that they can use a wide range of organic substrates like sugars, fatty acids, organic acids, and waste materials. They can survive under a wide range of physiological conditions with a perfect metabolic diversity and they are able to use a wide variety of wavelengths of the light spectrum (Afsar et al., 2011).

Photofermentation and growth of photosynthetic bacteria are affected by some environmental and nutritional factors such as carbon and nitrogen sources, the carbon to nitrogen ratio, temperature, pH levels and light intensity. Temperature and light intensity are two of these factors which strongly affect hydrogen production by PNS bacteria (Wu et al., 2012). As it is seen, not only one parameter affects the photofermentation. When more than one parameter is of concern, there might be some combined effects of these operational parameters, which should be investigated in detail.

Photofermentation seems to be a favorable option among the biological hydrogen production processes, yet, there are also some limitations. Main limitations in photofermentation process can be itemized as follows (Boodhun, 2017; Ljunggren et al., 2011):

- High nitrogen ingredient can reduce hydrogen production.
- The rate of biohydrogen production is directly related with bacterial growth, thus selection of the bacterial strain and cultivation is highly important.
- Carbon to Nitrogen (C/N) ratio should be adjusted.
- Activity of hydrogenase should be minimal and activity of nitrogenase should be maximal.
- Color of the wastewater affects the light penetration. Thus, dilution or some pre-treatment methods should be applied to the wastewater.
- Because of the polyhydroxybutyrate (PHB) synthesis, hydrogen production metabolism can be affected negatively and hydrogen production yield can decrease.
- Concerns regarding low hydrogen production rate and, in turn, practical applicability of the process have been raised in photofermentation research field.

To increase the energy yields and production rates, two-stage energy systems are of research interest. Sequential dark fermentation and photofermentation or combined dark fermentation and photofermentation processes are two-stage systems in order to increase hydrogen production yields. In these methods, conversion of simple sugars or carbohydrates to organic acids occurs in dark fermentation stage and the products of dark fermentation are used in the subsequent photofermentation stage as substrate. The two-stage dark fermentation and photofermentation is the most encouraging strategy for biological hydrogen production (Uyar et al., 2009). Higher hydrogen yields obtained from these two-stage systems might be promising/encouraging for other potential multi-stage systems. Multi-stage systems,

which might integrate other energy-producing reactor types, remain to be researched.

Considering the above mentioned points, this thesis study aims to investigate the effects of operational parameters on photofermentation in batch and semi-batch reactors, and to research the application of photofermentation in multi-stage energy systems, the latter as an attempt to increase the total energy obtained from the whole system. This thesis study is part of the studies performed under a TUBITAK (The Scientific and Technological Research Council of Turkey) Project (112M252) with the aim to improve total energy from unit organic matter via integrated multi-stage systems. The specific objectives of this thesis study are given as follows;

- To investigate the effects of three parameters, namely, initial substrate concentration, initial biomass concentration and light intensity on photofermentation and their combined effect on hydrogen production by Response Surface Methodology.
    - To optimize these parameters in order to the maximize the hydrogen production rate in a single-stage
    - To determine optimum substrate to biomass (S/X_o) ratio
- To investigate photofermentation in a two-stage dark fermentation and photofermentation system
- To investigate the photofermentation in a three-stage system composed of dark fermentation, methanogenesis and photofermentation reactors.
- To compare photofermentation efficiency in two-stage and three-stage systems.
- To investigate the optimum hydraulic retention time (HRT) parameter of semi-batch photofermentation reactor leading to the highest hydrogen production rate.

CHAPTER 2

LITERATURE REVIEW

2.1. Hydrogen as an Energy Carrier

Energy demand in direct proportion to industrialization and rapid population growth in developing countries shows a tendency of continuous growth. In this respect, energy production and use are considered as the indicators of the economic and social development or development potential of a country. Within this scope, it is an important requirement that industrial development, the rise in living standards, and the energy supply needed by the growing population are adequately and reliably ensured.

The growing energy demand of continuous increase in the world population and the developing industry is met today with a great deal of fossil sources. However, due to the limited formation of fossil fuel reserves, the increase in energy prices, the technical, administrative and financial aspects of the environmental and social effects of energy production based on fossil resources, and the operation of related plants depend on natural and human factors has led today's technologies to focus on the search and use of renewable and low carbon emission sources in energy production (World Energy Council, 2013).

Because the growing energy demand causes more pollution, the emissions of greenhouse gases and the global warming become important issues in science and global policy. Therefore, the necessity for replacing fossil fuels with renewable energy sources is accelerating (Veras et al., 2017). The winds, tides, waves and solar radiation are among the energy sources which generaterenewable, environmental friendly and, therefore, sustainable solutions over the long term. Waste and biomass

are also viewed as sustainable energy sources. By way of waste-to-energy technologies, it can be possible to convert waste materials to useful energy forms like hydrogen (biohydrogen), biogas, bioalcohol, etc. (Kothari et al., 2010).

Because it is replaceable with fossil fuels and it is an important and promising energy carrier which can be play a significant role in the reduction of greenhouse gas emissions, hydrogen fuel gains more importance in recent times. Hydrogen is a potential non-carbon energy source that does not contribute to harmful oxides of carbon, sulfur, nitrogen, etc. like fossil fuels. Thus, hydrogen is considered as an alternative clean and green fuel source. Because of carbon free and environmental friendly quality and high energy content, hydrogen is thought as the most attractive candidate future fuel and energy carrier, and it is expected to play an essential role in future energy systems. (Dutta, 2014). Hydrogen is a light, colorless and odorless element with different characteristics from other gaseous fuels. Its main properties and energy content comparisons among hydrogen and some common conventional and alternative fuels are presented in Table 2.1, Table 2.2 and Table 2.3.

Table 2.1 Main properties of hydrogen (BACAS, 2006)

Gas density	0.0899 kg/Nm^3
Liquid density	70.99 kg/m^3
Boiling point	20.4 K
Melting point	14 K
Lower Heating Value (LHV)	121 MJ/kg
Burning range	4–74.5 % volume
Detonation range	18.3–59 % volume
Stoechiometric ratio (with air)	34.5

Table 2.2 Weight and volume based energy density among hydrogen and some common fuels (BACAS, 2006)

Energy carrier	**Form of Storage**	**Energy density by weight (kWh/kg)**	**Energy density by volume (kWh/L)**
Hydrogen	gas (30 MPa)	33.3	0.75
	liquid (-253°C)	33.3	2.36
Natural gas	gas (30 MPa)	13.9	3.38
	liquid (-162°C)	13.9	5.8
LPG (Propane)	liquid	12.9	7.5
Methanol	liquid	5.6	4.42
Gasoline	liquid	12.7	8.76
Diesel	liquid	11.6	9.7
Electricity	Pb battery (chemical)	0.03	0.09

Table 2.3 Comparison among hydrogen, methane and propane (BACAS, 2006)

Parameter	**Unit**	**Hydrogen (H_2)**	**Methane (CH_4)**	**Propane (C_3H_8)**
Lower heating value	MJ/kg	121	50	46.4
	kWh/kg	33.33	13.90	12.88
	MJ/Nm^3	10.78	35.88	93.21
Upper heating value	kJ/kg	141 890	55 530	50 410
	kWh/kg	39.41	15.42	14.00
	MJ/Nm^3	12.74	39.82	101.24
Lower Wobbe index	MJ/Nm^3	40.89	48.1	74.74
Upper Wobbe index	MJ/Nm^3	48.34	53.45	81.18
Density	kg/m^3	0.08988	0.7175	2.011
Gas constant	J/kg K	4124	518.8	188.5
Ignition temperature in air	°C	530	645	510

The most abundant resource of hydrogen is water which is made of 11.2% hydrogen by weight. The density of gaseous hydrogen is 0.09 kg/m^3 which is 14.4 times lighter than air and 8 times lighter than methane. Boling point of hydrogen is -253°C. Energy to weight ratio of hydrogen is the highest among all fuels. 1 kg of hydrogen is equal to 2.1 kg of natural gas or 2.8 kg of gasoline on energy basis. Hydrogen contains 122 MJ/kg of energy that is about 2.75 times greater than the energy content of methane. The explosive concentrations of hydrogen in air lie between 18.3% to 59%, whereas explosive concentrations in air for methane are from 6.3% to 14%. The explosive range for hydrogen is explicitly much greater and methane is explosive at a much lower concentration. The diffusion coefficient of hydrogen is 0.61 cm^3/s which is 4 times greater than methane so hydrogen mixes with air faster than methane or petrol (BACAS, 2006).

The main reasons for encouraging hydrogen as a future energy carrier are its superior properties for environmental protection. Under proper conditions, burning hydrogen in engines or turbines causes very low or negligible emissions. CO and trace hydrocarbon emissions can only come from the combustion of engine grease in the combustion chamber. Nitrous oxide emissions can be minimized with appropriate process control because they are related exponentially with combustion temperature. Hydrogen is more flexible than other fuels, so combustion can be achieved at lower temperatures. Thus this leads to a significant reduction in NO_x emissions compared to natural gas and petroleum products. Generally particulate matter and sulphur emissions are completely prevented (BACAS, 2006).

Some advantages of hydrogen against fossil fuels can be listed as follows:

- Because of being a gas, hydrogen can be stored easier than electricity.
- Including renewable resources, hydrogen could be derived from primary energy sources.

- Because decentralized production is possible, hydrogen is shown as capable of supply services where the electricity is unavailable, especially as an energy storage in remote fields and a fuel for vehicles.

- Hydrogen is the most versatile fuel, because hydrogen could be converted to practical energy forms such as mechanical, thermal and electrical by way of five different processes for end users. However, flame combustion is the only process that fossil fuels could be converted.

- When hydrogen is converted to practical energy forms such as thermal, electrical and mechanical at the user end, it has the highest utilization efficiency. Hydrogen is called as the most energy-conserving fuel because it could save primary energy sources and hydrogen is nearly 39% more efficient than fossil fuels.

- Hydrogen has very good safety records when toxicity and fire hazards are considered (BACAS, 2006; Dinçer and Zamfirescu, 2016).

For sustainable hydrogen production pathways, it is needed to take inventory natural sources of hydrogen, hydrogen production methods which are applicable, and the present resources of energy which could be used to extract hydrogen from natural sources. These elements and factors are summarized in Figure 2.1. Water, biomass, fossil hydrocarbons, H_2S, biological and anthropogenic wastes as indicated in Figure 2.1a are the hydrogen-containing natural sources. Farm wastes such as manure, municipal wastewater, crops residues, garbage residues, organic wastes, cellulosic materials, recycled plastics are some biological and anthropogenic wastes where hydrogen could be extracted.

In order to extract hydrogen from any source in a nonpolluting and clean manner, sustainable energy is a requirement. The main sustainable energy sources such as solar, thermal, biomass, geothermal, hydro, tidal, wind, and nuclear are listed in Figure 2.1b. With minor environmental impacts or no any impacts, high temperature heat, nuclear radiation or electricity could be generated from any of these sources

by using carefully. These energies are used for hydrogen production by way of one of the methods listed in Figure 2.1c. These hydrogen production methods can be categorized in six main classes which are photochemical, thermochemical, electrochemical, biochemical, radiochemical and hybrid methods. The hybrid methods are integrated systems which are any kind of combination of first five methods.

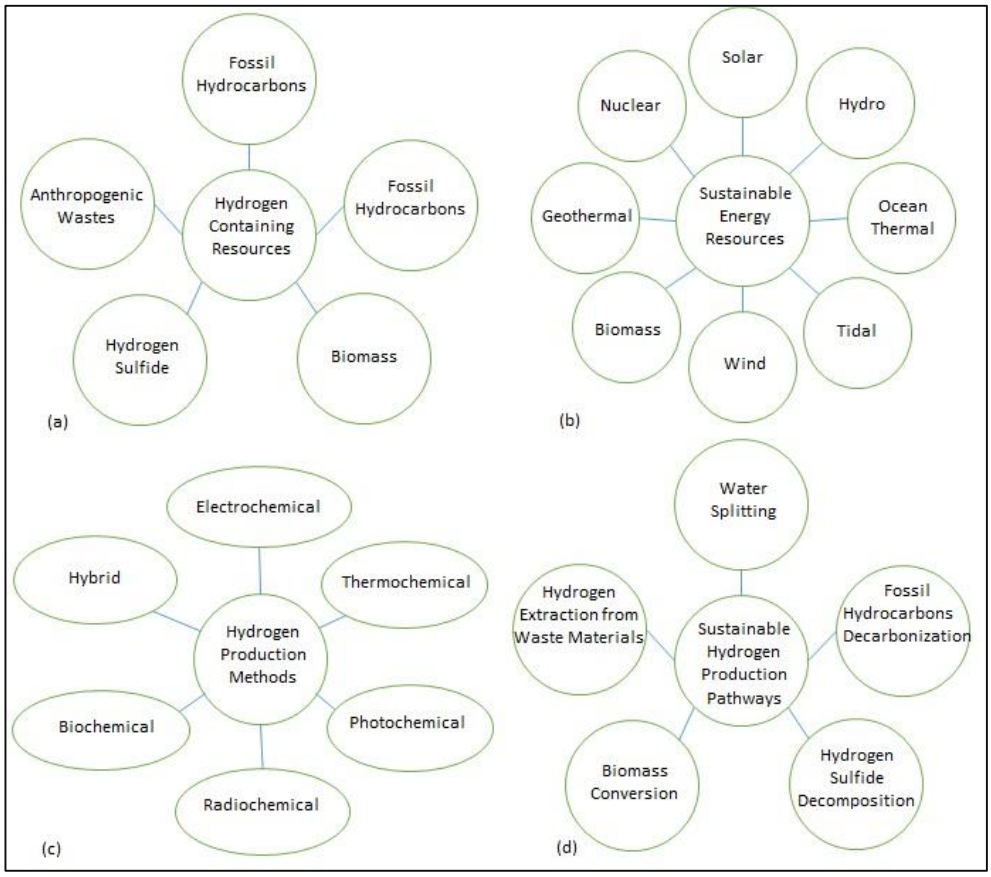

Figure 2.1 (a) Natural hydrogen containing resources, (b) sustainable energy sources, (c) hydrogen production methods, (d) sustainable hydrogen production pathways (Dinçer and Zamfirescu, 2016)

It can be identified that there are five possible processes for hydrogen generation in a sustainable manner. These processes, which are water splitting, H_2S decomposition, hydrocarbons decarbonization, extraction from waste materials and biomass conversion, are indicated in Figure 2.1d. Hydrogen can be extracted from a natural resource corresponded to each process (Dinçer and Zamfirescu, 2016). Energy conversion pathways for hydrogen production methods are shown in Figure 2.2 (Dinçer and Zamfirescu, 2016;). The four forms of energy, namely, biochemical, electrical, thermal and photonic (or radiation) are extracted from basic energy resources.

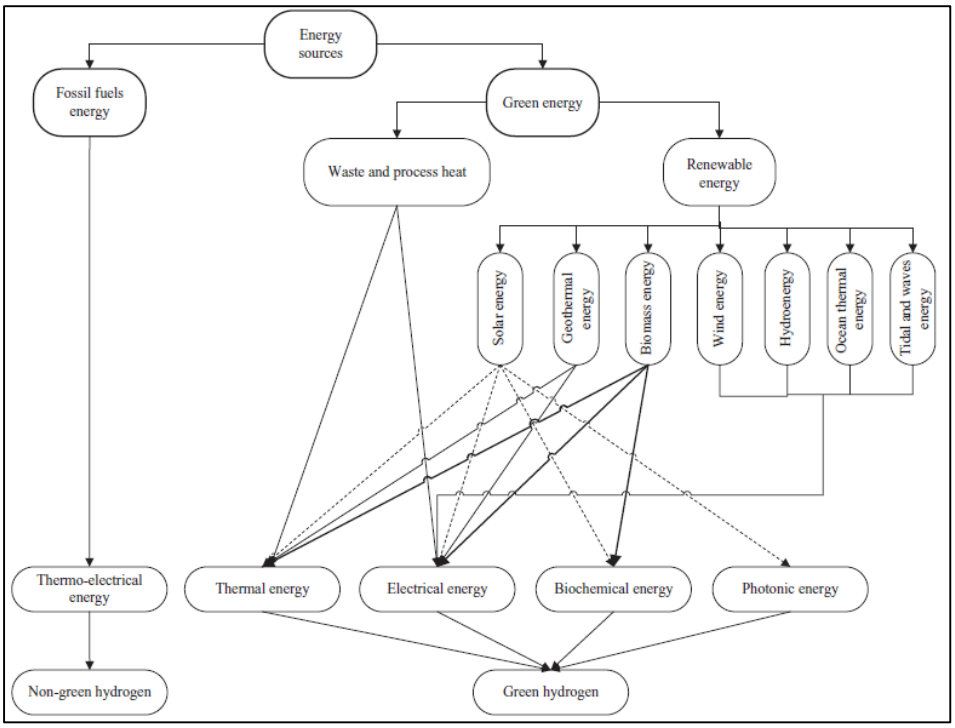

Figure 2.2 Energy conversion pathways for hydrogen production (Dinçer and Zamfirescu, 2016)

2.2. Hydrogen Production Methods

Various hydrogen production methods (Figure 2.3) are available and these processes can be divided into two major categories according to the raw materials used (Nikolaidis and Poullikkas, 2017). The first category accommodates the methods which produce hydrogen from fossil fuels and includes the methods of pyrolysis and hydrocarbon reforming. Steam reforming, autothermal reforming and partial oxidation are chemical techniques in hydrocarbon reforming process. The second category processes renewable sources either from water or biomass. Biological and thermochemical processes are two general sub-categories of biomass utilization as a feedstock. Direct biophotolysis, indirect biophotolysis, dark fermentation and photofermentation are major biological processes. Thermochemical processes are mainly pyrolysis, gasification, liquefaction and combustion. Water splitting processes which can produce hydrogen through electrolysis, thermolysis and photoelectrolysis methods are the second class of renewable technologies (Nikolaidis and Poullikkas, 2017).

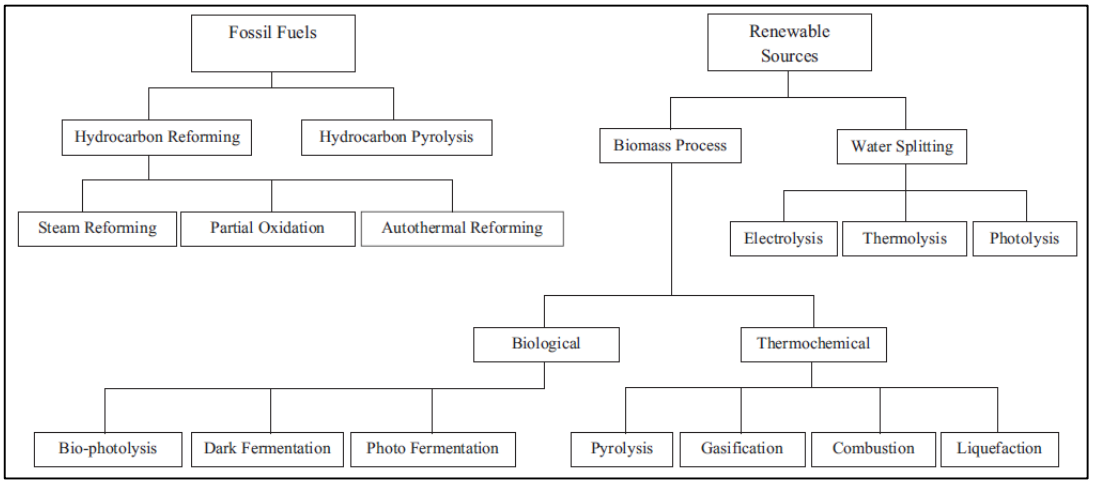

Figure 2.3 Hydrogen production methods (Nikolaidis and Poullikkas, 2017)

2.2.1. Hydrogen Production from Fossil Fuels

There are many technologies and methods for hydrogen production from fossil fuels, the main of which are hydrocarbon reforming and pyrolysis. Almost the entire hydrogen demand is met by these methods which are commonly used and the most developed technologies. Currently, hydrogen is produced 48% from natural gas, 30% from oil and naphtha and 18% from coal. So, 96% of the hydrogen production comes from fossil fuels (Nikolaidis and Poullikkas, 2017).

2.2.1.1. Hydrocarbon Reforming Methods

Hydrocarbon fuel is converted to hydrogen via three primary routes with hydrocarbon reforming methods, namely, steam reforming, partial oxidation and autothermal reforming (Dalena et al., 2017). The endothermic reaction is known as steam reforming where steam is the reactant for the reforming process. Partial oxidation is an exothermic reaction where oxygen is the reactant for the reforming process. When steam reforming and partial oxidation reactions are combined, it is known as the autothermal reaction (Nikolaidis and Poullikkas, 2017).

2.2.1.1.1. Steam Reforming Method

Steam reforming method is a catalytic conversion of hydrocarbons and steam to hydrogen and carbon oxides (Nikolaidis and Poullikkas, 2017). Currently, the least expensive method is steam reforming of natural gas, and almost half of the worldwide hydrogen production is performed via this method. Firstly, sulphur compounds are cleaned from natural gas by desulphurization and then it is mixed with steam and send over a tubular externally heated reactor with the reforming catalyst which is generally based on nickel-alumina. CO and H_2 are generated here. The catalytic water-gas shift reaction is a second step reaction where water and CO are converted to H_2 and CO_2. Then the hydrogen gas is purified.

The endothermic reaction of reforming is:

$$CH_4 + H_2O + 206\ kJ/kg \rightarrow CO + 3H_2 \qquad \text{(Eq. 2.1)}$$

The exothermic shift reaction is:

$$CO + H_2O \rightarrow CO_2 + H_2 + 41\ kJ/kg \quad \text{(Eq. 2.2)}$$

The overall reaction is:

$$CH_4 + 2H_2O + 165\ kJ/kg \rightarrow CO_2 + 4H_2 \quad \text{(Eq. 2.3)}$$

The required heat is supplied from the residual steam from initial purification step (Nikolaidis and Poullikkas, 2017; BACAS, 2006).

2.2.1.1.2. Partial Oxidation Method

Hydrocarbons, steam and oxygen are converted to hydrogen and carbon oxides in the partial oxidation method (BACAS, 2006). In this process, liquid or gaseous hydrocarbons such as natural gas and oxygen are injected to the high pressure reactor. In order to avoid of soot formation and to maximize hydrogen yield, oxygen to carbon ratio is optimally set. The large amount of heat generated by the oxidation reaction is removed in the next steps, CO with water is converted to CO_2 and H_2, and then CO_2 is captured and hydrogen gas is purified.

The partial oxidation for natural gas is:

$$CH_4 + \tfrac{1}{2}O_2 \rightarrow CO + 2H_2 \quad \text{(Eq. 2.4)}$$

The process gas in this method is similar with the gas in the steam reforming process. This reaction is exothermic, so heating is not required. This is the major advantage of this method. However, steam reforming is typically more energy efficient than partial oxidation (BACAS, 2006).

2.2.1.1.3. Autothermal Reforming Method

The exothermic partial oxidation reaction is used in order to provide the sufficient heat and endothermic steam reforming reaction is used for increasing the hydrogen production in the autothermal reforming method (Nikolaidis and Poullikkas, 2017). In this process, oxygen and steam are injected to a vessel which includes a combustion zone and reforming zone and they are reacted in a vessel. The heat

provided from exothermic partial oxidation balances that for the endothermic steam reforming. The standard shift reaction and hydrogen purification steps are the next steps for the process gas. The autothermal reforming method is compact and flexible for load just as partial oxidation method and it almost reaches the higher efficiency of steam reforming method (Nikolaidis and Poullikkas, 2017).

2.2.1.2. Hydrocarbon Pyrolysis Method

The hydrocarbon is the only source of hydrogen in the hydrocarbon pyrolysis process which is considered as an indirect hydrogen production method. Hydrocarbons pass thermal decomposition process through the following main reaction:

$$C_mH_n \rightarrow mC + \tfrac{1}{2}nH_2 \quad \text{(Eq. 2.5)}$$

Light liquid hydrocarbons are decomposed thermo-catalytically and elemental carbon and hydrogen are produced. Hydrogen is produced in two-step which are hydrogasification and cracking of methane. This two-step scheme (Nikolaidis and Poullikkas, 2017) is as follows;

$$CH_{1.6} + 1.2H_2 \rightarrow CH_4 \text{ (hydrogasification)} \quad \text{(Eq. 2.6)}$$

$$CH_4 \rightarrow C + 2H_2 \text{ (cracking of methane)} \quad \text{(Eq. 2.7)}$$

$$CH_{1.6} \rightarrow C + 0.8H_2 \text{ (overall)} \quad \text{(Eq. 2.8)}$$

2.2.2. Hydrogen Production from Renewable Sources

Currently, fossil fuels are the main feedstock used for hydrogen production. However, there is a need to increase the integration of renewable technologies and methods. Because of the greenhouse effect and depletion of fossil fuels, it is expected to increase the share of the renewable technologies in the near future and these methods will dominate over conventional technologies. There are many methods for hydrogen production from renewable sources. These are mainly classified as biomass based processes and water splitting techniques (Nikolaidis and Poullikkas, 2017).

2.2.2.1. Water Splitting Methods

Water which is the most common hydrogen resource is one of the most abundant and exhaustless raw material in Earth. Water splitting methods, namely electrolysis, photoelectrolysis and thermolysis use water for hydrogen production (Nikolaidis and Poullikkas, 2017).

2.2.2.1.1. Electrolysis

Water electrolysis is a basic process, the cleanest way and the most effective technique in order to produce pure hydrogen (Nikolaidis and Poullikkas, 2017; Dincer and Acar, 2015). Significance of electrolysis is expected to increase in near future. Electrolysis method is based on electrons movement supported by external circuit. A basic and typical electrolysis unit, namely electrolyzer, consists of an anode and a cathode. Basically, water splits when the electrical current is applied and hydrogen is produced at the cathode side and oxygen is evolved at the anode side through the following reaction:

$$2H_2O \rightarrow 2H_2 + O_2 \qquad \text{(Eq. 2.9)}$$

Alkaline, solid oxide electrolysis cells (SOEC) and polymer or proton exchange membrane (PEM) are the commonly used electrolysis technologies. Extremely pure hydrogen is produced easily from water by electrolysis method, however, electrical consumption by electrolyzers are considerably high (Nikolaidis and Poullikkas, 2017; Dincer and Acar, 2015).

2.2.2.1.2. Thermolysis

Water thermolysis or thermochemical water splitting is a dissociation process where water is heated to high temperature and it is decomposed to hydrogen and oxygen via the following reaction:

$$H_2O + heat \rightarrow H_2 + \tfrac{1}{2}O_2 \qquad \text{(Eq. 2.10)}$$

The decomposition of water is affected by temperature over 2500°C. When it is satisfied and Gibbs function (ΔG) equals zero, hydrogen separation from the

equilibrium mixture becomes feasible Nikolaidis and Poullikkas, 2017; Dincer and Acar, 2015).

2.2.2.1.3. Photoelectrolysis

Photoelectrolysis or photolysis is the process where photocatalysts are applied to the electrodes (Dincer and Acar, 2015). Visible light energy absorbed with the help of these catalysts is utilized in order to decompose water to hydrogen and oxygen. Semiconducting materials absorb the sunlight and water splitting process is similar to electrolysis. The energetic view of hydrogen production is represented in the following equations (Nikolaidis and Poullikkas, 2017; Dincer and Acar, 2015):

Anode:

$$2p^{+} + H_2O \rightarrow \frac{1}{2}O_2 + 2H^{+} \quad \text{(Eq. 2.11)}$$

Cathode:

$$2e^{-} + 2H^{+} \rightarrow H_2 \quad \text{(Eq. 2.12)}$$

Overall:

$$H_2O \rightarrow H_2 + \frac{1}{2}O_2 \quad \text{(Eq. 2.13)}$$

2.2.2.2. Biomass Process

Biomass is a renewable resource of primary energy which can be used for sustainable hydrogen production. Energy crops, agricultural and crop residues, forest residues, industrial residues, municipal waste, animal and farm waste, grass are some biomass derived fuels from animal and plant materials. Instead of fossil fuels, using biomass for hydrogen production reduces CO_2 emissions. Hydrogen production from biomass is mainly based on two processes, namely thermochemical and biological methods. Biological processes are more environmental friendly and less energy consuming methods. However, these processes provide low hydrogen production rates and yields depending on the raw material. Besides, thermochemical

processes are much faster and provide higher hydrogen yields (Nikolaidis and Poullikkas, 2017).

2.2.2.2.1. Thermochemical Methods

Thermochemical processes, which are pyrolysis, gasification, combustion and liquefaction, are based on the technique where biomass and biomass derived fuels could be converted to hydrogen and hydrogen rich gases (Dalena et al., 2017). Hydrogen rich gases are produced from synthesis gas which is obtained from thermochemical processes and the production of hydrogen rich gases is an effective solution for greenhouse effect with zero emission of greenhouse gases and necessary for sustainable development. Pyrolysis and gasification are the main thermochemical technologies. Because of emitting polluting byproducts, requiring difficult operational conditions and offering low hydrogen production, combustion and liquefaction processes are less preferable methods (Nikolaidis and Poullikkas, 2017; Dalena et al., 2017).

- *Pyrolysis*

Biomass pyrolysis, which is considered as an indirect production method, is the thermochemical process of converting biomass to bio-oil, biochar and gaseous compounds by heating the biomass. Pyrolysis process takes place in the individual steps through the following reactions:

Pyrolysis of biomass $\rightarrow H_2 + CO + CO_2 +$ hydrocarbon gases + char + tar (Eq. 2.14)

$C_mH_n + m\ H_2O \rightarrow mCO + (m + ½n)\ H_2$ (Eq. 2.15)

$CO + H2O \rightarrow CO_2 + H_2$ (Eq. 2.16)

The hydrogen production yield of biomass pyrolysis depends on the feedstock type, catalyst type, residence time and temperature. Pyrolysis occurs in the anoxic conditions except for some conditions of partial combustion processes which provide the thermal energy needed for the process (Nikolaidis and Poullikkas, 2017; Dalena et al., 2017).

- *Gasification*

Biomass gasification is a process of thermochemical conversion of biomass to gas which is applied for organic waste conversion to CO, CO_2, CH_4 and H_2 via high temperature reactions in a gasification medium such as air, oxygen and steam (Dalena et al., 2017). The major product of gasification is syngas. There are three main reactor types used for gasification process, namely fixed bed, fluidized bed and indirect gasifiers. The conversion of biomass to syngas takes place through the following pathways according to the reaction with air or steam:

$$\text{Biomass} + \text{Air} \rightarrow H_2 + CO_2 + CO + N_2 + CH_4 + \text{other CHs} + H_2O + \text{char} + \text{tar} \quad \text{(Eq. 2.17)}$$

$$\text{Biomass} + \text{Steam} \rightarrow H_2 + CO_2 + CO + CH_4 + \text{other CHs} + H_2O + \text{char} + \text{tar} \quad \text{(Eq. 2.18)}$$

Hydrogen yield is affected mainly by parameters such as type of biomass, size of particle, catalyst type, steam to biomass ratio and temperature (Nikolaidis and Poullikkas, 2017; Dalena et al., 2017).

2.2.2.2.2. Biological Methods

Hydrogen produced from renewable resources or biomass with the inclusion of the biological agents such as enzymes, microorganisms and plants is called biohydrogen. Because of sustainable development and waste minimization strategies, biological hydrogen production researches have accelerated over the last several years (Nikolaidis and Poullikkas, 2017). Because of operating at ambient pressure and temperature, biological processes are less energy intensive methods. They are playing a role in recycling of waste materials by using and utilizing various waste materials. They utilize inexhaustible renewable resources and they provide environmental friendly solutions. However, they are time-consuming methods. Direct and indirect biophotolysis, dark fermentation and photofermentation processes are the major biological processes for hydrogen production which are

discussed in detail in Section 2.3 (Nikolaidis and Poullikkas, 2017; Dalena et al., 2017).

2.3. Biological Hydrogen Production Strategies

Several strategies are present in order to produce hydrogen through biological pathways: 1) direct and indirect biophotolysis by green algae and cyanobacteria which use sunlight to separate water to hydrogen and oxygen molecules; 2) dark fermentation by bacteria which ferment organic materials such as sugars; 3) photofermentation by photosynthetic bacteria which use sunlight to split organic compounds to hydrogen and carbon dioxide molecules. There are also hybrid systems such as sequential dark fermentation and photofermentation processes in order to improve hydrogen yields (Lin and Wilson, 2016).

Microorganisms catalyze the biological hydrogen production in an aqueous environment at optimum temperature and pressure conditions. These microorganisms' characteristics differ from one another according to feedstock and process conditions. Compared to the chemical and electrochemical processes, biological hydrogen production technologies are much adapting for energy production and are decentralized in pilot scale plants. They are applicable and practicable at any location where wastes and biomass are easily available. The catalyzing chemical reaction of hydrogen production is represented in the following equation:

$$2H^+ + 2e^- \leftrightarrow H_2 \qquad \text{(Eq. 2.19)}$$

Enzymes have an essential role for catalyzing the biological hydrogen production. Nitrogenase, Fe-hydrogenase and Ni-hydrogenase are three widespread enzymes involved in the biohydrogen production reactions (Bharathiraja et al., 2016).

2.3.1. Biophotolysis

Biophotolysis is a biological hydrogen production method which uses the basic principles found in plants and algal photosynthesis (Nikolaidis and Poullikkas, 2017). The carbon dioxide reduction is observed in green plants, whereas catalytic enzymes for hydrogen production are absent. On the other hand, algae include hydrogen-producing enzymes and they generate hydrogen under particular conditions. Green and blue green algae can split water to hydrogen and oxygen ions through direct and indirect biophotolysis (Nikolaidis and Poullikkas, 2017).

2.3.1.1. Direct Biophotolysis

Direct biophotolysis is a biological method using microalgae photosynthesis system to split water to hydrogen and oxygen by converting solar energy to chemical energy (Azwar et al., 2014). The reaction is generally as follows (Azwar et al., 2014):

$$2H_2O + \text{light energy} \rightarrow 2H_2 + O_2 \quad \text{(Eq. 2.20)}$$

In direct biophotolysis, water is splitted to hydrogen and oxygen ions by green algae. Hydrogenase enzyme then convert hydrogen ions produced into hydrogen gas. This is an oxygen sensitive enzyme and oxygen level should be kept under 0.1% (Nikolaidis and Poullikkas, 2017; Azwar et al., 2014).

2.3.1.2. Indirect Biophotolysis

Indirect biophotolysis is a biological method using microalgae and cyanobacteria photosynthesis system to split water to hydrogen and oxygen ions by converting solar energy into chemical energy through basically two steps as follows (Azwar et al., 2014):

$$12H_2O + 6CO_2 + \text{light energy} \rightarrow C_6H_{12}O_6 + 6O_2 \quad \text{(Eq. 2.21)}$$

$$C_6H_{12}O_6 + 12H_2O + \text{light energy} \rightarrow 12H_2 + 6CO_2 \quad \text{(Eq. 2.22)}$$

The overall reaction as follows:

$$12H_2O + \text{light energy} \rightarrow 12H_2 + 6O_2 \quad \text{(Eq. 2.23)}$$

In direct biophotolysis, water is splitted to hydrogen and oxygen ions by blue green algae and cyanobacteria. Both nitrogenase and hydrogenase enzymes then convert hydrogen ions produced into hydrogen gas and the hydrogen production rate is comparable to direct biophotolysis which consists hydrogenase based production by green algae (Nikolaidis and Poullikkas, 2017; Azwar et al., 2014).

2.3.2. Dark Fermentation

Dark fermentation is a biological fermentative process to convert organic materials for biohydrogen production in anaerobic conditions with the absence of light (Veras et al., 2017). Dark fermentation uses various groups of bacteria on carbohydrate rich organic substrates by involving biochemical reaction series. Glucose is a model substrate and preferred source for dark fermentation process. Acetic acid (acetate) and butyric acid (butyrate) constitute over than 80% of total end products and theoretical hydrogen yields are 4 moles per mole of glucose in acetate type fermentation and 2 moles per mole of glucose in butyrate type fermentation as follows:

$$C_6H_{12}O_6 + 2H_2O \rightarrow 2CH_3COOH + 4H_2 + 2CO_2 \text{ (acetate fermentation)} \quad \text{(Eq. 2.24)}$$

$$C_6H_{12}O_6 \rightarrow CH_3CH_2CH_2COOH + 2H_2 + 2CO_2 \text{ (butyrate fermentation)} \quad \text{(Eq. 2.25)}$$

Dark fermentation has various advantages in comparison with other biological hydrogen production methods such as no illumination requirement, production of by-products with organic acids having commercial value, using wide variety of carbon sources, higher hydrogen production rate, simple reactor technology and process simplicity (Veras et al., 2017; Nikolaidis and Poullikkas, 2017; Azwar et al., 2014).

2.3.3. Photofermentation

Photofermentation is another biological fermentative process which is realized in deficient nitrogen conditions utilizing organic acids and solar energy. Photofermentation is the focus of this thesis study, so it is examined in detail in the next topic, Section 2.4.

2.4. Detailed Information on Photofermentation

Fermentation is biochemical processes which occurs without oxygen and converts organic compounds to alcohols, hydrogen, acetone and carbon dioxide (Nikolaidis and Poullikkas, 2017). This method is attractive for biohydrogen production due to waste materials' usage and provision of energy with simultaneous waste treatment. Photofermentation is a light dependent biological process where photosynthetic bacteria absorb sunlight and convert biomass to hydrogen (Nikolaidis and Poullikkas, 2017). While anaerobic photosynthetic bacteria absorb light energy, they perform electron transport and this generates a proton drive force which is required for ATP synthesis. Purple sulfur, purple non-sulfur (PNS) and green sulfur bacteria are mainly photosynthetic bacteria which produce molecular hydrogen using light energy and reduced sources such as organic acids as proton source (Eq. 2.26-2.29). These process are catalyzed by nitrogenase enzyme (Gandia et al., 2013).

$CH_3COOH + 2H_2O + \text{light energy} \rightarrow 2CO_2 + 4H_2$ (Acetic acid) (Eq. 2.26)

$C_3H_6O_3 + 3H_2O + \text{light energy} \rightarrow 3CO_2 + 6H_2$ (Lactic acid) (Eq. 2.27)

$C_4H_6O_5 + 3H_2O + \text{light energy} \rightarrow 4CO_2 + 6H_2$ (Malic acid) (Eq. 2.28)

$C_4H_8O_2 + 6H_2O + \text{light energy} \rightarrow 4CO_2 + 10H_2$ (Butyric acid) (Eq. 2.29)

There are different photofermentation bioprocesses such as single stage and two-stage (sequential) photofermentation processes and combined (co-culture) photofermentation processes. Figure 2.4 shows the different photofermentation

processes (Pandey et al., 2013). Various substrates including different waste streams can be used for photofermentation process. Organic acids can be directly converted to hydrogen and carbon dioxide in a single stage photofermentation process by PNS bacteria. Moreover, some simple sugars can be directly converted by these organisms. Sugars are also used as substrates for hydrogen and organic acid production by dark fermentation. Thus, complex carbohydrates such as cellulose and starch should be first degraded to simple sugars and/or organic acids by dark fermentation before being converted to hydrogen by photofermentation. The effluent of the dark fermentation process can be suitably converted to hydrogen in a second photofermentation stage. In an alternative way, organic acid conversion to hydrogen through photofermentation can occur in a combined co-culture process (dark fermentation and photofermentation in the same close system) (Pandey et al., 2013).

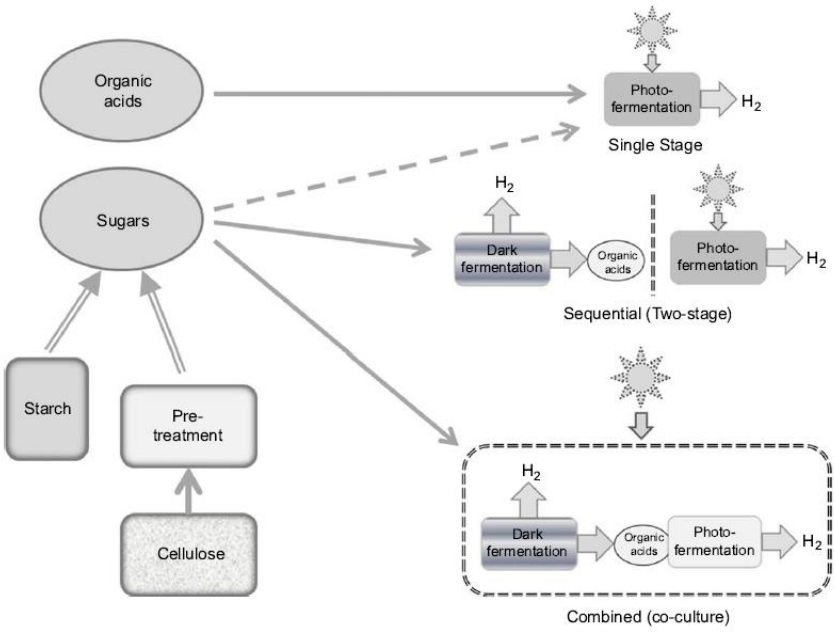

Figure 2.4 Different photofermentation bioprocesses (Pandey et al., 2013)

2.4.1. Photofermentative Organisms and Metabolic Pathways

Although there are many types of bacteria such as purple sulfur, green sulfur and PNS bacteria which could be used in photofermentation process, hydrogen production was performed mainly through PNS bacteria in photofermentation; because PNS bacteria particularly suit to photoheterotrophic lifestyle. PNS bacteria are less sensitive to oxygen existence than purple and green sulfur bacteria. Besides, PNS bacteria have higher growth rates and nitrogenase activities (Azwar et al., 2014; Gandia et al., 2013; Pandey et al., 2013). By using their single photosystem in the presence of light, they generate the energy which is necessary for growth and producing ATP to survive photosynthetically. They use organic compounds and inorganic ions (Fe^{2+}) as electron donors which are necessary for their metabolic activities (Pandey et al., 2013).

Photofermentation studies have been carried out mainly through five species of PNS bacteria, namely, *Rhodobacter spheroides*, *Rhodobacter capsulatus*, *Rhodosprilllum rubrum*, *Rhodovulum sulfidophilum*, and *Rhodopseudomonas palustris*. Although PNS bacteria are not strong enough to split water, they are able to use organic acids, amino acids, alcohols, simple sugars, agricultural and industrial effluents to produce hydrogen. PNS bacteria are found in a variety of natural environment and they can use a wide range of substrates which depends on the strain type (Gandia et al., 2013; Pandey et al., 2013).

Nitrogenase (N_2ase), an oxygen complex iron-sulfur molybdenum enzyme, is the key enzyme in photofermentation. There are some particular requirements and specific conditions for its regulation, enzyme activity, biosynthesis and hydrogen production. Large quantities of iron and molybdenum is nutritional requirement and regulatory factor for nitrogenase. High concentrations of fixed nitrogen (N_2) and oxygen repress the nitrogenase synthesis. Therefore, effective photofermentation only takes place under anoxic conditions and when very limited quantities of ammonium are present. Nitrogen is generally supplied in the form of amino acids such as glutamate or yeast extract for cell growth and this supports hydrogen

production better than ammonium. Nitrogen limitation prevents also excess cell synthesis which can be a problem in reduction of light diffusion and, in turn, photofermentation (Pandey et al., 2013).

A schematic diagram given in Figure 2.5 shows photofermentation of organic compounds by photosynthetic bacteria. Chemical energy is produced by photosynthetic bacteria from light and this energy are used to drive reverse electron to nitrogenase. Protons are released through metabolism and nitrogenase reduces protons to hydrogen with ATP hydrolysis. Normally, the fuction of nitrogenase is to catalyze biological dinitrogen reduction to ammonia with releasing of 1 mole hydrogen per 1 mol nitrogen reduced (Eq. 2.30). Nitrogenase also proceeds to reduce protons to hydrogen gas (Eq. 2.31).

$$N_2 + 8H^+ + 8e^- + 16ATP \rightarrow 2NH_3 + H_2 + 16ADP + 16Pi \quad \text{(Eq. 2.30)}$$

$$2H^+ + 2e^- + 4ATP \rightarrow H_2 + 4ADP + 4Pi \quad \text{(Eq. 2.31)}$$

As seen in Figure 2.5, organic acids are imported and metabolized through central metabolic pathways. Carbon dioxide is given off and NADH is produced. NADH is used in order to reduce ferredoxin which is the electron donor to nitrogenase through a reverse electron transport. ATP is necessary for protons reduction by nitrogenase and it is generated by bacterial photosynthesis (Pandey et al., 2013).

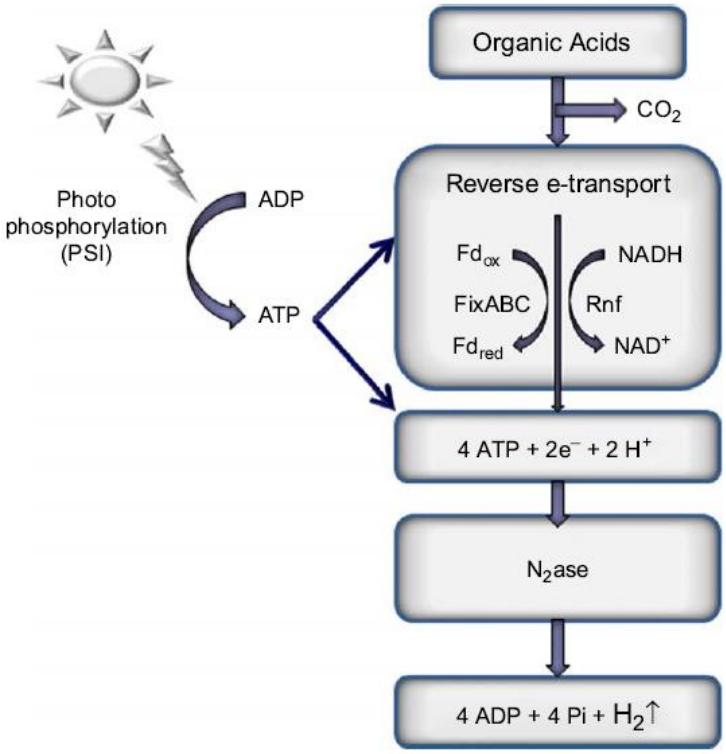

Figure 2.5 The outline of metabolic processes involved in photofermentation (Pandey et al., 2013)

2.4.2. Factors Affecting Photofermentative Hydrogen Production

Photofermentative hydrogen production is influenced by many factors and operational parameters. Carbon and nitrogen sources, carbon to nitrogen (C/N) ratio, type of photobioreactors, operational parameters such as light source and intensity, pH, temperature and mode of operation are the major factors which affect the hydrogen production in photofermentation process (Basak et al., 2014).

2.4.2.1. Carbon and Nitrogen Sources

Although the substrate type can change depending on the bacterial strain, photosynthetic bacteria prefer organic acids as substrates. Acetic acid, malic acid, formic acid, butyric acid, propionic acid and succinic acid are the organic acids which can be utilized as carbon sources for hydrogen production by photosynthetic

bacteria in photofermentation process (Basak et al., 2014). Nitrogen sources mainly used are glutamic acid, yeast extract, ammonium chloride and ammonium sulphate. Both concentrations and types of nitrogen sources vary from one type of bacteria to other. Nitrogen concentration, especially ammonium ion, NH_4^+, in the substrate plays an important role for hydrogen production. As mentioned previously, the activity of nitrogenase enzyme is inhibited by the presence of ammonium. In the absence of ammonium salts and molecular nitrogen in the substrate, both hydrogen production and activity of nitrogenase are enhanced (Gandia et al., 2013; Basak et al., 2014). Glutamate was found a favorable nitrogen source for hydrogen production among the other amino acids (Hillmer and Gest, 1977). It was also conducted in the same study that when the glutamate concentration increased from 7 mM to 22 mM, both hydrogen production rate and hydrogen yield decreased progressively.

Initial organic acid concentrations have an impact on bacterial growth rate, lag period and hydrogen production. According to the study conducted by Barbosa et al. (2011), acetate was found as the best carbon source leading to the highest hydrogen production among acetate, malate, lactate and butyrate for *Rhodopseudomonas spheroides*. In that study, acetate concentrations between 6-22 mM were studied and 22 mM acetate gave the best result for the highest hydrogen yield. In a study conducted by Özgür et al. (2010), the highest hydrogen production was observed at 40 mM acetate concentration and the highest substrate conversion efficiency was obtained at 30 mM acetate concentration for *Rhodobacter capsulatus*. Asada et al. (2008) stated that acetate concentrations higher than 84 mM inhibit the hydrogen production in immobilized batch systems.

2.4.2.2. Type of Reactors

Photobioreactor type and its design are among important factors for effective hydrogen production in photofermentation process (Gandia et al., 2013). Photobioreactors are still in the development stage. Large scale hydrogen production requires a proper photobiorector design. Performance of photobioreactors not only

depend on the bacterial strain selected and its light requirement, but also on some physical operational parameters such as dissolved oxygen and carbon dioxide, pH, temperature, which can affect the metabolic pathways. Mass transfer of carbon dioxide, surface to volume ratio, mixing, removal of oxygen, control of temperature and construction material are the main criteria for bioreactor design in photofermentation (Gandia et al., 2013; Rezania et al., 2017).

Photobioreactors must be closed systems in order to satisfy anaerobic conditions and prevent dispersion of hydrogen gas. While collecting hydrogen gas efficiently by satisfactory gas exchange system, photobioreactors should protect bacteria from contamination. High illuminated surface to volume ratio and efficient mixing system to allow the culture to be illuminated must be satisfied (Basak et al., 2014; Adessi and Philippis, 2014). The amount of light entering the system is determined by surface to volume ratio. Therefore, the higher surface to volume ratio provides the cell concentration and greater volumetric productivities. However, too high surface to volume ratios can accumulate oxygen which inhibits the photosynthetic bacteria. The construction material of photobioreactors should not be only highly transparent, durable and flexible, but also they must be nontoxic for microorganisms and resistant to weather and chemicals. Mixing is also a highly important parameter in order to prevent gradients of nutrient, light and temperature. Settling of biomass, stagnant zones, aggregation of cells and multiphase behaviors can be observed in case of inadequate mixing. The general method of mixing is inert gas bubbling and sometimes collected gas can be also recirculated (Gandia et al., 2013).

Tubular reactors (Figure 2.6b) and flat panel reactors (Figure 2.6a) are main photobioreactor types used for hydrogen production. Tubular reactors, which consist of transparent tubes, have high surface to volume ratio leading to high photosynthetic efficiencies. Transparent tubes are either horizontal, vertical or helical. Horizontal tubular reactors, which are oriented toward sunlight, have higher light conversion efficiencies but efficient temperature control is a main problem. Vertical tubular reactors, which consist of a single column, are generally constructed

by polyethylene and allow efficient light irradiation and temperature control. Flat panel reactors, which are rectangular transparent boxes, have very high surface to volume ratio. They consist of plates made with the minimal thickness which can be placed either horizontal or inclined in the direction of sun. Because construction and modification of flat panel reactors are easy and simple, they are very suitable for base studies on light distribution and mixing. This kind of reactors refer to small scale reactors with innovative systems to get higher yields (Gandia et al., 2013; Adessi and Philippis, 2014).

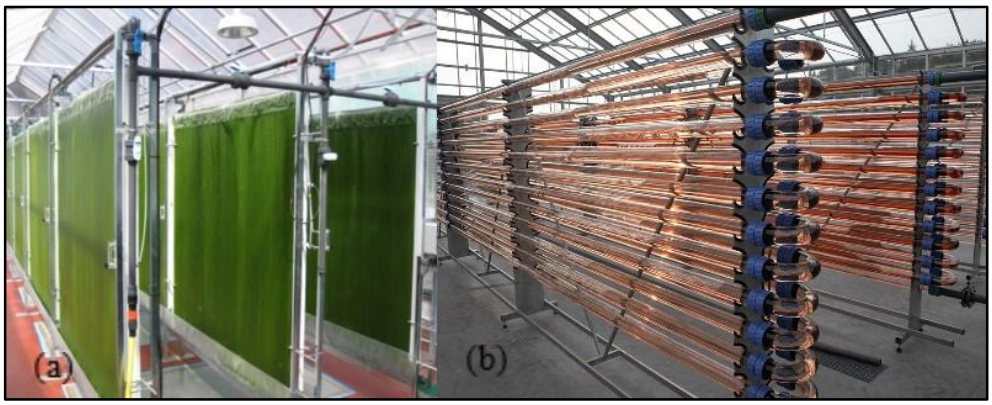

Figure 2.6 (a) Flat panel reactors, (b) Tubular reactors (URL-1)

2.4.2.3. Operational Parameters

The light source and intensity, temperature, pH, micronutrient concentrations and mode of operation are the main operational parameters which influence hydrogen production and required to control strictly (Gandia et al., 2013; Rezania et al., 2017). These operational parameters must be optimized for each process in order to enhance hydrogen production in photofermentation.

Light Intensity: Distribution of light inside of the photobioreactor is one of the most important operational parameters which strongly affects the hydrogen production. Light is also a requirement for bacterial growth. The light intensity controls the photosynthetic mechanisms that converts the light energy to ATP. Hydrogen

production rates and yields increase with increasing light intensities until a threshold. The high ATP demand of nitrogenase for hydrogen production is not met by the light energy at low light intensities. On the other hand, under high light intensities, the saturation of photosynthetic mechanism prevents hydrogen production. Moreover, stronger light intensities cause a decrease in hydrogen production because of the adverse effects such as cell shading resultant of high biomass growth (Sasikala et al., 1999; Uyar et al., 2007; Shi and Yu, 2005). The study about the effect of light intensity on hydrogen production conducted by Uyar et al. (2007) showed that hydrogen production increased with increasing light intensity, reaching saturation at 270 W/m^2. Hydrogen production did not increase after this saturation level. Androga et al. (2014) optimized the light intensity, and 285 W/m^2 and 287 W/m^2 of optimum light intensities were obtained for maximum hydrogen yield and maximum hydrogen production rate, respectively. In the literature, optimal range of light intensities are reported as 4000-6000 lux (Uyar et al., 2007; Shi and Yu, 2005; Sevinc et al., 2012; Castillo et al., 2012) corresponding to 267-400 W/m^2.

Sunlight or artificial light sources are utilized by photobioreactors as light sources. Sunlight can be used alone or combination with one or more artificial light sources. Artificial light sources can be florescent lamps, halogen lamps, neon tubes, optical fibers, light emitting diodes etc. Because the light energy decreases with the distance from light sources, high light efficiency is achieved with short light path. Moreover, light sources cannot be in close contact with the bacterial culture because of substantial amount of heat generation (Basak et al., 2014).

Temperature: Temperature is another essential operational parameter for photofermentative hydrogen production since it plays an important role in the metabolic reactions for hydrogen production. The optimum temperature range for *Rhodobacter* species is between 31°C and 36°C (Basak and Das, 2007). In the study conducted by Eroğlu et al. (2010), the highest hydrogen production rate was found at 30°C by *Rhodobacter capsulatus*. Optimum temperature is also reported as

around 30°C in other studies (Özgür et al., 2010; Sasikala et al. 1991; Sevinc et al., 2012). Increasing the temperature above 30°C enhances hydrogen production, while heat stress and reversible enzyme inactivation affect hydrogen production adversely at temperatures above 30°C (Doğan, 2011). The optimum temperature for the activity of nitrogenase was reported as 30°C and temperatures above or below result in lower activities which leads to lower hydrogen production (Koku et al., 2002; Jouanneau et al., 1985).

pH: The optimum pH level for photofermentation is between 6.5-8 (Zannoni and Philippis, 2014). The optimal pH for hydrogen production for *Rhodobacter sphaeroides O.U.001* was determined in the range between 6 and 9 by Sasikala et al. (1991). The optimum pH range was also reported to be 6.8-7.5 (Argun and Kargi, 2011). Moreover, the pH range between 6.5-7.5 was found as the optimum for bacterial growth (Bergey and Holt, 1994).

Micronutrients: Micronutrients such as essential metal ions play an important role on the activity of nitrogenase enzyme and photofermentative hydrogen production. The nitrogenase activity reduces in the absence of essential metal ions such as iron and molybdenum which are required cofactors for higher nitrogenase activity. Thus, especially iron and molybdenum salts should be supplemented to the culture media to enhance hydrogen production yield of various *Rhodobacter* species (Laurinavichene et al., 2013; Kars et al., 2006; Koku et al., 2002; Zhu et al. 2007).

Operation Mode: The mode of operation is another operational parameter which influences the amount of hydrogen produced (Gandia et al., 2013). Commonly, photobioreactors operate in batch, continuous or semi-batch modes. When the cells reach the stationary phase in the batch systems, cumulative hydrogen production stops. However, bacterial concentration of the exponential growth phase can be maintained for longer periods with a specific dilution rate. Semi-batch processes are alternative systems where the substrate is added with a specific rate that is sufficient to support bacterial community and to eliminate inhibitions of substrate and products with no effluent removal. When the feeding rate and substrate consumption

rate are equal, substrate concentration in the reactor reaches a quasi-steady state. In the study conducted by Avcıoğlu et al. (2009) it was shown that hydrogen production rate and yield of *Rhodobacter capsulatus* were lower in continuous operation than in batch mode. However, while continuous operation could be stable for 3 months, it was approximately 150 hours for batch mode. Thus, continuous operation was suggested as more suitable operation for the scale-up and long term hydrogen production.

Combined Effects of Operational Parameters: Photofermentation studies in the literature generally investigate the effects of one parameter or separate effects of more than one parameter on hydrogen production (Eroglu et al., 2014; Uyar et al., 2007; Argun et al., 2008). Yet, the optimum value which was found for one parameter may not necessarily result in the highest hydrogen production, when there are other potential parameters affecting the influence of this predetermined parameter. For instance, cell concentration and light intensity are two important parameters which influence hydrogen production by PNS bacteria. However, cell concentration might affect the distribution of the light intensity in reactors, and, in turn, the hydrogen production. Therefore, when there are more than one parameter influencing the hydrogen production, possible potential interactions of them should be considered. The studies investigating the combined effects of parameters on photofermentative hydrogen production are limited in literature (Shi et al., 2005; Androga et al., 2014) and these only focus on two parameters. However, the combined effect of three operational conditions of the substrate, the biomass (VSS) and the light intensity on photofermentation has not been investigated so far. Moreover, the effect of initial substrate concentration to initial volatile suspended solids (VSS) concentration ratio (S/X_o) has not been studied so far. In this scope, the combined effects of these three parameters were investigated in this thesis study (Akman et al., 2015).

2.5. *Rhodobacter Capsulatus* (DSM 1710)

Rhodobacter capsulatus is a gram negative PNS bacteria which belongs to α-proteobacteria (Imhoff, 1995). *Rhodobacter capsulatus* is rod shaped and has a diameter of 0.5-1.2 μm. It produces slime and capsule. It can store poly-β-hydroxybutyric acid as the storage material. The microscopic image of *Rhodobacter capsulatus* is given in Figure 2.7. The taxonomy of *Rhodobacter capsulatus* is presented in Table 2.4 (Imhoff, 1995).

Rhodobacter capsulatus has been a favorite research tool in the areas of photosynthesis, energetics and nitrogen fixation for many years (Gandia et al., 2013). *Rhodobacter capsulatus* has been studied for its versatile metabolism, hydrogen production and nitrogen fixation. Moreover, it can be easily mutated by classical procedures, thus offering good opportunities for biochemical and genetic approaches (Weaver, 1975).

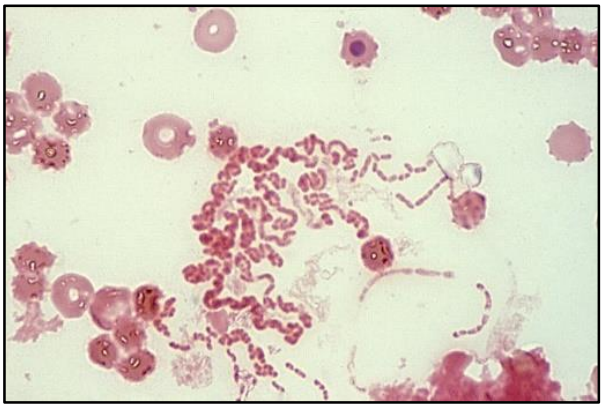

Figure 2.7 The microscopic image of Rhodobacter capsulatus (URL-2)

Table 2.4 The taxonomy of Rhodobacter capsulatus (Imhoff, 1995).

Super Kingdom	Prokaryota
Kingdom	Monera
Sub Kingdom	Eubacteria
Class	Photosynthetic eubacteria
Family	Rhodospirillaceae
Genus	Rhodobacter
Species	Capsulatus

2.5.1. Photofermentative Hydrogen production via Rhodobacter Capsulatus

Hydrogen production by PNS bacteria breaks down the organic materials (such as acetate, butyrate, malate, propionate and lactate) under illumination under anaerobic and nitrogen-limited conditions (Wu et al., 2012). *Rhodobacter capsulatus*, is frequently used in photofermentative hydrogen production (Table 2.5). Hydrogen production of *Rhodobacter capsulatus* was improved by eliminating polyhydroxyalkanote synthesis and knocking out the uptake hydrogenase. Another improvement strategy used in PNS bacteria involved the genetic modification of the electron transfer chains in *Rhodobacter capsulatus*. The uptake hydrogenase of *Rhodobacter capsulatus* can be eliminated and genetically mutant *Rhodobacter capsulatus* types can be generated (i.e *Rhodobacter capsulatus* YO3) (Mathews and Wang, 2009). Hydrogen production rate of various studies with *Rhodobacter capsulatus* in literature are given in Table 2.5. The hydrogen production rate was obtained in the range of 0.14-2.04 mmol/L.h in the studies conducted with *Rhodobacter capsulatus* and its mutants so far. The highest hydrogen production rate observed was 2.04 mmol/L.h (Elkahlout et al., 2016). This was obtained in batch reactor with *Rhodobacter capsulatus* YO3. The highest hydrogen production rate of 0.75 mmol/L.h from acetate was achieved with *Rhodobacter capsulatus* DSM 1710 in a batch reactor.

Table 2.5 Hydrogen production rate (HPR) of various studies performed with *Rhodobacter capsulatus*

Feed Type	**Bacteria Type**	**HPR (mmol/L.h)**	**References**
DFE of thick juice	*R.capsulatus* YO3	1.05	Uyar et al., 2015
DFE of thick juice	R.capsulatus DSM1710	1.01	Uyar et al., 2015
Acetate	*R.capsulatus* YO3	2.04	Elkahlout et al., 2016
Acetate	*R.capsulatus* DSM1710	0.75	Elkahlout et al., 2016
Sucrose	*R.capsulatus* YO3	0.72	Sagir et al., 2017
Acetate	*R.capsulatus* DSM1710	0.31	Boran et al., 2010
DFE of molasses	*R.capsulatus* YO3	0.67	Avcioglu et al., 2011
DFE of molasses	*R.capsulatus* DSM1710	0.55	Avcioglu et al., 2011
Acetate	*R.capsulatus* YO3	0.51	Androga et al., 2011
DFE of thick juice	*R.capsulatus* YO3	1.36	Ozkan et al., 2012
Molasses	*R.capsulatus* YO3	0.31	Yetis et al., 2000
Sucrose	*R.capsulatus* YO3	0.62	Sagir et al., 2017
Acetate, Lactate	*R.capsulatus* DSM155	0.74	Gebicki et al., 2010
Acetate	*R.capsulatus* YO3	0.37	Boran et al., 2012
Acetate, Lactate	*R.capsulatus* DSM1710	0.14	Özgür et al., 2010
Acetate, Lactate	*R.capsulatus* YO3	0.32	Özgür et al., 2010

CHAPTER 3

MATERIALS AND METHODS

This chapter covers the cultivation of bacteria, analytical methods used in experimental set-ups, namely, Set-1 to Set-4, Response Surface Methodology (RSM) and experimental procedure of each set.

3.1. Cultivation of Bacteria and Growth Medium

The strain of photosynthetic PNS bacteria, namely, *Rhodobacter capsulatus* DSM 1710 was used in this thesis study. This strain was obtained from DSMZ (Deutsche Sammlung von Mikroorganismen und Zellkulturen GmbH – German Collection of Microorganisms and Cell Cultures) and it was stored at -80°C in the stocks of Middle East Technical University – Hydrogen Research Laboratory.

Bacterial stocks taken from -80°C were thawed at room temperature and plated in petri dishes with agar and growth media by streak plate method (Figure 3.1.a). The modified Biebl and Pfennig medium containing 20 mM acetate and 10 mM glutamate was used as growth media. The plated petri dishes were kept in the incubator at 30°C for 7 days in the dark. The single colonies formed in petri dishes (Figure 3.1.a) were inoculated in Eppendorf tubes containing 1.5 mL Biebl and Pfennig medium. These tubes were inoculated in the dark at 30°C in the incubator. After 3 days, each 1.5 mL bacteria culture in eppendorf tubes were inoculated to 15 mL sterile cone tubes and these tubes were stored in the dark at 30°C for 2 days in the incubator (Figure 3.1.b). After that, the bacteria cultured in 15 mL tubes were inoculated to 50 mL glass reactors with 10% v/v dilution.

After inoculation, the air in the reactors was purged with argon gas in order to create anaerobic environment and reactors were kept to grow in the light at 30°C for 2 days in the incubator (Figure 3.1.c). At the end of this period, the same process was once again carried out for transfering bacterial culture from 50 mL glass bottles to 150 mL glass bottles and replication process was continued from 150 mL glass bottles to 150 mL glass bottles at the intervals of approximately 4-5 days. All these procedures were carried out in a sterile cabinet under sterile conditions (Figure 3.1.d). All the materials and media used were autoclaved at 121°C and 1 atm pressure for 20 minutes.

Figure 3.1 Rhodobacter capsulatus (DSM 1710) growth and replication phases (a) bacterial growth by streak plate method, (b) bacterial cultivation in Eppendorf tubes, (c) bacterial cultivation in glass reactors, (d) sterile working procedure

3.2. Analytical Methods

3.2.1. Analyses Performed to Monitor Reactor Performance

Cell Concentration: Cell concentration in reactors was determined by a spectrophotometer (Shimadzu UV-1201) at a wavelength of 660 nm (Uyar, 2008). An Optical Density (OD) value of 1 at 660 nm corresponded to 0.6334 g VSS/L dry cell weight for *Rhodobacter capsulatus* (DSM 1710) according to the OD-VSS calibration curve given in Appendix A (Figure A.1). Distilled water was used as blank.

pH: pH of the liquid solutions prepared for growth media and liquid solutions in the reactors was measured using a pH meter (Mettler Toledo 3311). The pH meter was calibrated with pH 4, pH 7 and pH 10 buffer solutions before each use.

Light Intensity: The light intensity in experiments was measured using luxmeter (Lutron LX-105 Light Meter).

Temperature: The reactors were placed in a cooling incubator (Nüve ES 250 incubator) to keep the temperature constant. The inner temperature was also checked by a digital thermometer (Maxi-T). The surface temperature of the reactors was manually checked using an infrared thermometer (Testo T1).

Volatile Suspended Solids (VSS): VSS concentration was determined according to Standard Methods (2540) (APHA, AWWA and WEF 2005).

Volatile Fatty Acids (VFA): The daily samples taken from reactors were centrifuged at 13,600 rpm for 10 minutes in a bench-top centrifuge (Eppendorf MiniSpin) to precipitate the bacterial cells. The supernatant of the centrifuged samples was used for VFA analysis. High Performance Liquid Chromatography (HPLC) (Shimadzu 20A Series) was used to analyze VFAs concentrations. The liquid samples were filtered through 0.22 μm pore-sized filters (Millipore SLGS033) and analyzed by an

Alltech IOA-1000 (300 mm x 7.8 mm) HPLC column. The oven temperature was maintained at 66°C and for mobile phase 0.085 M H_2SO_4 was used. The mobile phase flow rate of 0.4 mL/min was kept by using a low gradient pump (Shimadzu LC-20AT) with a degasser (Shimadzu DGU-14A). 10 µL of sample was injected to the system by autosampler (Shimadzu SIL-20AC) and a UV detector (Shimadzu FCV-10AT) detected the VFA at 210 nm wavelength. The VFA measured in samples were acetic acid, lactic acid, formic acid, propionic acid and butyric acid. The calibration curves prepared for determination of VFA concentrations are given in Appendix B (Figure B.1).

Gas Composition Analysis: Gas samples were collected from the headspace of the reactors by gas-tight syringes (Hamilton, 22 GA). The composition of the gas produced in the reactors was measured by a gas chromatograph (GC) with a thermal conductivity detector (Agilent Technologies 6890N). The Supelco Carboxen 1010 column was used. Argon gas with a flow rate of 26 mL/min was used as a carrier gas and the oven temperature was 140°C. The temperatures of injector and detector were 160°C and 170°C, respectively. The Agilent Chemstation ver.B.01.01 (Agilent Technologies) was used as software.

Chemical Oxygen Demand (COD): EPA approved digestion method (COD range of 0-1500 mg/L) was carried out for COD analyses (Hach Water Analysis Handbook, 2012, GT). Aqualytic AL 38 heater and PC Multidirect Spectrophotometer (Program 130-131) were used for COD measurements. Samples were filtered through 0.45 µm pore sized filters (Millipore) for soluble COD (sCOD) analysis.

Alkalinity: Alkalinity was measured according to Standard Methods (2320B Titration Method) (APHA, AWWA and WEF 2005).

Evaluation of Hydrogen Production Performance: Hydrogen production performance of each photofermentation reactor was specified by hydrogen production rate, hydrogen yield, substrate conversion efficiency and light conversion efficiency. The hydrogen production rate was calculated from the linear hydrogen production phase during the exponential phase of bacterial growth by Equation 3.1:

Hydrogen Production Rate (mmol/L/h) = Amount of H_2 produced (mmol)/time (h)/working volume of the photobioreactor (L) (Eq. 3.1)

The hydrogen yield was determined as a ratio of mass of hydrogen produced per mass of acetate utilized. Substrate conversion efficiency (for acetate) was calculated as a ratio of moles of hydrogen produced per stoichiometric number of moles of hydrogen which would be produced from full use of initial substrates. Light conversion efficiency, η, was calculated as a ratio of the obtained total energy of hydrogen to the total energy input to the photobioreactor by light radiation and defined as Equation 3.2:

$$\eta\ (\%) = (33.6 * \rho * V) * 100 / (I * A * t) \quad \text{(Eq. 3.2)}$$

where, Constant number 33.6 is the energy density of hydrogen gas in Watt·h/g, ρ is the density of hydrogen in g/L, V is the volume of hydrogen produced in L, I is the light intensity in W/m^2, A is the irradiated area in m^2 and t is the duration of hydrogen production in hours. Equations and examples used in photofermentation sets are given in Appendix C.

3.2.2. Response Surface Methodology (RSM) for Design and Analysis of Set-1

Standard experimental design, which investigates the effects of a variety of variables on a specific objective (a response – such as hydrogen production rate), generally depends on only one factor at a time approach (Wang and Wan, 2009). However, this standard approach for experimental design misses some effects of the interaction of multiple variables which can change the magnitude of the objective (Wang and Wan, 2009). Moreover, standard experimental design requires multiple experiments to cover several levels of a variable, so it is a time-consuming operation (Xing et al., 2011). A statistical design approach such as RSM, on the other hand, provides a statistical impression of results via reducing the number of experiments and involving the interactions of the variables in the resulting objective (Liu et al., 2011).

In order to apply RSM, firstly, independent variables (for example, substrate concentration (S), VSS concentration (X_o), etc.) which can have effect on a response, such as hydrogen production rate, are chosen (in the light of preliminary studies or literature survey). After that, the maximum and minimum values (a range) for each independent variables (parameters) are introduced to RSM (for example 20 and 60 mM HAc, for the variable S). These selected ranges for each independent variable are based on the preliminary results or information of previous studies in the literature. There are several modeling methods (such as central composite design, Box-Behnken design, etc.) in RSM tool. These models determine the levels (values) of each independent variable tested in the defined range. In this thesis, Box-Behnken design method was used because it is a commonly used method when the reactor set ups are to be performed with less design points than other methods (Wang and Wan, 2008). The RSM – Box-Behnken design method develops a mathematical model, which defines the relationships between the response and the independent variables. In this thesis study, independent variables were selected as the initial substrate concentration, initial VSS concentration and light intensity. In other words,

to develop the model, three independent variables (each one defined with maximum and minimum value) were used. It was specified that each independent variable combination should be performed in two replicas. Accordingly, the design method set 30 design points (30 reactors) including replicas or 13 different reactor types with different independent variable combinations.

Set-1 was designed by RSM-Box-Behnken design method. The factors and levels used in the design model of Set-1 are given in Table 3.1. MiniTab Software (MiniTab Pro (16.1.0.0)) was used to employ RSM. Using RSM, the effects of the independent variables (i.e., the substrate (S), VSS (X_o) and the light intensity (I)) on the response (hydrogen production rate) were evaluated. Experimental results were used to develop favorable models and 3-D graphs. In order to examine the validity of this model, Analysis of Variance (ANOVA) was performed. ANOVA results were further modified to improve the model and better define the relationship between the response and the variables of concern. When ANOVA indicated the insignificance of a specific variable or interaction of variables, it was eliminated from the model. P-value of larger than 0.05 in the ANOVA results indicates the insignificance of a variable. A change in insignificance variable does not considerably affect the value of the response for studied range. The surface and contour plots were drawn for defined responses. Then the optimum independent variable points, which maximize the responses, were calculated using the response optimization tool of RSM.

Table 3.1 Factors and levels used in Box-Behnken Design Method

Independent variables	Symbols	Ranges and levels		
		-1	0	1
Initial VSS concentration (X_o)	X_0	0.05	0.2	0.35
Initial substrate concentration (S)	X_1	20	40	60
Light intensity (I)	X_2	100	200	300

Hydrogen yield, light conversion efficiency and substrate conversion efficiency were also selected as responses. ANOVA and optimization tests for hydrogen yield and conversion efficiencies were also performed using RSM. However, the ANOVA analysis results showed that the model could not be developed for hydrogen yield and conversion efficiencies. The hydrogen yield and conversion efficiencies cannot be explained by S, X_o and I variables and (or) their interactions; and optimization studies were not succesful. For this reason, RSM and ANOVA analyses and results of these mentioned responses were not given in the Results and Discussion Section. Only the hydrogen production rate related results were discussed.

3.3. Experimental Procedure

3.3.1. Set-1: Investigation of the Effects of Initial Substrate Concentration, Initial VSS Concentration and Light Intensity

The aim of Set-1 was to investigate the effect of three parameters, namely, initial substrate concentration (S), initial VSS concentration (X_o, biomass) and the light intensity (I) on photofermentation and their combined effect on hydrogen production by RSM – Box-Behnken Design Method. This study also aimed to optimize three operational conditions of the substrate, the VSS and the light intensity leading to the maximization of hydrogen production in a single stage. The optimum S/X_o ratio would be also determined via this study.

Acetate (of 20 mM, 40 mM and 60 mM) was used as substrate in this study. In the view of the literature studies, it was observed that frequently studied acetate concentrations were generally in the range of 10-80 mM (Eroğlu et al., 2008; Özgür et al., 2010; Androga et al., 2011 Lo et al., 2011). Acetate concentration of 168 mM was even studied (Asada et al., 2008). The optimum acetate concentrations recommended for *R. Capsulatus* is 30 mM (Özgür et al., 2010), 22-42 mM for another *Rhodobacter* culture (Asada et al., 2008) and 22 mM for

Rhodopseudomonas species (Barbosa et al., 2001). Therefore, the limit values for substrate concentration interval were set as 20 and 60 mM in this study.

As microorganism concentrations, *Rhodobacter capsulatus* cultures were inoculated in different amounts to achieve 0.05 g VSS/L, 0.2 g VSS/L and 0.35 g VSS/L in the reactors. OD analyses and VSS-OD calibration curve (Appendix A) were used in order to determine the amount of bacteria to be innoculated and the concentration of VSS in the reactors.

The light intensity is one of the most important parameters in hydrogen production with PNS bacteria (Sevinç et al., 2012). Sevinç et al. (2012) studied at light intensities between 1500 lux and 5000 lux, and stated that this range was suitable for hydrogen production for PNS bacteria. Therefore, in this study, three values were studied in the light intensity range of 1500-5000 lux and it was aimed to determine the light intensity that ideally influence the hydrogen production rate and yield. Thus, illumination was provided to have the intensity value of 1500 lux (100 W/m^2), 3000 lux (200 W/m^2) and 4500 lux (300 W/m^2).

Experiments were performed in 30 batch reactors with effective volume of 50 mL and total volume of 55 mL. Biebl and Pfennig medium was used as hydrogen producing medium (Biebl and Pfennig, 1981). Being different from the growth medium (Section 3.1), this medium contained 20 mM, 40 mM or 60 mM of acetate, and 1.33 mM, 2.67 mM or 4 mM of glutamate concentrations, respectively. Thus, carbon to nitrogen (C/N) ratio of all reactors were kept constant at 15, which is recommended in literature to be between 13-35 (Savasturk et al., 2018).

Experiments were carried out in three different incubators to provide three different light intensities mentioned above. Eight of the 30 reactors were incubated at a light intensity of 1500 lux (Fig 3.2 c-d), 8 of the 30 reactors at a light intensity of 4500 lux (Fig 3.2 b) and 14 of the 30 reactors at a light intensity of 3000 lux (Fig 3.2 a). As mentioned previously in Section 3.2.2, RSM reactor types and number of replicates of each type were designed by RSM – Box-Behnken Design Method. The

factors and levels determined by the RSM – Box-Behnken Design Method are already given in Table 3.1 (Section 3.2.2). According to this method, 6 replicate reactors were operated for the middle points of 3 variables (S=40 mM acetate, X_o=0.2 g VSS/L, I=3000 lux). Other reactor types (reactors' variants with different compositions of three variables) were operated in 2 replicates. The characteristics of the reactors conducted in the experiments are given in Table 3.2.

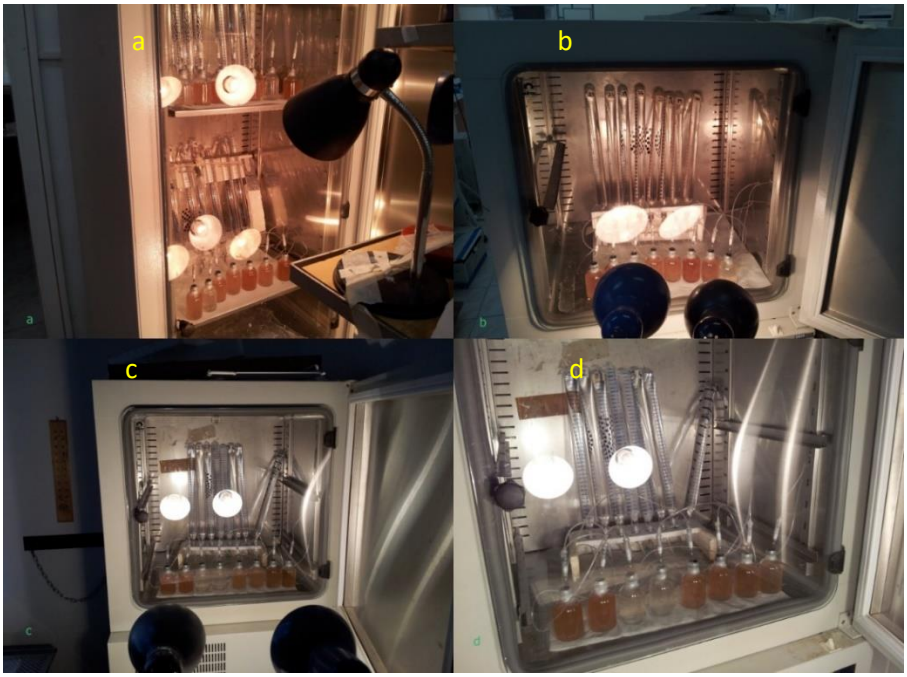

Figure 3.2 Set-up used in batch photofermentation reactors in Set-1, (a) in 3000 lux light intensity, (b) in 4500 lux light intensity, (c) in 1500 lux light intensity, (d) in 1500 lux light intensity

Table 3.2 The characteristics of the batch photofermentation reactors run in Set-1

Reactor No.	VSS Concentrations, X_o (g VSS/L)	Substrate, S (mM acetate)	Illumination, I (lux)	Calculated S/X_o, (g COD/g VSS)
1	0.35	40	1500	8.4
2	0.35	40	1500	8.4
3	0.05	40	1500	58.9
4	0.05	40	1500	58.9
5	0.2	20	1500	7.4
6	0.2	60	1500	22.1
7	0.2	60	1500	22.1
8	0.2	20	1500	7.4
9	0.05	20	3000	29.4
10	0.2	40	3000	14.7
11	0.35	60	3000	12.6
12	0.05	60	3000	88.4
13	0.2	40	3000	14.7
14	0.05	20	3000	29.4
15	0.35	20	3000	4.2
16	0.2	40	3000	14.7
17	0.05	60	3000	88.4
18	0.2	40	3000	14.7
19	0.2	40	3000	14.7
20	0.35	60	3000	12.6
21	0.2	40	3000	14.7
22	0.35	20	3000	4.2
23	0.2	60	4500	22.1
24	0.35	40	4500	8.4
25	0.05	40	4500	58.9
26	0.2	20	4500	7.4
27	0.2	20	4500	7.4
28	0.35	40	4500	8.4
29	0.2	60	4500	22.1
30	0.05	40	4500	58.9

After inoculation, the reactors were taped with rubber stoppers and the headspace of all the reactors were flushed with oxygen-free argon gas for 4-5 minutes. The reactors were then incubated at 30°C. During the incubation period, 2.5 mL liquid samples were taken regularly from reactors every day. One mL of samples were used for pH and OD analyses and 1.5 mL of samples were used for VFA analyses. As seen in Figure 3.2, the gas produced in each reactor was collected in the columns separately connected to each reactor. The composition of the gas produced in reactors was measured from the gas samples taken from the headspace of the reactors.

3.3.2. Set-2: Photofermentation as a Second-stage of a Two-stage System

The aim of Set-2 was to study photofermentation as a second-stage of a two-stage dark fermentation and photofermentation system. The photofermentative hydrogen production yields obtained in this two-stage dark fermentation and photofermentation, which are frequently encountered in literature studies, provide a preliminary knowledge and comparison for the future three-stage system experiments.

In this study, photofermentation reactors were conducted with the effluents of a dark fermentative Sequencing Batch Reactor (SBR). Dark fermentative SBR was studied by Ekin Güneş Tunçay in Environmental Engineering Department of Middle East Technical University, Ankara, Turkey (Tunçay, 2015). In this dark fermentative SBR, sucrose was used as substrate; thus the effluent of dark fermentation SBR was fermented sucrose. Dark fermentative SBR was run at different operational conditions, so, two effluent types, namely, Influent-1 and Influent-2 were withdrawn from the SBR. Both Influent-1 and Influent-2 were filtered with 0.45 μm pore size filters (Millipore) after withdrawal from dark fermentation SBR and both of them were kept at -20°C until their to use as substrates of photofermentation batch reactors in this study (Set-2). Table 3.3 indicates the characteristics of the filtered Influent-1 and Influent-2 used in Set-2 batch reactors.It can be seen that both

Influent-1 and Influent-2 had similar characteristics with the exception of higher COD and slightly lower total VFA content of the former. According to Table 3.3, the effluents of dark fermentative SBR contained high concentrations of acetic acid and butyric acid compared to other VFA types and total VFA concentration majorly consisted of these two types. Because the optimum acetate concentration recomended for *Rhodobacter capsulatus* is 30 mM (Özgür et al., 2010), and 21-42 mM for another *Rhodobacter sphaeroides* (Asada et al., 2008) and 22 mM for *Rhodopseudomonas* species (Barbosa et al., 2001). Thus, it can be said that 21 mM acetic acid concentration in Influent-1 and Influent-2 was suitable for photofermentation reactors and the effluent of dark fermentative SBR was used in batch photofermentation reactors. Total Ammonia Nitrogen (TAN) was 8 mg/L (0.5 mM). Akköse et al. (2009) stated that hydrogen production was not observed when the concentration of ammonium ion was greater than 2 mM (36 mg/L). This indicated that the effluent of dark fermentative SBR would not cause any toxic effect for PNS bacteria regarding its TAN concentration and it could be directly used in photofermentation reactors without any need of pretreatment.

Table 3.3 The characteristics of the filtered Influent-1 and Influent-2 used in batch photofermentation reactors of Set-2

Parameter	**Substrate type of Set-2**	
	Influent-1	Influent-2
sCOD (mg/L)	10750±254	9000±312
TAN (mg/L)	8±0.2	14±0.8
Alkalinity (mg/L $CaCO_3$)	2122± 68	2057±93
pH	6.2	6.3
Acetic acid (mM)	21	21
Propionic acid (mM)	4	2
Butyric acid (mM)	17	8
Iso-butyric acid (mM)	1	2
Total VFA (mM HAc)	37	30

Two batch reactor types, each conducted in three replicates, were conducted with either Influent-1 or Influent-2. The total and effective volume of reactors were 55 and 50 mL, respectively. Homogeneously mixed and filtered Influents were autoclaved and each reactor was filled with 50% diluted influents (approximately 45 mL of 50% diluted influents were fed to the reactors). The aim of this dilution was to decrease the high COD concentration and reduce the possible inhibition effects originating from organic matters except VFA. According to the results of Set-1 mentioned in Section 4.1, S/X_o ratio leading to the highest hydrogen production rate was found as 9.4 g COD/g VSS. Thus, *Rhodobacter capsulatus* culture was inoculated to the reactors by satisfying 9.4 g COD/g VSS (8.3 g COD_{HAc}/g VSS) substrate to biomass (S/X_o) ratio. Moreover, according to the results of Set-1, the light intensity satisfying the highest hydrogen production rate was observed as 3995 lux and thus, reactors in Set-2 were illuminated at a light intensity of 3955 lux.

After inoculation, the reactors were taped with rubber stoppers and the headspace of all the reactors were flushed with oxygen-free argon gas for 4-5 minutes. The reactors were then incubated at 30°C. During the incubation period, 2.5 mL liquid samples were taken regularly from reactors every day. One mL of liquid samples were used for pH and OD analysis and 1.5 mL of samples were used for VFA analyses. Gas produced in each reactor was collected in the columns connected to each reactor separately. The composition of the gas produced in the reactors was measured with gas samples taken from the headspace of the reactors.

3.3.3. Set-3: Photofermentation as a Third-stage of a Three-stage System

The aim of Set-3 was to investigate photofermentation as a third-stage of a three-stage system composed of dark fermentation, methanogenesis and photofermentation processes. In other words, Set-3 was conducted to investigate the photofermentative hydrogen production from the effluents of a methanogenesis reactor. Both the photofermentative hydrogen production yields and total energy

yields obtained in this three-stage system, which is not studied so far in literature, provide a preliminary knowledge for future three-stage systems and comparison for two-stage systems frequently encountered in literature studies.

In Set-3, batch photofermentation reactors were conducted with the effluents of methanogenesis process operated in SBR mode. Methanogenesis SBR was studied by Engin Koç in Environmental Engineering Department of Middle East Technical University, Ankara, Turkey (Koç, 2015). In this methanogenesis SBR, the effluents of dark fermentation SBR (Tunçay, 2015) were used as influents. Thus, this is a novel three-stage system composed of dark fermentation, methanogenesis and photofermentation in sequence.

Six differrent influents, namely, Influent-A, Influent-B, Influent-C, Influent-D, Influent-E and Influent-F, were used in the experiments in Set-3. This is due to the fact that methanogenesis SBR was operated at six different periods with different hydraulic retention time (HRT) and solid retention time (SRT) combinations. The characteristics of these six influents, which were withdrawn from the methanogenesis SBR at six different HRT-SRT combinations and used as substrate in Set-3, are given in Table 3.4. All influents were filtered via 0.45 μm pore size filters (Millipore) after withdrawal from methanogenesis SBR. As shown in Table 3.4, TAN concentrations of the influents were between 90-162 mg/L NH_4^+-N (116-208 mg/L NH_4). It has been reported in literature that hydrogen production in photofermentation reactors ceased when ammonium ion concentration was equal to or greater than 2 mM (36 mg/L NH_4^+ or 28 mg/L NH_4-N) (Akköse et al., 2009). Therefore, it was decided to remove ammonia from the effluents of methanogenesis SBR, before using them as influents of photofermentation reactors, with a preliminary treatment. Among ammonia removal methods, two methods were initially selected to investigate the ammonium removal from the effluents, namely, ammonia stripping and zeolite (clinoptilolite) adsorption. Preliminary experiments were performed for both methods. These two methods, the experiment performed and the results were explained in Appendix D in detail. Comparing the results of

these two preliminary studies/methods, ammonia stripping method was chosen for achieving higher removal efficiencies and applied to remove ammonia from influents. Ammonia concentrations of methanogenesis SBR effluents and the influents of photofermentation after applying stripping method are presented in Table 3.4. As seen in Table 3.4, the ammonia concentrations of all the influents decreased to the levels which are well below the potential inhibitory level of 28 mg/L NH_4-N (Akköse et al., 2009).

The VFA contents of only two influents among six influents appeared to be sufficient (22 mM and 16 mM for Influent-D and Influent-E, respectively) for photofermentation. For each of these two Influents, 3 replicate batch photofermentation reactors were conducted. For the remaining 4 Influents, one reactor was conducted for each influent type in order to observe the potential bacterial growth and hydrogen production, if any. Blank reactors containing only the influent, and control reactors containing only the bacterial culture were also conducted. The total and effective volume of reactors were 55 and 50 mL, respectively. Each reactor was filled with autoclaved and homogeneously mixed and filtered Influents. S/X_o ratio of Set-3 was set as 9.4 g COD/g VSS, regarding the results of Set-1. Accordingly, *Rhodobacter capsulatus* culture was inoculated to the reactors by satisfying S/X_o of 9.4 g COD/g VSS (8.3 g COD_{HAc}/g VSS). The reactors were illuminated at a light intensity of 3955 lux according to the results of Set-1 (Section 4.1).

After inoculation, the reactors were taped with rubber stoppers and the headspace of all the reactors were flushed with oxygen-free argon gas for 4-5 minutes. The reactors were then incubated at 30°C. During the incubation period, 2.5 mL liquid samples were taken regularly from reactors every day. One mL of liquid samples were used for pH and OD analysis and 1.5 mL of samples were used for VFA analyses. Gas produced in each reactor was collected in the columns connected to each reactor separately. The composition of the gas produced in the reactors was measured with gas samples taken from the headspace of the reactors.

Table 3.4 The characteristics of six influents used in batch photofermentation reactors of Set-3.

Parameters	Effluents withdrawn from methanogenesis SBR					
	Influent-A	Influent-B	Influent-C	Influent-D	Influent-E	Influent-F
tVFA (mM HAc)	3.9±2.4	2.7±1.1	2.6±0.8	21.7±4.1	16.4±1.7	2.6±0.8
sCOD (mg/L)	1345±65	1220±55	1100±40	2625±45	1605±40	1215±75
TAN (mg/L NH_4-N)[a]	100.8	89.6	89.6	106.4	112	162.4
TAN (mg/L NH_4-N)[b]	12.5	14	12.3	13.8	11.6	18.2
pH	7.4	7.5	7.8	7.6	7.6	7.5

[a] TAN concentrations of the effluents of methanogenesis SBR

[b] TAN concentrations after applying ammonia stripping method

3.3.4. Set-4: Semi-batch Reactor Experiments

The aim of Set-4 was to investigate the optimum HRT leading to the highest photofermentative hydrogen production rate in semi-batch reactors. In this study, reactors were run with the effluents of methanogenesis SBR operated at different operational conditions and fed with the effluents of dark fermentative SBR. In other words, reactors in Set-4 were third-stage of a three-stage system as in batch reactors of Set-3. Thus, the results of Set-4 and Set-3 were also used to compare the effect of operation mode (batch or semi-batch) in photofermentative hydrogen production.

Three HRT values of 2, 4 and 6 days were studied. As mentioned previously for Set-3 (Section 3.4.3), the VFA contents of only the two of the influents among six were sufficient for photofermentation (22 mM and 16 mM for Influent-D and Influent-E, respectively). Moreover, according to the results of Set-3 mentioned in Section 4.3, hydrogen production was only observed in the reactors fed either Influent-D or Influent-E. In the light of these information, Influent-D and Influent-E were used as influents in photofermentation reactors of Set-4. The characteristics of Influent-D

and Influent-E were given in Table 3.5. Both Influent-D and Influent-E were filtered via 0.45 μm pore size filters (Millipore) after withdrawal from methanogenesis SBR and both of them were stored at -20°C until their use as substrates in Set-4. Prior to the feeding to the reactors, air stripping method (Appendix D) was applied to each 500 mL of Influents taken from -20°C to reduce ammonia concentrations. This procedure was repeated to each 500 mL Influents.

In this study, 2 replicate semi-batch reactors were run for each HRT value studied. In other words, 12 semi-batch photofermentation reactors were conducted totally for 3 different HRT values and two influent types. The characteristics of reactors' set up are given in Table 3.6. The total and effective volume of reactors were 55 and 50 mL, respectively. Each reactor was fed with autoclaved and homogeneously mixed and filtered influents on daily basis. According to the results of Set-1 mentioned in Section 4.1, S/X_o ratio leading to the highest hydrogen production rate was found as 9.4 g COD/g VSS and it was used in Set-4. *Rhodobacter capsulatus* culture was inoculated to the reactors by satisfying S/X_o ratio of 9.4 g COD/g VSS (8.3 g COD_{HAc}/g VSS). The reactors were illuminated at a light intensity of 3955 lux according to the results of Set-1 (Section 4.1).

Table 3.5 The characteristics of Influent-D and Influent-E used in semi-batch photofermentation reactors of Set-4

Parameters	Effluents withdrawn from methanogenesis SBR	
	Influent-D	Influent-E
Total VFA (mM HAc)	21.7±4.1	16.4±1.7
sCOD (g/L)	2625±45	1605±40
TAN (mg/L NH_4-N)[a]	106.4	112
TAN (mg/L NH_4-N)[b]	6.8-15.4	5.6-14.9
pH	7.6	7.6
[a] TAN concentrations of the effluents of methanogenesis SBR [b] TAN concentrations range after applying ammonia stripping method to influents stored at -20°C in volumes of 500 mL		

Table 3.6 The characteristics of reactors in Set-4

Reactor No	Influent type	HRT (day)		Reactor No	Influent type	HRT (day)
1	Influent-D	2		7	Influent-E	2
2	Influent-D	2		8	Influent-E	2
3	Influent-D	4		9	Influent-E	4
4	Influent-D	4		10	Influent-E	4
5	Influent-D	6		11	Influent-E	6
6	Influent-D	6		12	Influent-E	6

After inoculation, the reactors were taped with rubber stoppers and the headspace of all the reactors were flushed with oxygen-free argon gas for 4-5 minutes. The reactors were then incubated at 30°C. During the incubation period, 2.5 mL liquid samples were taken regularly from reactors every day. One mL of liquid samples were used for pH and OD analysis and 1.5 mL of samples were used for VFA analyses. Gas produced in each reactor was collected in the columns connected to each reactor separately. The composition of the gas produced in the reactors was measured with gas samples taken from the headspace of the reactors.

CHAPTER 4

RESULTS AND DISCUSSION

The results of batch reactor studies of Set-1, Set-2, Set-3; semi-batch reactor study of Set-4 and the comparison of batch to semi-batch reactors in photofermentation efficiencies are given in this section.

4.1. Results of Set-1: Determination of the effects of Initial Substrate and Biomass Concentrations and Light Intensity Values on photofermentation

Set-1 was conducted to investigate the effect of three parameters, namely, substrate (S), the biomass (X_o) and the light intensity (I) on photofermentation and their combined effect on hydrogen production by RSM. The results of this study optimized three parameters of the substrate, the biomass and the light intensity leading to the maximization of hydrogen production in a single stage. The optimum S/X_o ratio was also determined as a result of this study.

Because reactor types and contents were conducted by RSM, trying to interpret the results obtained from the reactors with other methods apart from methods used for RSM does not reflect the truths. In other words, trying to find the optimum conditions by comparing the reactors directly with the raw data, especially when there are three variables, may not reflect the results correctly. However, hydrogen production rates, hydrogen production yields, substrate conversion efficiencies and light conversion efficiencies calculated for each reactor were compared in order to get an opinion. To this purpose, the results of Set-1 were represented in Table 4.1 by taking the mean values of the reactor types conducted with 2 and 6 replicas. The detailed results were given in Table E.1 and Table E.2 (Appendix E).

As it is seen in Table 4.1, hydrogen production rates (productivities) changed in the range of 0.27-0.91 mmol H_2/L.h. The highest hydrogen production rate of 0.91 mmol H_2/L.h was obtained in the reactors where the initial substrate, biomass (*Rhodobacter capsulatus)* and light intensity values were 20 mM, 0.2 g VSS/L and 4500 lux, respectively. Next highest hydrogen production rates were obtained as 0.88 mmol H_2/L.h in the reactors where S= 40 mM, X_o= 0.35 g VSS/L and I= 4500 lux and as 0.87 mmol H_2/L.h in the reactors where S= 40 mM, X_o= 0.2 g VSS/L and I=3000 lux. The results of this study were supported by related literature (Mars et al., 2010; Özgür et al., 2010). In a photofermentation study using *Rhodobacter capsulatus*, the highest hydrogen production rate was obtained as 1.10 mmol H_2/L.h at 29 mM initial acetate concentration (Mars et al., 2010). Moreover, in study of Özgür et al. (2010) using different acetate concentrations (10 mM, 20 mM, 30 mM, 40 mM, 50 mM) of same medium (Biebl and Pfennig medium) and *Rhodobacter capsulatus*, the highest hydrogen production rate (1.17 mmol H_2/L.h) was observed at 40 mM acetate concentration, and the highest substrate conversion efficiency (%72) was observed at 30 mM acetate concentration (Özgür et al., 2010). It can be seen that the highest hydrogen production rates obtained in this study are close to the highest hydrogen production rate Mars et al. (2010) and Özgür et al. (2010) found. In the later sections of this study, RSM optimization analyses were conducted and the acetate concentration providing the highest hydrogen production rate was found as 35.35 mM. Thus, literature data support the results of this study on the basis of optimum acetate concentration (Mars et al., 2010; Özgür et al., 2010).

As mentioned previously, according to the experimental data, the highest hydrogen production rate was 0.91 mmol H_2 L.h (20.4 mL H_2/L.h) where S= 20 mM acetate, X_o= 0.2 g VSS/L and I= 4500 lux. The hydrogen yield obtained at these conditions was 0.09 g H_2/g acetate (2.7 mol H_2/mol Acetate, 41.5 mmol H_2/g COD_{HAc}). The second highest substrate conversion efficiency was again obtained at these conditions with 68.1%. On the other hand, the highest hydrogen yield was obtained in the reactors with the initial acetate concentration, initial biomass concentration and light intensity values of 20 mM acetate, 0.35 g VSS/L and 3000 lux,

respectively. The highest hydrogen yield obtained was 0.11 g H_2/g acetate (3.3 mol H_2/mol acetate, 51.6 mmol H_2/g COD_{HAc}). The hydrogen production rate obtained under these conditions was 0.86 mmol H_2/L.h (19.3 mL H_2/L.h). The highest substrate conversion efficiency was achieved in this reactor with 83%.

Table 4.1 The hydrogen production performance of photobioreactors in Set-1

X_o (g VSS/ L)	**S (HAc, mM)**	**I (W/m^2)**	**H_2 production rate (mmol H_2/L.h)**	**Substrate conv. efficiency (%)**	**H_2 yield (g H_2/g acetate)**	**Light conv. efficiency (%)**
0.35	40	100	0.27	34.9	0.05	0.41
0.05	40	100	0.32	37.4	0.05	0.40
0.2	20	100	0.37	53.3	0.07	0.43
0.2	60	100	0. 32	30.0	0.04	0.36
0.05	20	200	0.42	42.9	0.06	0.16
0.2*	40*	200*	0.87±0.05	57.1±4.4	0.08±0.01	0.31±0.06
0.35	60	200	0.73	49.4	0.07	0.35
0.05	60	200	0.28	18.2	0.02	0.11
0.35	20	200	0.86	83.0	0.11	0.39
0.2	60	300	0.68	36.6	0.05	0.17
0.35	40	300	0.88	56.5	0.08	0.27
0.05	40	300	0.60	34.3	0.05	0.14
0.2	20	300	0.91	68.1	0.09	0.22

* The middle point, corresponding to 40 mM acetate, 0.2 g VSS/L bacterial concentration and 200 W/m^2 light intensity combination, was conducted in six replicates, the other combinations were replicated twice. The values given are the average of the result of replicated reactors.

Considering the total hydrogen gas produced, the maximum hydrogen production was achieved in reactors which had 60 mM initial acetate concentration, 0.35 g VSS/L initial biomass concentration and 3000 lux illumination (Figure 4.1). The second highest hydrogen production was achieved in the reactors which had 40 mM initial substrate concentration, 0.20 g VSS/L initial biomass concentration and 3000 lux illumination; 60 mM initial substrate concentration, 0.20 g VSS/L initial biomass concentration and 4500 lux illumination and 40 mM initial substrate concentration, 0.35 g VSS/L initial biomass concentration and 4500 lux illumination (Figure 4.1). On the other hand, the minimum hydrogen production was observed in

the reactors which had 20 mM initial acetate concentration, 0.05 g VSS/L initial biomass concentration and 3000 lux illumination. As seen in Figure 4.1, there is a big difference (105 mL) between maximum and minimum hydrogen production amounts. Yet, it is not possible to conclude that the initial substrate or VSS concentration was the main parameter for this high difference in volume of hydrogen produced. Actually, it can be seen from Table 4.1 and Figure 4.1 that there is an interaction among initial acetate concentration, initial biomass concentration and initial light intensity values. Therefore, this interaction, i.e. the combined effect of the three variables on hydrogen production, could not be clarified directly from Table 4.1 or Figure 4.1. In order to get the optimum parameters (combination of variables) leading to the maximum hydrogen production and rate, and to better analyze the combined effects RSM results should be taken into consideration.

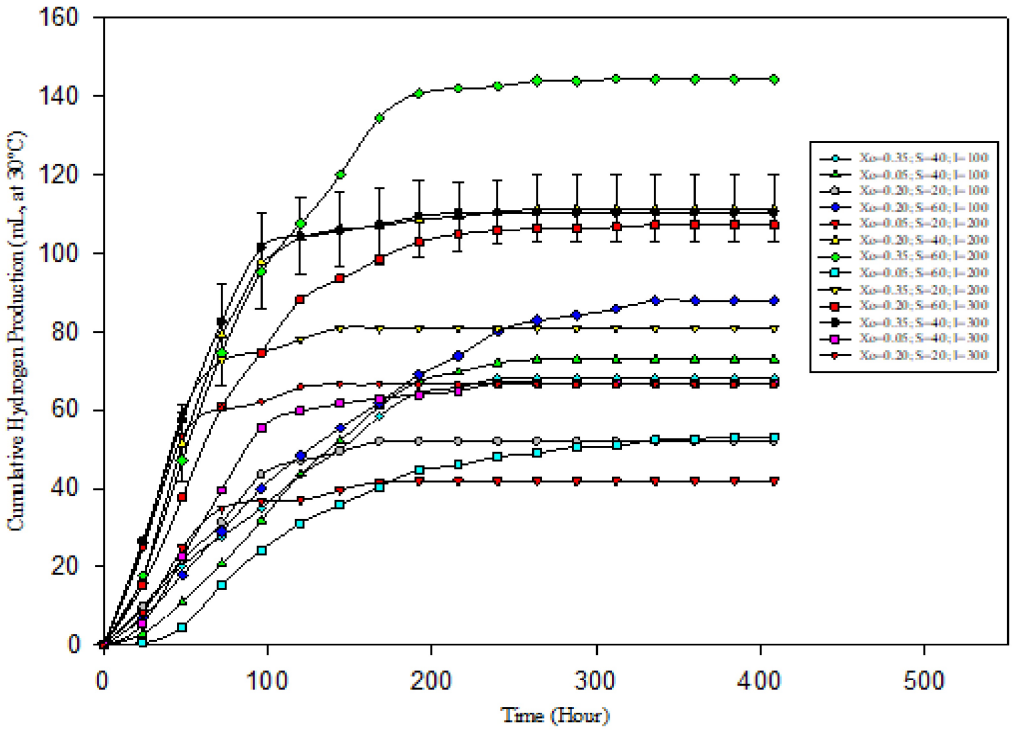

Figure 4.1 Total hydrogen gas production observed in Set-1 (30°C, acetate)

In the GC analysis, it was determined that 92% of the headspace gas in the reactors was hydrogen gas. Theoratically, *Rhodobacter capsulatus* is expected to produce 4 mol H_2 gas and 2 mol CO_2 gas from 1 mol acetic acid (Equation 4.1). The fact that the measured H_2 fraction was higher than the theoretical value can be explained by the carbon dioxide-carbonic acid balance. During the incubation, the pH values in the reactors varied between 6.5-8. As it is known, when CO_2 is dissolved in water, bicarbonate (HCO_3^-) is the dominant product in the range of pH 6.5-8 (Kirby and Cravotta III, 2005). Thereby, the percentage of hydrogen in the headspace gas was observed as 92% because the majority of CO_2 gas produced during the photofermentation period was present as bicarbonate in the reactor.

$$CH_3COOH + 2H_20 + \text{‘luminous energy’} \rightarrow 4H_2 + 2CO_2 \qquad \text{(Equation 4.1)}$$

4.1.1. Results of RSM Study for Set-1

After applying RSM to the results obtained on the basis of the hydrogen production rate using MiniTab and performing the corresponding sequential ANOVA analysis, the following Equation 4.2 was obtained.

$$y_{coded} = 0.92833 + 0.14377\ x_0 - 0.06750\ x_1 + 0.22127\ x_2 - 0.20669\ x_0^2 - 0.14914\ x_1^2 - 0.20919\ x_2^2 + 0.08995\ x_0\ x_2 \qquad \text{(Equation 4.2)}$$

where;

x_0= Initial biomass concentration, X_o

x_1= Initial acetate concentration, S

x_2= Light intensity, I

The symbols and intervals used in Box-Behnken design was already shown in Table 3.1 (Section 3.2.2). Equation 4.2 displayed the coded regression model, which related the hydrogen production rate by Rhodobacter capsulatus DSM 1710 to initial substrate concentration, initial biomass concentration and the light intensity. In order to test the significance of the fit of the second order polynomial Equation 4.2 to the experimental data, an ANOVA analysis was performed. The results of the ANOVA for the regression model were shown in Table 4.2. The F-value of 36.5 indicated that the model was significant, with a $p < 0.01\%$. Because the low p-values correspond to a high statistical significance of the variables, p-values less than 0.05 were accepted to be significant. The linear (X_0, X_1 and X_2), quadratic (X_0^2, X_1^2 and X_2^2) and the interaction (X_0X_2) effects of initial substrate concentration, initial biomass concentration and light intensity on the model were found to be significant ($p < 0.05$). The lack-of-fit F-value of 7.56, which corresponds to a p-value of 0.001, indicates that the lack of fit is significant. This means that the model does not explain the data well. However, the measure of the goodness of fit ($R^2 = 0.9207$) was close to 1, which shows a good agreement between predicted and observed values.

When optimization analysis was applied for hydrogen production rate equation (Equation 4.2), the optimum values at which the highest hydrogen production rate could be obtained in the range of values studied were found as 35.35 mM initial substrate (acetate) concentration, 0.27 g VSS/L initial biomass concentration and 3955 lux (263.6 W/m^2) light intensity. When these optimum values were used, the estimated response value (hydrogen production rate) was calculated as 1.04 mmol H_2/L.h. Because Mathcad did not make a significance comparison between the variables, the optimum variable values of the Equation 4.2 were not reinvestigated using Mathcad. It was considered that the results of MiniTab, in which the interactive statistical analyses were performed, were sufficient.

Table 4.2 ANOVA results for hydrogen production rate by *R.capsulatus* DSM 1710

Factors	**Df***	**Ss****	**Mean squares**	**F-value**	**p-value**
Model	7	1.95131	0.278758	36.5	<0.0001
X_0	1	0.33074	0.33074	43.3	<0.0001
X_1	1	0.07290	0.07290	9.6	0.005
X_2	1	0.78340	0.78340	102.6	<0.0001
X_0^2	1	0.31548	0.31548	41.3	<0.0001
X_1^2	1	0.16426	0.16426	21.5	<0.0001
X_2^2	1	0.32316	0.32316	42.3	<0.0001
X_0 X_2	1	0.06473	0.06473	8.5	0.008
Residual error	22	0.16797	0.007635		
Lack-of-fit	5	0,11588	0.023177	7.56	0.001
Pure error	17	0.05208	0.003064		
Total	29	2.11928			

* Degrees of freedom

** Sum of squares

Figure 4.2 shows the three-dimensional response surface and contour plots for the hydrogen production rate as a function of initial substrate concentration, initial biomass concentration and light intensity, which was formulated as Equation 4.2. As seen from the response surface plot (Figure 4.2 (a), (b), (c)), hydrogen production rate was observed to increase as the initial substrate and biomass concentrations and light intensity increase. After reaching a peak, hydrogen production rate decreases when the initial substrate and biomass concentrations and light intensity continue to increase. At constant substrate concentrations, light intensity highly affects the rate of hydrogen production. The hydrogen production rate increases sharply as light intensity increases (Figure 4.2 (b)). Furthermore, at high initial biomass concentrations, light intensity affects the hydrogen production rate more sharply than at low initial biomass concentrations (Figure 4.2 (e)). Both

surface plots (Figure 4.2 (d), (e)) exhibited steeper slopes on light intensity axes. The surface plots (Figure 4.2 (d), (e), (f)) revealed that the hydrogen production rate was more sensitive to the light intensity changes than those of initial biomass and substrate concentrations. Both Figure 4.2 and Equation 4.2 showed that these three variables significantly affected the hydrogen production rate. The interaction between initial biomass and light intensity was also important as each parameter separately.

As it can be seen in Figure 4.2 (c) and (f), the highest hydrogen production rate was observed in the area where the initial biomass (X_o) was between 0.20-0.30 g VSS/L and the initial acetate concentration (S) was between 30-40 mM acetate. When analyzing the plots and comparing initial biomass-light intensity binomial (Figure 4.2 (b), (e)), it can be seen that the areas, where the hydrogen production rate was high, corresponded to the ranges between 0.20-0.30 g VSS/L for the initial biomass concentration and between 3000-4500 lux (250-300 W/m^2). When comparing the plots of acetate concentration-light intensity binomial (Figure 4.2 (a), (d)), it can be said that the hydrogen production rate was high in the region where the light intensity was high in the range of 3000-4500 lux (200-300 W/m^2) and the initial substrate concentration was in the range of 30-40 mM acetate. The optimum values given by RSM (Equation 4.2) for maximum hydrogen production rate of 1.04 mmol H_2/L.h match up with the graphs given in Figure 4.2.

As stated previously, the optimum values given by RSM optimization analyses were found as 35.35 mM initial substrate (acetate) concentration, 0.27 g VSS/L initial biomass concentration and 3955 lux (263.6 W/m^2) light intensity. Taking into account the optimum biomass concentration and the optimum substrate concentration, S/X_o ratio leading to the highest hydrogen production rate was calculated as 9.4 g COD/g VSS (8.3 g COD_{HAc}/g VSS, 7.7 g acetate/g VSS). As far as it is known, this S/X_o result had been obtained for the first time in photofermentation studies. The optimum light intensity value of 263.6 W/m^2 obtained was slightly close to the optimum value (287 W/m^2) reported by Androga

et al. (2014). Androga et al. (2014) investigated the effect of temperature and light intensity on photofermentative hydrogen production with 3^k general full factorial design. Optimum light intensity leading to the highest hydrogen production rate of 0.566 mmol H_2/L.h was found as 287 W/m^2 (Androga et al., 2014).

ANOVA and optimization tests were also performed for hydrogen yields and light conversion efficiencies using RSM. However, the results of ANOVA analysis showed that the model could not clarify hydrogen yields and light conversion efficiencies. The significance of the obtained equations was limited at only 10-50% as a result of ANOVA analysis. In other words, hydrogen yield and light conversion efficiency could not be explained by S, X_o and light intensity variables and (or) interactions and the optimizations of hydrogen yield and light conversion efficiency could not be successful. For this reason, RSM was optimized only for hydrogen production rate results.

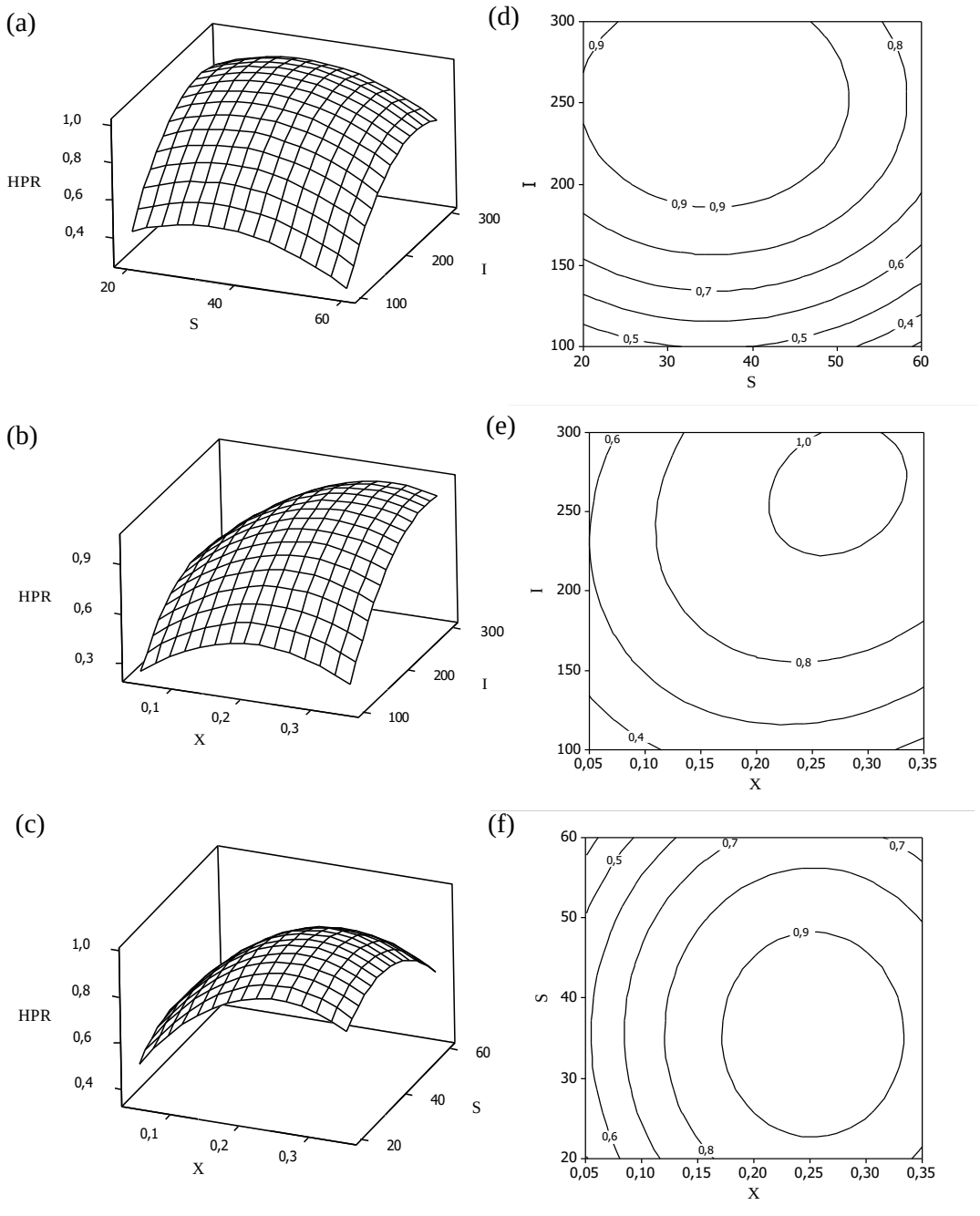

Figure 4.2 Plots for the hydrogen production rate (HPR) model using batch cultures of Rhodobacter capsulatus DSM 1710. (a), (b), (c) Three-dimensional response surface plots, and (d), (e), (f) Two-dimensional contour plots

As described in the Materials and Methods (Section 2.1), the initial biomass concentration was chosen as one of the variables because the initial biomass concentration was also important as well as the initial substrate concentration effect in the hydrogen production. The reactors were inoculated with three different biomass concentrations used in this study were 0.05, 0.20 and 0.35 g VSS/L as mentioned previously. The change in each biomass concentration in time was given in Figure 4.3. Figure 4.3 indicated that the concentrations of *Rhodobacter capsulatus* increased to 2.5-3.5 g VSS/L in the reactors where the initial biomass concentration was the highest (X_o=0.35 g VSS/L). The concentrations of *Rhodobacter capsulatus* in the reactors with initial biomass concentration of 0.20 g VSS/L increased to 2-2.5 g VSS/L; and the concentrations of *Rhodobacter capsulatus* in the reactors with initial biomass concentration of 0.05 g VSS/L increased to 1-1.8 g VSS/L. As can be seen in Figure 4.3 (a), (b), (c), the increase in the microorganism concentration of the reactors with the same initial biomass concentration and the same light intensity, where the initial substrate concentration was higher, was prominently greater. At the same initial biomass and acetate concentrations, the rate of increase in the microorganism concentration of reactors with higher light intensity was higher. Yet, despite the lower light intensity, the biomass concentration in the reactor increases and reaches to similar levels as observed in reactors with higher light intensity.

To summarize, it can be stated that, the results of Set-1 was interpretted by RSM Box-Behnken Design Method and the effect of initial acetate, initial biomass (*Rhodobacter capsulatus*) and light intesity and their interactions on hydrogen production rate was investigated with RSM. According to RSM results, hydrogen yields and light conversion efficiencies can not be explained by S, X_o and I variables and/or interactions (with these 3 variant models). Optimum values leading to the highest hydrogen production rate were found as 35.35 mM HAc initial substrate concentration, 0.27 g VSS/L initial biomass (*Rhodobacter capsulatus*) concentration and 3955 lux (263.6 W/m^2) light intensity. When these values were used, the highest estimated hydrogen production rate to be obtained was 1.04 mmol

H_2/L.h. The S/X_o ratio providing the highest hydrogen production rate was 9.4 COD/g VSS, (8.3 g COD_{HAc}/g VSS, 7.7 g acetate/g VSS). Experimentally, the hydrogen production rates (productivity) were between 0.27-0.91 (mmol H_2/L.h); while the hydrogen production yields ranged between 0.02-0.11 g H_2/g acetate (0.60-3.27 mol H_2/mol acetate, 0.019-0.10 g H_2/g COD).

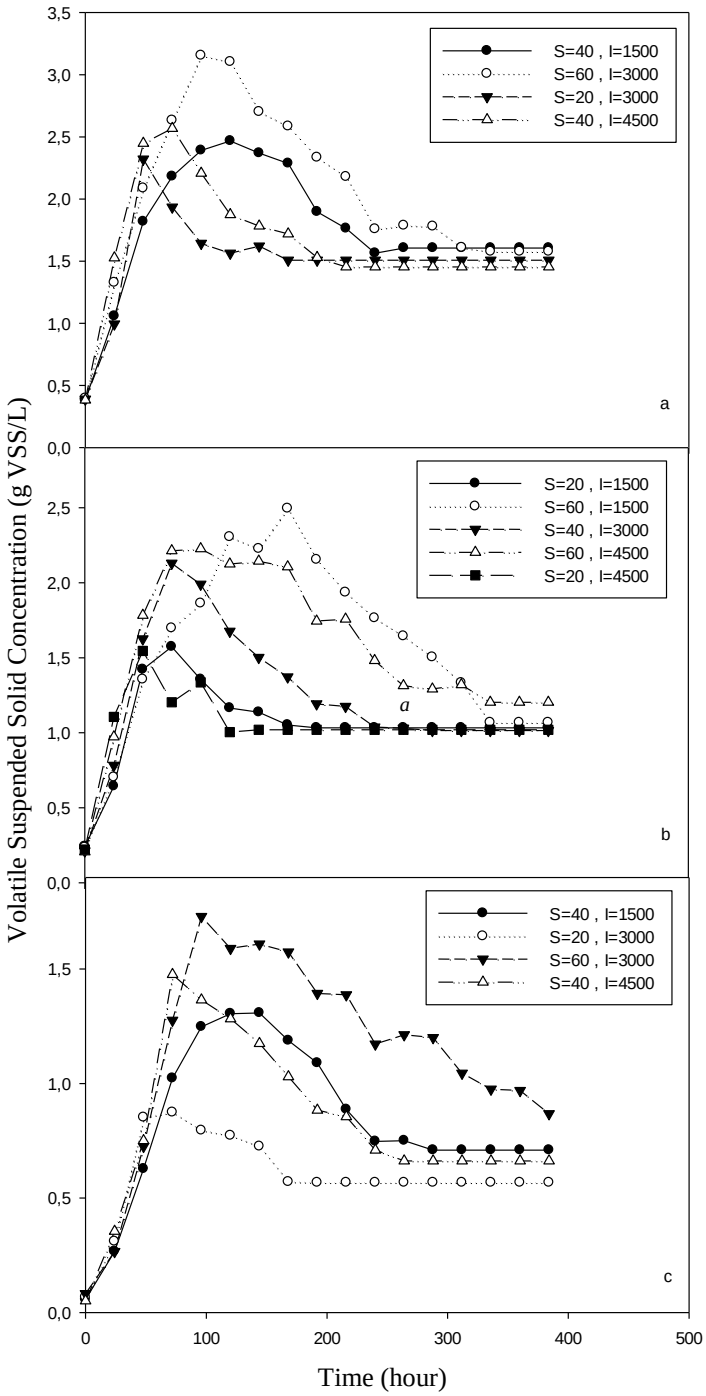

Figure 4.3 Rhodobacter capsulatus DSM 1710 concentration change with time in reactors with initial biomass (X_o) concentrations of (a) 0.35 g VSS/L, (b) 0.2 g VSS/L, (c) 0.05 g VSS/L (30°C, acetate)

4.2. Results of Set-2: Photofermentation as a Second-stage of a Two-stage System

The aim of Set-2 was to investigate photofermentation in a two-stage dark fermentation and photofermentation system. The results obtained in this two-stage dark fermentation and photofermentation, which are frequently encountered in literature studies, provided a preliminary knowledge and were used to compare with the results of three-stage systems conducted in further experiments (Set-3 and Set-4).

The photofermentation reactors conducted in Set-2 were operated for 8 days (192 hours). Hydrogen production was observed only in the reactors which were fed with Influent-2 (Table 3.3). Therefore, any data related to the reactors fed with Influent-1 was not given. The cumulative hydrogen gas production observed in the reactors fed with Influent-2 was given in Figure 4.4. The hydrogen production rate, substrate conversion efficiency, light conversion efficiency values of these reactors (conducted in three replicas) are presented in Table 4.3. The average hydrogen yield values are presented in Table 4.4.

As shown in Table 4.3, close hydrogen gas production volumes and conversion efficiencies were obtained in 3 replica reactors with same properties. The average hydrogen production rate was calculated as 0.48±0.08 mmol H_2/L.h. The total amount of hydrogen gas produced was 1.52±0.22 mmol on average. The hydrogen yield based on the initial acetic acid concentration (21 mM HAc) was found as 1.61±0.24 mol H_2/mol HAc (0.054±0.008 g H_2/g acetate, 0.050±0.008 g H_2/g COD_{HAc} (Table 4.4). Hydrogen production yield was also calculated on the basis of acetic acid, butyric acid and propionic acid determined to be consumed in the reactors. Accordingly, the initial concentrations of these three acids were calculated as HAc equivalent and the hydrogen yield was found as 1.13±0.16 mol H_2 / mol (HAc + HBu + HPr, based on HAc equivalent).

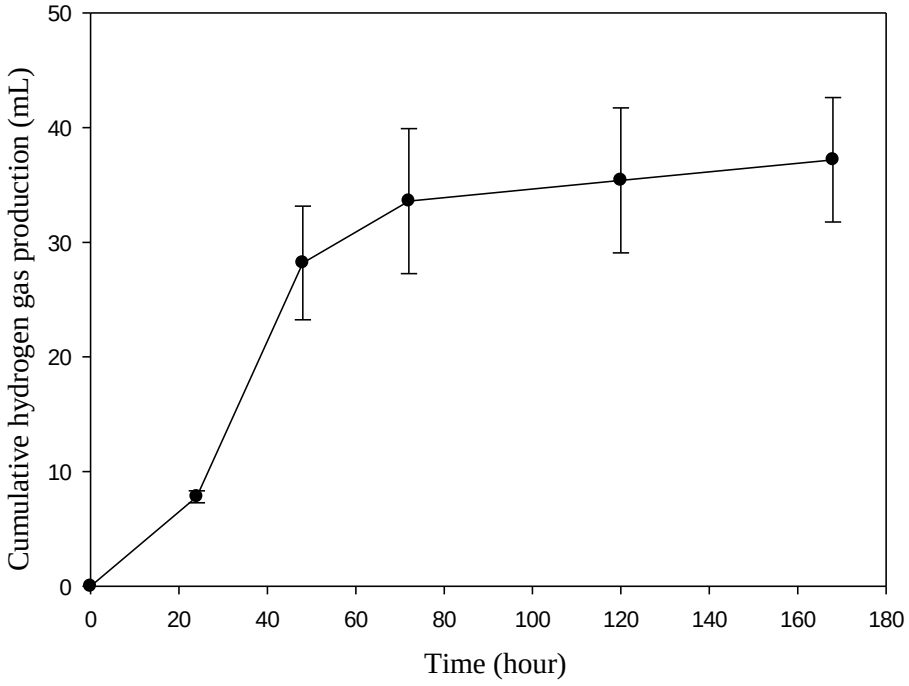

Figure 4.4 The average cumulative hydrogen gas production of reactors in Set-2

Table 4.3 Hydrogen production rates and efficiencies of reactors in Set-2

3 Replica Reactors	**Hydrogen Production Rate (mg H_2/L.h)**	**HPR (mmol H_2/L.h)**	**Substrate Conversion Efficiency (%)**	**Light Conversion Efficiency (%)**	**Total H_2 Produced (mmol)**
Reactor 1	0.80	0.40	23.9	0.30	1.29
Reactor 2	0.95	0.48	28.7	0.36	1.55
Reactor 3	1.14	0.57	32.1	0.40	1.73
Average	0.96±0.17	0.48±0.08	28.2±4.1	0.36±0.05	1.52±0.22

Table 4.4 Hydrogen yields of reactors in Set-2

Reactor No.	**Hydrogen Yield (g H_2/g COD_{HAc})**	**Hydrogen Yield (mol H_2/mol HAc)**	**Hydrogen Yield[a] (mol H_2/mol HAc+HBu+HPr)**
1	0.043	1.37	0.96
2	0.051	1.64	1.15
3	0.057	1.84	1.28
Average[b]	0.050±0.008	1.61±0.24	1.13±0.16
[a] When the yields were calculated, the indicated acids were converted to HAc (acetic acid) equivalent concentration; all yield units are based on mol H_2/mol HAc_{added}.			
[b] The yields on the basis of COD were calculated considering that all of the added HAc and other acids were consumed. 1 g of acetic acid is equivalent of 1.066 g of COD.			

In a photofermentation study using *Rhodobacter capsulatus*, the effluent of dark fermentation set-up with molasses was used as influent with 4 different dilution ratios (1/2, 1/3, 1/5, 1/10) (Mars et al., 2010). The hydrogen production rates obtained ranged within 0.08-1.10 mmol/L.h and it was stated that the highest hydrogen production rate (1.10 mmol/L.h) was obtained in the condition of 29 mM initial acetate concentration (1/3 dilution). In addition, light conversion efficiencies ranged from 0.09% to 0.66%. In Set-2, the average hydrogen production rate and light conversion efficiency were 0.48±0.08 mmol H_2/L.h and 0.36%, respectively, in the reactors conducted with the effluent of dark fermentation reactor without any dilution (21 mM acetate, HAc). In another photofermentation study using *Rhodobacter capsulatus*, the effluent of dark fermentation with 135 mM acetate concentration was diluted in the ratio of 1/4 and used for photofermentation reactors (Özgür and Peksel, 2013). The hydrogen production rate found by Özgür and Peksel (2013) was 0.22±0.02 mmol H_2/L.h and light conversion efficiency was 0.4%±0.0. As a result, it can be stated that comparable hydrogen production rate and light conversion efficiency results were obtained in this study.

In Set-1, the optimum values leading to the highest hydrogen production rate was determined as 35.35 mM initial acetate concentration, 0.27 g VSS initial biomass concentration and 3955 lux light intensity by using RSM optimization study. Moreover, the optimum S/X_o ratio was calculated as 8.3 g COD_{HAc}/g VSS (7.7 g acetate/g VSS). Lower hydrogen production rate (0.48±0.08 mmol H_2 / L.h) was observed in Set-2 compared to the hydrogen production rate obtained in Set-1 (0.91 mmol H_2 / L.h) where acetate was used as only carbon source. Uyar et al. (2009) reported that there was no problem with the growth of bacteria in different substrate mixtures, but changes in carbon source might cause a long lag period. It could be argued that the lower hydrogen production rate in Set-2, where the effluent of a dark fermentation SBR was used (Table 4.3) was due to the different carbon sources in the substrate and their effect on the bacteria. When the hydrogen yields were examined, the hydrogen yield obtained in this study as 1.61±0.24 mol H_2/mol HAc (0.054 g H_2/g HAc) was lower compared to the highest hydrogen yield (3.3 mol H_2/mol HAc, 0.11 g H_2/g HAc) obtained in Set-1. On the other hand, the photofermentative hydrogen was comparable with the hydrogen yields (0.72-1.56 mol H_2/mol HAc) obtained from the effluent of molasses dark fermentation (Uyar et al., 2009). As a result, it can be concluded that due to being the second-stage following dark fermentation, lower hydrogen yield was observed compared to the single-stage photofermentative hydrogen yields obtained at optimum conditions.

The change in biomass concentration over time is given in Figure 4.5. The highest biomass concentration reached during the experiment with Influent-2 was measured as 2.15 g VSS/L. Biomass production was much lower (0.8 g VSS/L) in the reactors conducted with Influent-1, where hydrogen production was not observed.

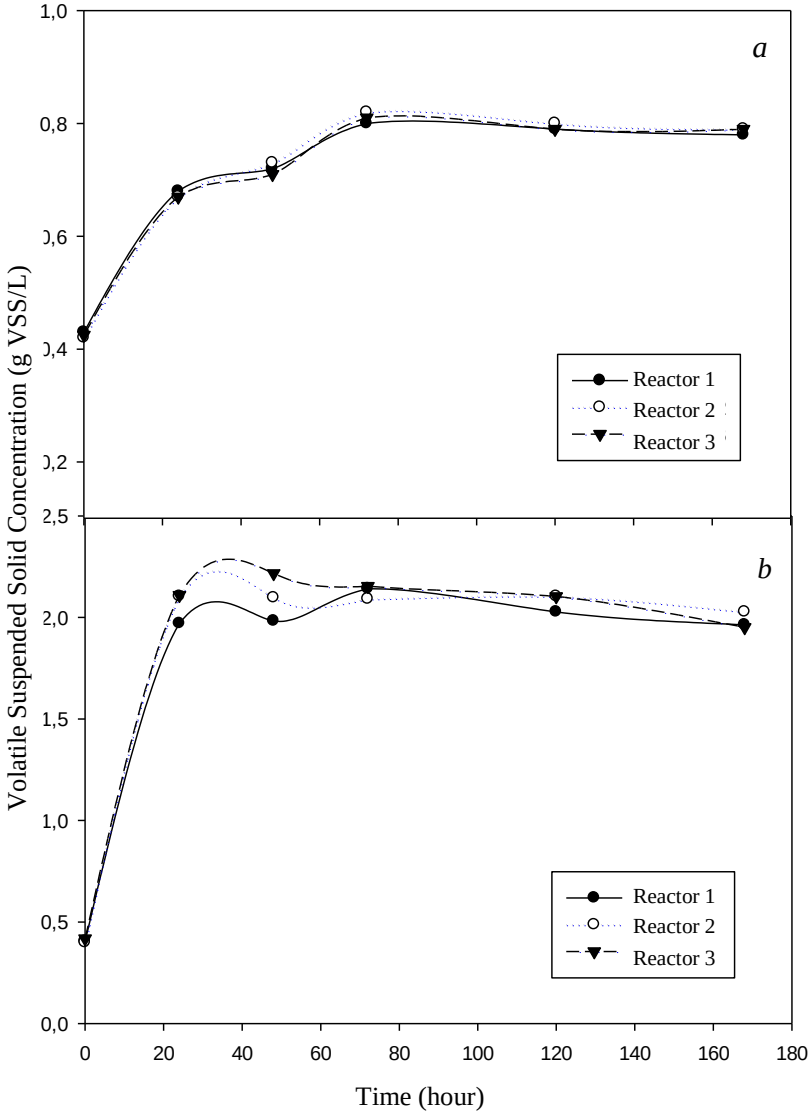

Figure 4.5 The change of Rhodobacter capsulatus concentration with time in photofermentation reactors conducted with a) Influent-1, and b) Influent-2 in Set-2.

During the study, VFA analyses were done with samples taken regularly. VFA concentrations of the reactors are given in Figure 4.6. As seen in Figure 4.5a, acetic acid was consumed in the first 168 hours (11.1±0.2 mM HAc) in the reactors set with Influent-2. Nearly half of butyric acid (1.1±0.2 mM) was removed simultaneously with lower rate. The trace amount of propionic acid (1.1±0.1 mM)

was also consumed in the first 48 hours of the experiment. In addition, formic acid production was observed up to a concentration of 2.3±0.2 mM.

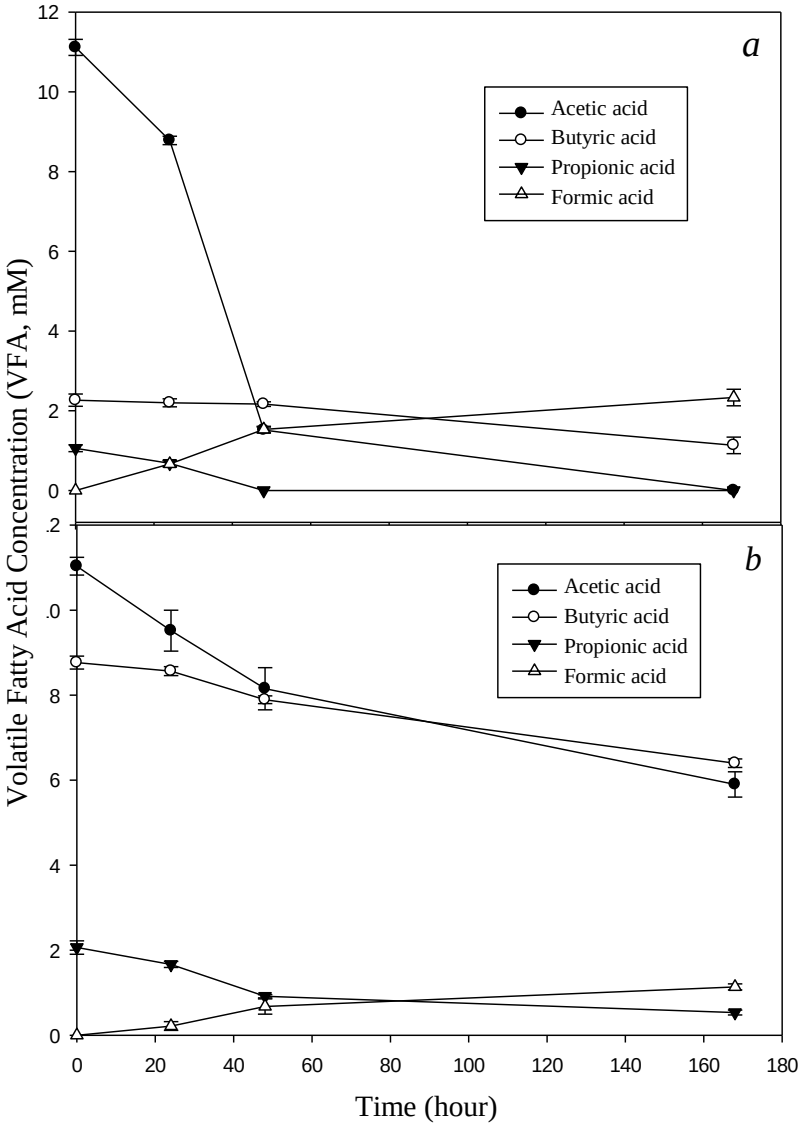

Figure 4.6 The change of VFA concentrations with time in photofermentation reactors conducted with a) Influent-2, and b) Influent-1 in Set-2.

As seen in Figure 4.6b, almost half of the acetic acid was removed in the first 168 hours (5.1±0.2 mM HAc) in the reactors conducted with Influent-1 with a much

lower rate compared to the reactors conducted with Influent-2. The butyric acid was also removed simultaneously with acetic acid with a lower rate. A small amount of propionic acid (2.1±0.2 mM) was also consumed in the first 48 hours of the experiment. In addition, formic acid production was observed up to 1.2±0.1 mM concentration as also observed in reactors conducted with Influent-2.

Hydrogen production was not observed in the reactors conducted with Influent-1. There was no inhibition due to any ammonium ion, pH, bacterial contamination, light intensity, total VFA or butyric acid concentration. Influent-1 and Influent-2 had similar characteristics (TAN, VFA type and concentrations, pH). However, hydrogen production was only observed for Influent-2. Thus, it was stated that presence of a substance or substances in Influent-1 might have prevented hydrogen production from Influent-1. This was attributed to the operational conditions of dark fermentative SBR and the related effluent characteristics. Influent-1 was withdrawn from the dark fermentative SBR when SRT was 10-15 days, while Influent-2 was withdrawn during the SRT application of 3-5 days. Longer SRTs might have resulted in production of inhibitory substance which prevents the hydrogen production.

4.3. Results of Set-3: Photofermentation as a Third-stage of a Three-stage System

The aim of Set-3 was to investigate photofermentation in three-stage system composed of dark fermentation, methanogenesis and photofermentation processes. The yields obtained in this three-stage system, which have not been studied so far in literature studies, provide a preliminary knowledge for future three-stage systems and comparison for two-stage systems frequently encountered in literature studies. In this study, batch photofermentation reactors were conducted with effluents of methanogenesis SBR (Koç, 2015). In this methanogenesis SBR, the effluents of dark fermentative SBR (Tunçay, 2015) were used as influents. Thus, this is a three-stage

system composed of dark fermentation, methanogenesis and photofermentation in sequence.

Batch photofermentation reactors of Set-3 were operated for 8 days (192 hours). Six different influents namely Influent-A, Influent-B, Influent-C, Influent-D, Influent-E and Influent-F were used in the experiments. These six influents were withdrawn from effluents of methanogenesis SBR study which were operated at six different HRT and SRT combinations. Hydrogen production was not observed during the whole incubation period of 8 days in the reactors conducted with Influent-A, Influent-B, Influent-C and Influent-F. This was associated with the lack of adequate VFA concentrations (2.5-4 mM, Table 3.4). Hydrogen production was also not observed in the first 48 hours of the incubation period in the reactors conducted with Influent-D and Influent-E. However, hydrogen production started at the end of 48 hours in these reactors as expected because they had sufficient initial VFA concentrations (16.4 and 21.7 mM, Table 3.4). The cumulative amounts of hydrogen gas produced in these reactors are presented in Figure 4.7. As seen in Figure 4.7, the volume of hydrogen gas produced was very low.

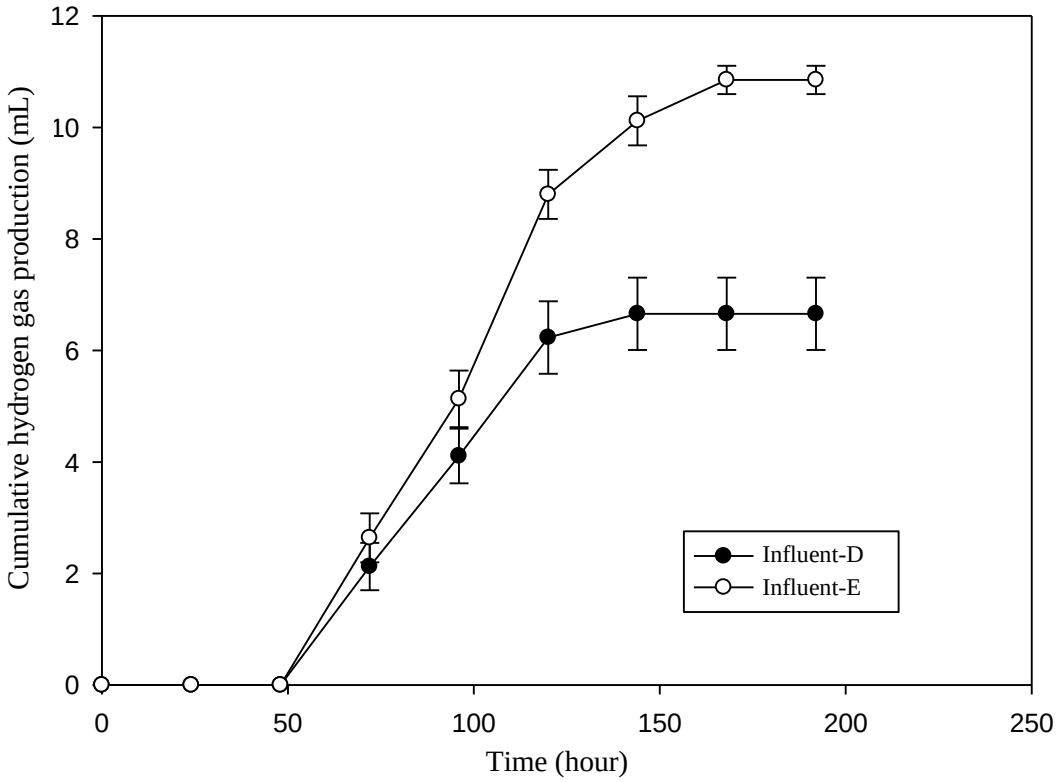

Figure 4.7 The average cumulative hydrogen gas production observed in Set-3.

In order to determine why hydrogen was produced in low amounts and there was a lag-phase at the beginning in the reactors fed with Influent-D and Influent-E, the main factors influencing the hydrogen production in purple non-sulphur bacteria were reviewed first. During the incubation, the temperature was monitored with an additional thermometer placed in the incubator and it was ensured that the temperature of 30 ° C was kept constant during the experiment. The pH change, which was an another factor that could affect the hydrogen production, was monitored daily. During the experiment, the pH value in replica reactors increased gradually from 6.8 to 7.2, decreased to 7.0 at the end of 125th hour and remained at that pH till the end. This indicated that there was no pH-related problem because incubation was carried out at the appropriate pH range (6.8-7.5) for photofermentation. Another factor, light intensity, was set at 3955 lux during the

experiment. It was known from previous experiments (Set-1 and Set-2) that any problem of light intensity would not occur. It was suspected that there might have been a bacterial contamination; thus a sample was taken from the stock bacteria culture, which had been used as inoculum of the reactors of concern, and plated in petri dishes by streak plate method. The bacterial colonies were observed, but no bacterial contamination occurred; therefore, bacterial contamination was also not the potential reason of not observing hydrogen production. Because ammonium ion (0.8 mM (13.8 mg/L) and 0.6 mM (11.6 mg/L), Table 3.4) was treated and decreased to the levels below the inhibition value (2 mM) (Appendix D), it was known that there was not any inhibition originating from ammonium ion concentration as well.

It has been reported that for efficient integrated (dark fermentation and photofermentation) hydrogen production, dark fermentation effluents' VFA concentrations should be lower than 2500 mg/L (~ 42 mM) and conditions where butyric acid is above 25 mM inhibits photofermentative hydrogen production (Argun et al., 2008; Su et al., 2009). Table 3.4 (Section 3.4.3) indicated that the concentration of total VFA was 21.7±4.1 mM and 16.4±1.7 mM for Influent-D and Influent-E, respectively. In addition, butyric acid concentrations were lower than the inhibitory level of 25 mM. In other words, total VFA and butyric acid concentrations were not the inhibition factors either. Therefore, low volumes of hydrogen produced in the reactors conducted with Influent-D and Influent-E did not originate from the aforementioned factors investigated.

It should be noted that granule formations were observed in the reactors conducted with both Influent-D and Influent-E starting from the first day (24 hours) in all replica reactors operated. Granulation is a defense mechanism of microorganism when they are exposed to environmental stress (Ergüder and Demirer, 2005). Therefore, it was thought that *Rhodobacter capsulatus* was exposed to an inhibition/stress that might lead to granulation. The hydrogen production started after 48 hours. The granular formation, on the other hand, decreased by the end of 72 hours and disappeared at the end of 4th day (96 hours). This dissappearance of

granule formation and parallel increase in the hydrogen production might be related to the possible reduction in the effect of the factor causing the stress/inhibition and/or adaptation of the microorganism to the environment. Thus, low volume of hydrogen production following the acclimation period and granule formation might be due to a possible inhibitory substance in the substrate source. The substance/chemical leading to the inhibition might be a product formed during the incubation of dark fermentation SBR or methanogenesis SBR. As mentioned in Set-2 (Section 4.2), similar inhibitory effect was also observed in the reactors conducted with Influent-1 (effluent of dark fermentative SBR). The comparison of Set-2 and Set-3 would be given in detail in Section 4.5.

In Set-3, hydrogen production rate, substrate conversion efficiency, light conversion efficiency and hydrogen yield values of the reactors fed with Influent-D and Influent-E conducted in three replicas are presented in Table 4.5, respectively. The highest hydrogen production rate and hydrogen yield were observed as 0.10±0.005 mmol H_2/L.h and 0.032±0.001 g H_2/g acetate, respectively, from Influent-E. These values are nearly one-tenth of the optimized hydrogen production rate (1.01 mmol H_2/L.h), experimental hydrogen production rate (0.91 mmol H_2/L.h) and experimental hydrogen yield (0.11 g H_2/g acetate) obtained in optimum batch photofermentation conditions in Set-1. Yet, it should be noted that substrate was acetate in Set-1, where, there was no potential inhibitory products for photofermentation and the conditions were optimum operational conditions obtained via the experiment. As seen in Table 4.5, hydrogen production rates, yields and conversion efficiencies of reactors fed with Influent-E were higher than those fed with Influent-D. It was speculated that the potential substance causing the inhibition/stress might be low in concentration in Influent-E.

Table 4.5 Average hydrogen production rates, efficiencies and yields in Set-3

Effluent of Methanogenesis SBR	Hydrogen Production Rate (mg H_2/L.h)	Hydrogen Production Rate (mmol H_2/L.h)	Substrate Conv. Efficiency (%)	Light Conv. Efficiency (%)	Hydrogen Yield (g H_2/g acetate)
Influent-D	0.14±0.02	0.07±0.01	8±0.8	0.11±0.01	0.012 ±0.001
Influent-E	0.19±0.01	0.10±0.005	17.1±0.4	0.15±0.003	0.032 ±0.001

The change in VFA concentrations over time is given in Figure 4.8. As seen in Figure 4.8a, in the reactors conducted with Influent-D, half of the acetic acid was consumed until the start of hydrogen production (48 hours) and the amount consumed in the remaining period caused low hydrogen production. On the other hand, in the reactors conducted with Influent-E, the amount of acetic acid consumed until the start of hydrogen production (48 hours) was less than that observed in the reactors conducted with Influent-D (Figure 4.8b). Besides, the consumption of acetic acid in the process of hydrogen production (48-192 hours) was higher in the reactors conducted with Influent-E. Despite the different acetic acid consumption rates during the experimental period, almost similar amounts of total VFA were consumed in these reactors. Yet, hydrogen production yield of the reactor fed with Influent-E was almost three times higher than that of the reactor fed with Influent-D, as mentioned previously. On the other hand, VSS concentration and/or biomass growth in the reactors fed with Influent-E was lower than those observed in the reactors fed with Influent-D (Figure 4.9). It is likely that *Rhodobacter capsulatus* in reactors fed with Influent-D diverted majority of the consumed VFA for bacterial growth initially, rather than hydrogen production. This might be a defense mechanism of bacteria as well, for Influent-D might have higher concentration of potential inhibitory substance compared to Influent-E, as aforementioned. As seen in Figure 4.9, bacterial growth was also observed in the reactors fed with Influents A, B, C, F yet growth was low due to low initial VFA concentrations (2.5-4 mM).

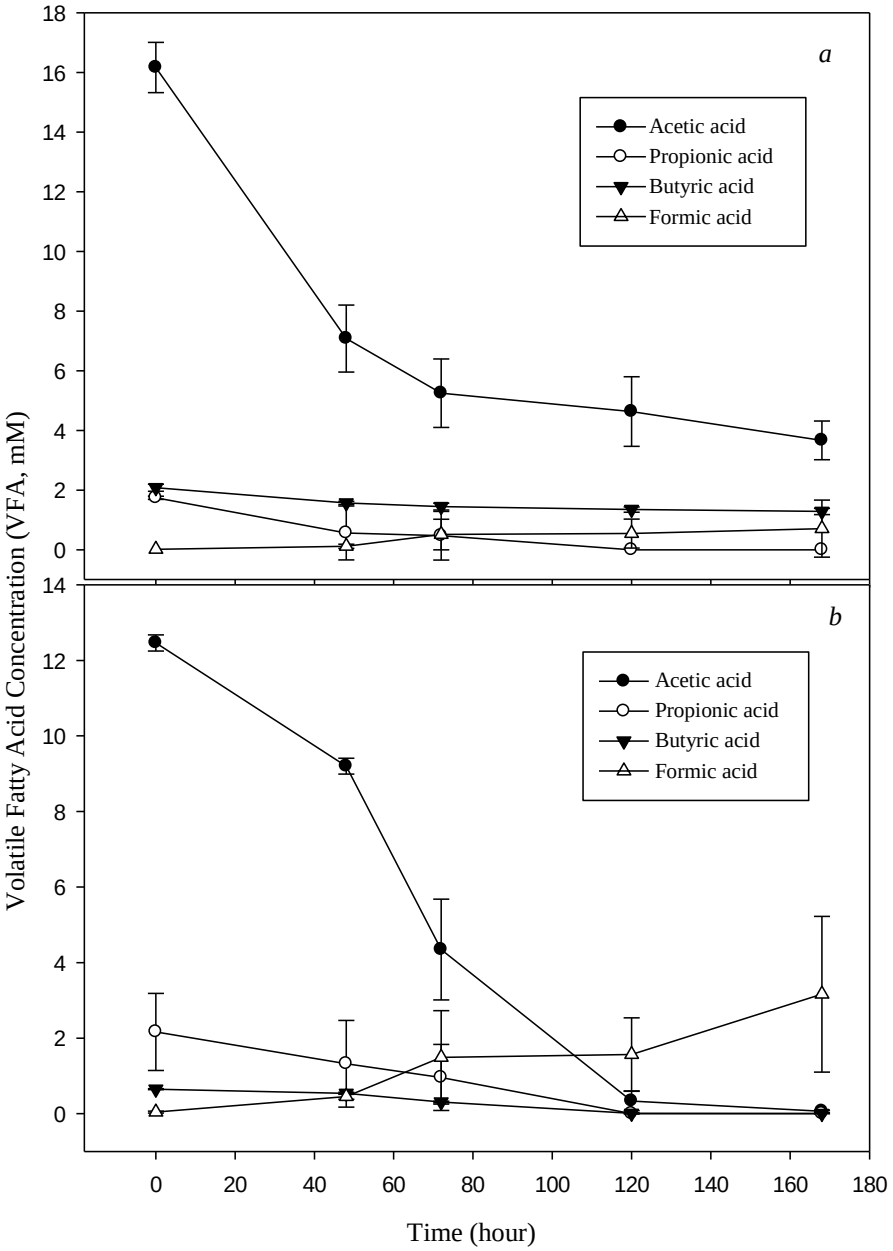

Figure 4.8 The change in average VFA concentrations over time in reactors of Set-3 conducted with a) Influent-D, b) Influent-E

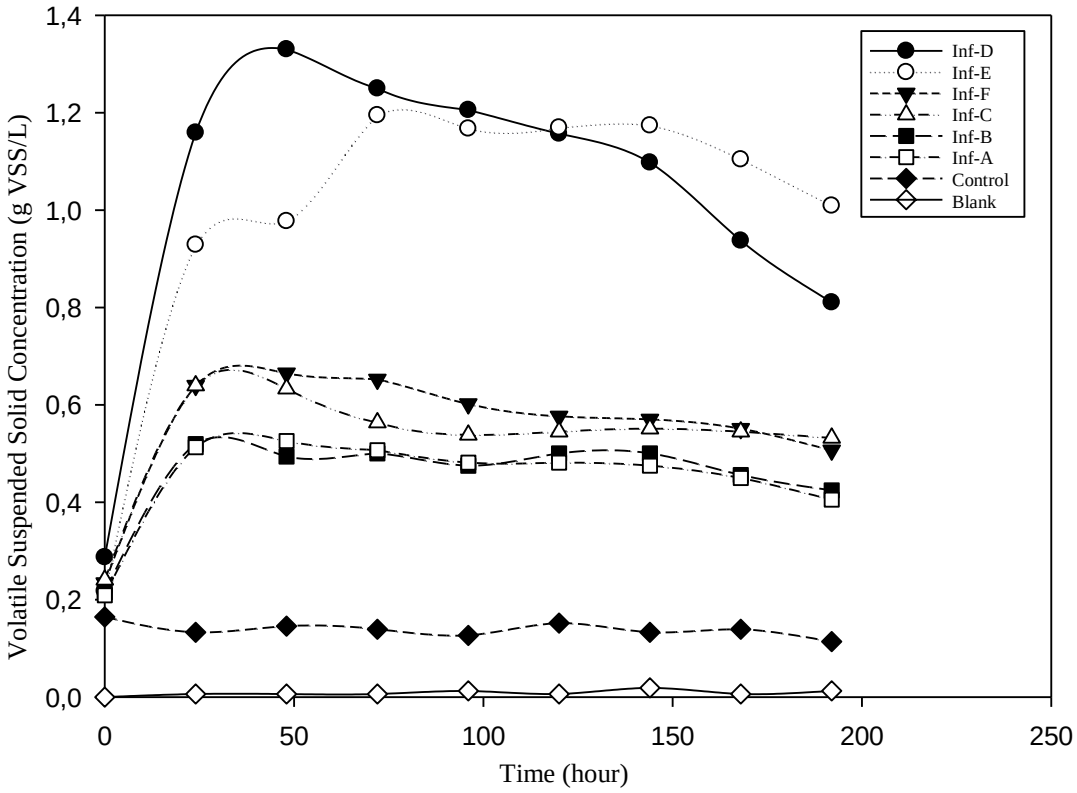

Figure 4.9 The change in average VSS concentration over time in reactors of Set-3

4.4. Results of Set-4: Semi-batch Reactor Experiments

The aim of Set-4 was to investigate the optimum HRT leading to the highest photofermentative hydrogen production rate in semi-batch reactors. In this study, reactors were run with the effluents of methanogenesis SBR operated at different operating conditions and fed with the effluents of dark fermentative SBR. In other words, reactors in Set-4 were also third-stage of a three-stage system as in batch reactors of Set-3.

Daily biogas and hydrogen production amounts observed in the reactors fed with Influent-D and Influent-E are given in Figure 4.10 and Figure 4.11, respectively. Semi-batch photofermentation reactors fed with Influent-D was operated for 38 days

(912 hours), semi-batch reactors fed with Influent-E was operated for 20 days (480 hours). Influent-E was not as much as Influent-D, so operational period of semi-batch reactors fed with Influent-E was less than those fed with Influent-D. Hydrogen production was not observed during the first 120 hours of the incubation period in all reactors. The formation of granules observed in Set-3 was also observed in Set-4 during the first 120 hours of the incubation period. It should be noted that hydrogen production had not been observed during the first 48 hours in Set-3. Considering the results of Set-3 and, thus, in order to provide acclimation period, the reactors in Set-4 were operated like batch reactors in the first 120 hours and any influent was not fed to the reactors till the observation of hydrogen production. Following the start of the hydrogen production (observed at the end of the 120 hours), it was started to operate reactors at semi-batch mode. After 120 hours, the formation of granules in the reactors reduced but granules were not completely disappeared. During the whole experimental period, granule formation was observed at a lower level compared to that observed at the beginning of the incubation of Set-1.

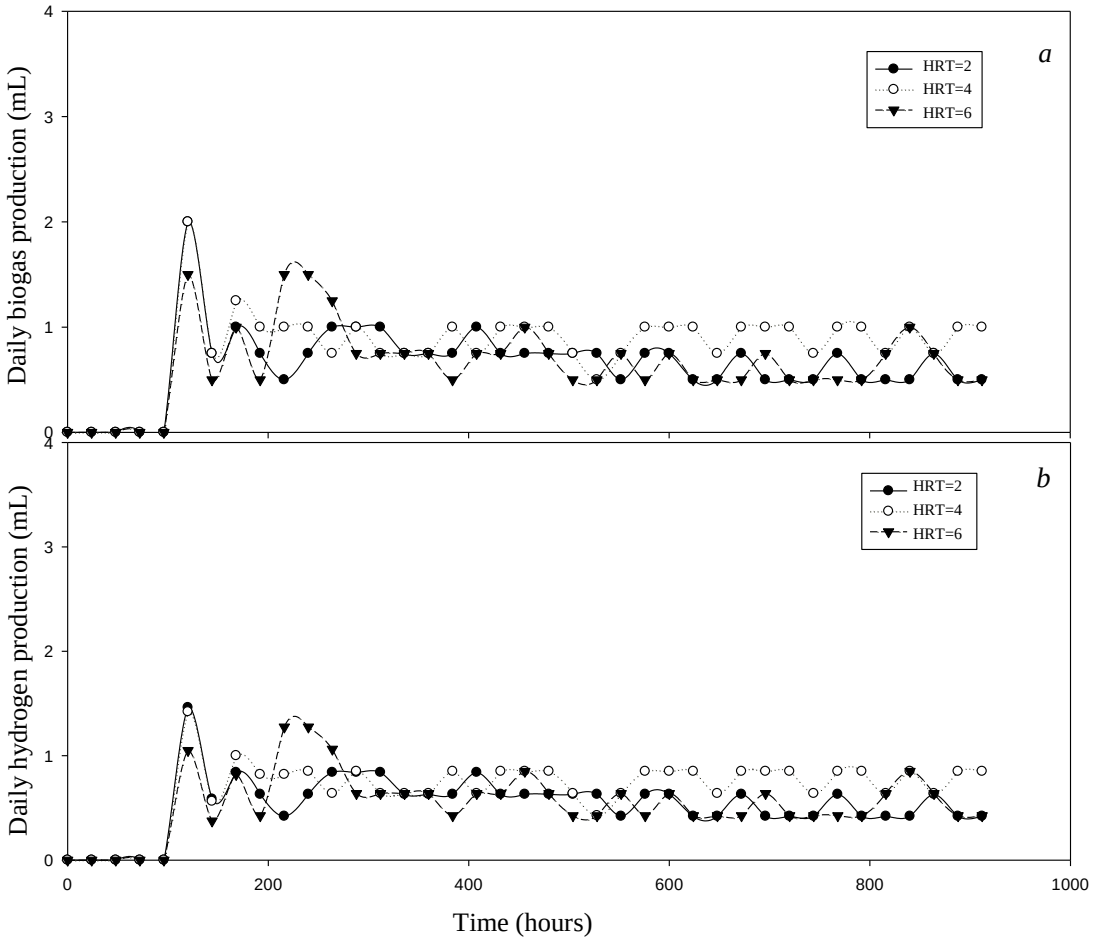

Figure 4.10 Average daily (a) biogas and (b) hydrogen production amounts observed in the reactors fed with Influent-D in Set-4 (30°C, S/X_o=8.3 g COD_{HAc}/g VSS, 3955 lux)

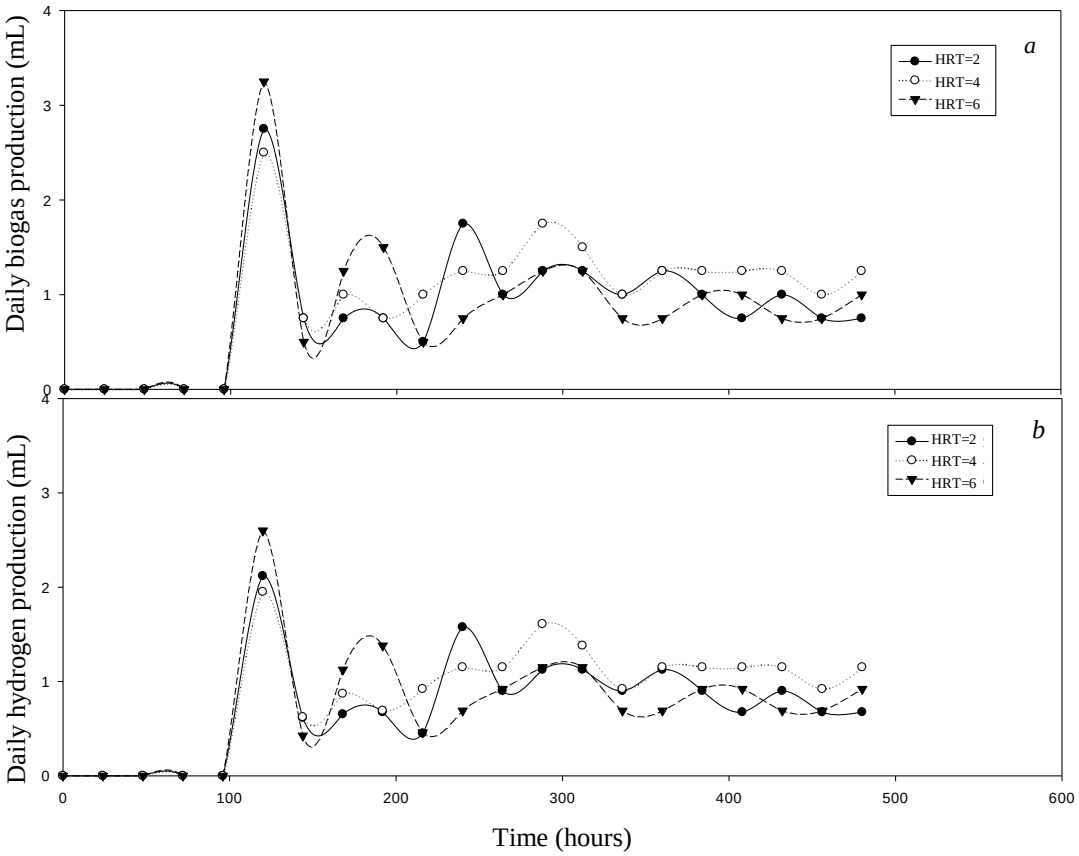

Figure 4.11 Daily (a) biogas and (b) hydrogen production amounts observed in the reactors fed with Influent-E in Set-4 (30°C, S/X_o=8.3 g COD_{HAc}/g VSS, 3955 lux)

The total amounts of hydrogen produced during the experimental period are given in Table 4.6. The changes in biomass concentration during the incubation period are given in Figure 4.12. As seen in Table 4.6, the total amounts of hydrogen produced were quite low. Among the reactors fed with either Influent-D or Influent-E, the highest hydrogen gas production was observed in the ones operated at an HRT of 4 days independent of the influent type. As mentioned previously, the reactors fed with Influent-D was operated 38 days and the reactors fed with Influent-E was operated 20 days. Despite the lower incubation period, hydrogen production amounts observed in the reactors fed with Influent-E was close to that of the reactors fed with Influent-D.

Table 4.6 The average amounts of total hydrogen gas produced in semi-batch reactors in Set-4

Reactor No	Influent type	HRT value (day)	Average amounts of total hydrogen gas produced (mmol)	Range of total hydrogen gas produced (mmol)
1-2	Influent-D	2	0.85	0.84-0.86
3-4	Influent-D	4	1.13	1.12-1.13
5-6	Influent-D	6	0.97	0.95-0.98
7-8	Influent-E	2	0.71	0.70-0.71
9-10	Influent-E	4	0.88	0.87-0.89
11-12	Influent-E	6	0.79	0.78-0.79

As seen in Figure 4.10 and Figure 4.11, the daily hydrogen gas production was very low (around 1 mL H_2/day) in all reactors fed with both Influent-D and Influent-E. The HRT value leading to the highest daily hydrogen production was observed as 4 days for both types of influents. As seen in Figure 4.12b, the biomass concentration in the reactors fed with Influent-E remained at higher levels (0.4-0.55 g VSS/L) during the incubation. It has been observed that the lowest biomass concentration of 0.38-0.41 g VSS/L was observed in the reactors with 2-day HRT compared to those also fed with Influent-D. This can be attributed to the fact that the daily liquid volume withdrawn from the reactors with 2-day HRT was higher than the reactors with 4 days and 6 days of HRTs and probably there was not enough time for bacterial growth at that HRT.

The daily hydrogen yields and substrate conversion efficiencies observed in reactors are presented in Table 4.7. The average daily hydrogen production rates obtained during the incubation are presented in Table 4.8. The average daily hydrogen yields obtained during the incubation are presented in Figure 4.13.

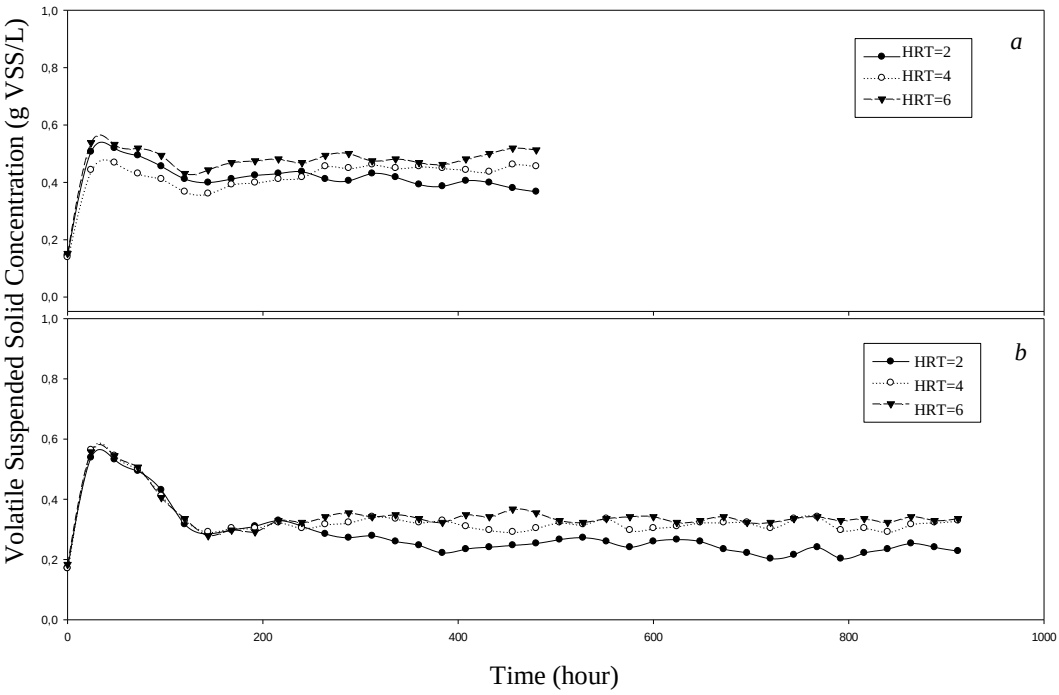

Figure 4.12 The changes in average bacterial concentration during the incubation period in semi-batch reactors fed with (a) Influent-E, (b) Influent-D conducted in two replicas in Set-4

Table 4.7 The range of daily average hydrogen yields and substrate conversion efficiencies in Set-4

Reactor No	**HRT (days)**	**Hydrogen yield (mol H_2/mol HAc)**	**Hydrogen yield (g H_2/g COD_{HAc})**	**Substrate conversion efficiency (%)**
1-2	2	0.038-0.077	0.0012-0.0024	1-1.9
3-4	4	0.077-0.182	0.0024-0.0048	2.6-5.2
5-6	6	0.103-0.351	0.0032-0.0109	2.6-8.8
7-8	2	0.067-0.235	0.0029-0.0073	1.7-5.9
9-10	4	0.185-0.478	0.0058-0.0150	5.1-12
11-12	6	0.207-0.622	0.0060-0.0163	4.8-15.5

As seen in Table 4.7, the highest hydrogen yields reached were observed in the reactors conducted with Influent-E and at 6 days of HRT. These reactors were followed by the reactors conducted with Influent-E and 4 days of HRT. As seen in Table 4.8, the reactors conducted with Influent-D and Influent-E, and HRT of 4 days achieved better results in terms of hydrogen production rate. The reactors with HRT of 2 days and 6 days and conducted with Influent-D or Influent-E, had same hydrogen production rates. In addition, the hydrogen production rates observed in the reactors conducted with Influent-E were higher than the rates in the reactors conducted with Influent-D. Higher yields and rates observed with Influent-E as also seen in Set-3 were attributed the lower levels of potential inhibitory compounds in it compared to Influent-D.

Table 4.8 The daily average hydrogen production rates observed in semi-batch reactors of Set-4

Reactor No	**HRT (days)**	**Amount of total hydrogen gas produced (mmol)**	**Hydrogen production rate (mg H_2/L.h)**	**Hydrogen production rate (mmol H_2/L.h)**
1-2	2	0.85	0.041	0.021
3-4	4	1.13	0.049	0.025
5-6	6	0.97	0.041	0.021
7-8	2	0.71	0.066	0.033
9-10	4	0.88	0.082	0.041
11-12	6	0.79	0.066	0.033

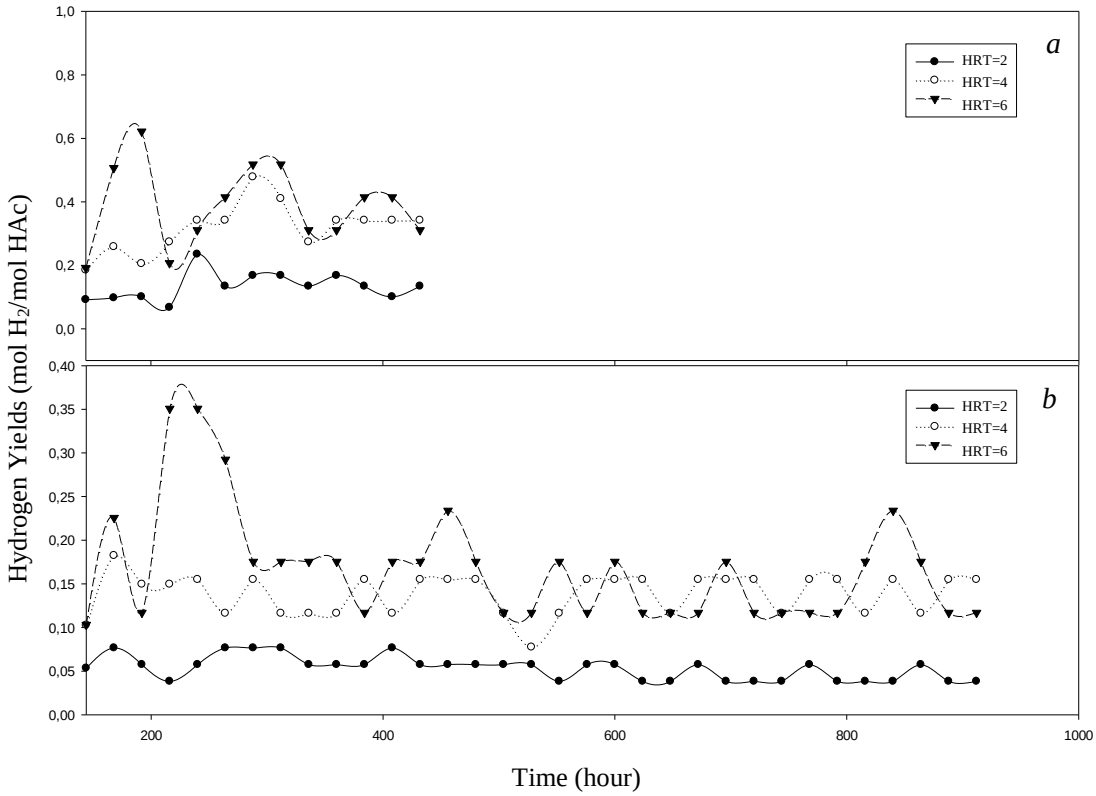

Figure 4.13 Average daily hydrogen yields obtained during the incubation in reactors fed with a) Influent-E b) Influent-D

The VFA concentrations monitored regularly during the incubation period are given in Figure 4.14 and Figure 4.15. As seen in Figure 4.14 and Figure 4.15, acetic acid in reactors conducted with Influent-E had been consumed in lower amounts than that in the reactors conducted with Influent-D during the first 120 hours of the incubation. Acetic acid concentration in the reactors increased after feeding as semi-batch mode (after 120th hour), it remained at nearly same concentration levels till the end of the incubation period, except slight fluctuations observed after 216 hours.

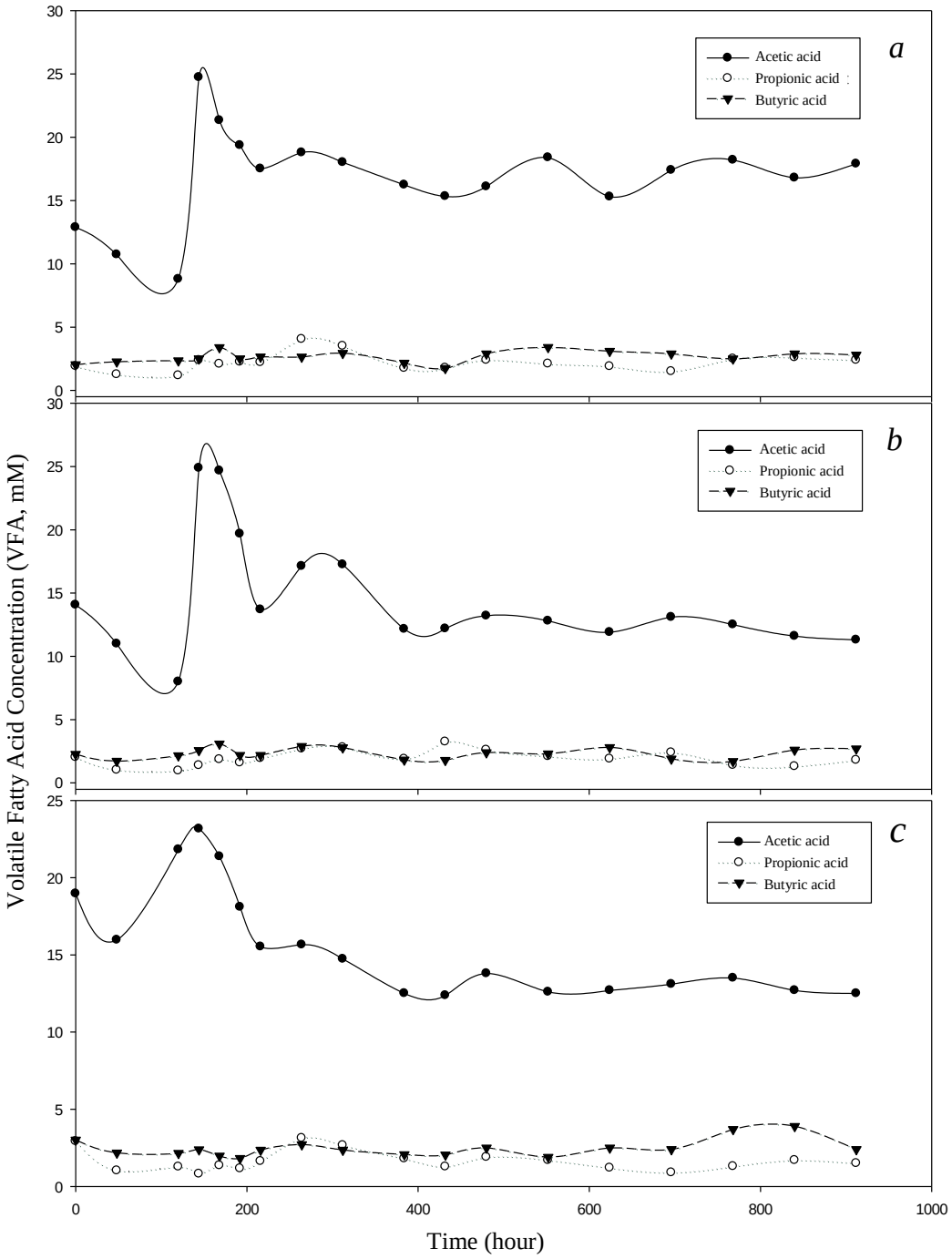

Figure 4.14 The change in the average VFA concentrations over time in reactors conducted with Influent-D, at (a) HRT=2 days; (b) HRT=4 days; (c) HRT=6 days

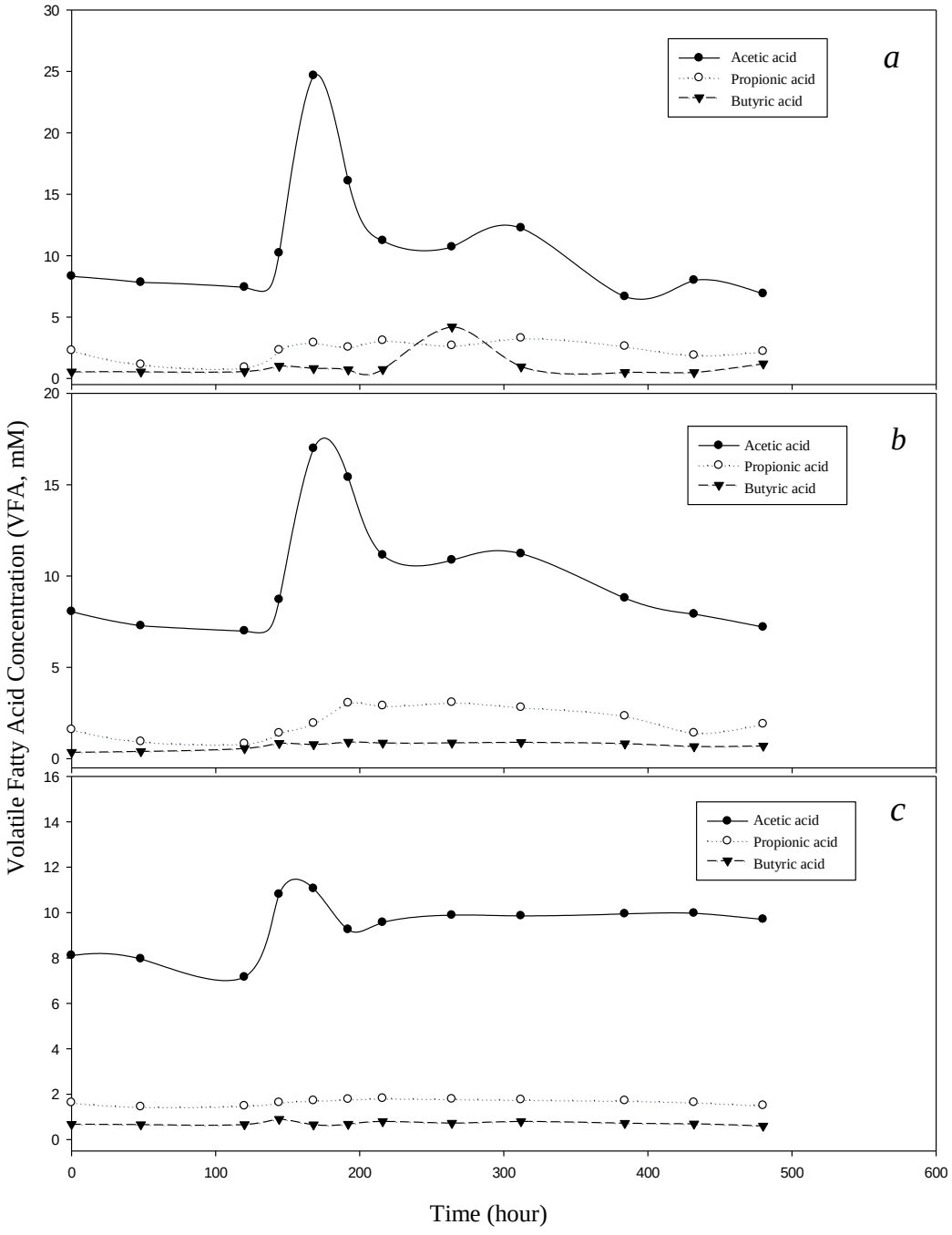

Figure 4.15 The change in the average VFA concentrations over time in reactors conducted with Influent-E, at (a) HRT=2 days; (b) HRT=4 days; (c) HRT=6 days

4.5. Comparison of Experimental Sets

Information of influents and effluents used in three-stage dark fermentation, methanogenesis and photofermentation system is given in Table 4.9. The reason of using this table is to indicate the relationship between influents and effluents used in photofermentation studies (Sets 2-3-4). Hydrogen production rates and yields in Set-1, Set-2, Set-3 and Set-4 are given in Table 4.10.

Table 4.9 The information on influents and effluents used in experimental studies

<table>
<tr><th colspan="3">Dark fermentative SBR[a]</th><th colspan="2">Methanogenesis SBR[b]</th><th>Photofermentation</th></tr>
<tr><th>Substrate</th><th>Operating Periods</th><th>Effluent name</th><th>Operating Periods</th><th>Effluent Name</th><th>Hydrogen Yield (mol H_2/mol HAc)</th></tr>
<tr><td rowspan="7">Sucrose</td><td>Period 1</td><td rowspan="4">Influent-1</td><td>Period I</td><td>Influent-A</td><td>n/a</td></tr>
<tr><td>Period 2</td><td>Period II</td><td>Influent-B</td><td>n/a</td></tr>
<tr><td>Period 3</td><td>Period III</td><td>Influent-C</td><td>n/a</td></tr>
<tr><td>Period 4</td><td>Period IV</td><td rowspan="2">Influent-D</td><td>0.36±0.03[c]
0.04-0.35[d]</td></tr>
<tr><td rowspan="3">Period 5</td><td rowspan="3">Influent-2</td><td>Period IV</td></tr>
<tr><td>Period V</td><td>Influent-E</td><td>0.95±0.03[c]
0.07-0.62[d]</td></tr>
<tr><td>Period VI</td><td>Influent-F</td><td>n/a</td></tr>
<tr><td colspan="6">n/a: not applicable (The initial VFA concentration was not adequate for hydrogen production (2.6-3.9 mM tVFA as HAc)
[a] Influent-1: Influent of Set-2 (Mixture of Periods 1-4 effluents of dark fermentative SBR)
Influent-2: Influent of Set-2 (Effluent of Period-5 of dark fermentative SBR)
[b] Influents-A to F: Influent of both Set-3 and Set-4
[c] Highest hydrogen yield observed in Set-3
[d] Hydrogen yields observed in Set-4</td></tr>
</table>

Set-1 was conducted to determine the optimum conditions for photofermentation studies to be used for other sets, therefore the results were not compared herein with other sets in terms of hydrogen production rate and yields. Besides, the substrate was acetate, the reactors were single-stage systems and the operating conditions were the optimum conditions leading to the highest hydrogen production rates and yields. Therefore, it might be misleading to compare the staged-reactors' performances (of Set-2, Set-3 and Set-4) with those of Set-1. Nevertheless, the yield and rates obtained in Set-1 were also given in Table 4.10.

In Set-2, inhibitory effect was observed in reactors conducted with Influent-1 and there was no hydrogen production in the reactors conducted with Influent-1 (Table 4.10). It was stated that, presence of a substance or substances in Influent-1 can cause bacterial inhibition effect. This situation was related to the operational conditions (i.e. SRT) of dark fermentative SBR. As seen in Table 4.9, Influent-1, which led to no hydrogen production in Set-2, was further used in Methanogenesis SBR, the effluent of which was Influents A-D of Set-3. As seen in Table 4.10, Influent-D resulted in lower hydrogen yield than Influent-E in Set-3. An inhibitory substance or substances found in Influent-1 might have caused such an effect and resulted in lower hydrogen yields. On the other hand, Influent-2 of Set-2 led to hydrogen production. Influent-2 was the substrate of Methanogenesis SBR, effluent of which was used as substrates, namely, Influent D, E and F.

Hydrogen production was observed in the reactors conducted with both Influent-D and Influent-E in Set-3. Influent-D was a mixture of effluents of Methanogenesis SBR conducted with Influent-1 and Influent-2. Possible inhibitory effect of Influent-1 might have affected Influent-D. Thus, the potential inhibitory reason might be related with the operational conditions of dark fermentative SBR, most probably with the long SRTs, in addition to that of Methanogenesis SBR. Influent-1 was withdrawn from dark fermentative SBR at 10-15 days of SRT, while Influent-2 was withdrawn at 3-5 days of SRT. Therefore, when higher SRT values than 3-5 days were applied in dark fermentation, a possible inhibitory substance or substances

might be produced. However, SRT parameter alone might not be responsible for the production of the inhibitory substance. Stable and effective dark fermentation refers to higher VFA/HAc production and higher hydrogen production on second-stage photofermentation process. Therefore, a stable dark fermentation should be provided, via achieving optimum operational conditions, such as SRT.

Table 4.10 The highest hydrogen production rates and yields in Set-2, Set-3 and Set-4

Experimental Set	**Influent Name**	**Hydrogen Production Rate (mmol H_2/L.h)**	**Hydrogen Yield (mol H_2/mol HAc)**
Set-1[a]	Acetate	0.91	3.27
Set-1[b]	Acetate	1.04	-
Set-2	Influent-1	n.p.	n.p.
Set-2	Influent-2	0.48±0.08	1.61±0.24
Set-3	Influent-D	0.07±0.01	0.36±0.03
Set-3	Influent-E	0.10±0.005	0.95±0.03
Set-4	Influent-D[c]	0.021-0.025	0.04-0.35
Set-4	Influent-E[c]	0.033-0.041	0.07-0.62

[a] Experimental results obtained in Set-1
[b] Estimated results according to optimum conditions in Set-1
[c] The range of hydrogen production rates and values in the reactors conducted in Set-4 and fed with related influent are presented.
n.p.: no production

As seen in Table 4.10, hydrogen yields observed in Set-2 was higher than those observed in Set-3. Thus, photofermentation in three-stage system had lower hydrogen production rate and hydrogen yields than photofermentation in two-stage. This can be related to possible inhibitory effect of methanogenesis SBR as well as dark fermentative SBR. This inhibitory effect might be due to production of an inhibitory substance(s) at long SRTs. Influent-E and Influent-D had been obtained at 10-day and 20-day SRTs from Methanogenesis SBR, respectively. Therefore, in

addition to the effect of dark fermentative SBR, an additional long SRT effect, this time resultant of methanogenesis SBR, which is much greater for Influent-D, might have increased the inhibitory factors in Influent-D. Therefore, additional SRT effect resultant of methanogenesis stage in a three-stage system, in addition to the dark fermentation stage, might be the reason of much lower yields obtained in Set-3 and Set-4, compared to those of Set-2.

Set-3 and Set-4 were conducted with same type of Influents (Influent-D and Influent-E). Yet, Set-3 had higher yields especially for Influent-E. This is attributed to the batch mode of Set-3. Set-4, which was conducted in semi-batch mode, was subjected to lower initial substrate concentration due to dilution with the reactor content after each feeding process. In addition, potential inhibitory substances(s) might have accumulated in semi-batch reactors. These might be the reasons of observing lower rates and yields in Set-4.

The highest hydrogen production rates obtained in Set-3 (0.10±0.005 mmol H_2/L.h) and Set-4 (0.041 mmol H_2/L.h) were quite lower than the studies in literature (Table 2.5). On the other hand, the highest hydrogen yields obtained in Set-3 (0.95±0.03 mol H_2/mol HAc) and Set-4 (0.62 mol H_2/mol HAc) were higher than those obtained in some literature studies. In photofermentation studies using *R. capsulatus*, the highest hydrogen yields were obtained as 0.438 mol H_2/mol VFA (mixture of acetic, propionic and butyric acid) and 0.534 mol H_2/mol VFA (mixture of acetic, propionic and butyric acid) (Shi and Yu, 2005a; Shi and Yu, 2005b). In the study of Androga et al. (2014) using *R. capsulatus*, the highest hydrogen yield was obtained as 0.326 mol H_2/mol substrate (acetate and lactate). Therefore, it is concluded that, despite the potential inhibitory substances and lower yields obtained in Set-3 and Set-4 compared to those of Set-2, photofermentative hydrogen production in three-stage systems is still promising and can be further improved / optimized.

CHAPTER 5

CONCLUSIONS AND RECOMMENDATIONS

The effects of operational parameters on photofermentation in batch and semi-batch reactors were investigated and the application of photofermentation in multi-stage energy systems was researched in this thesis study.

The starting point was to investigate the effect of three parameters, namely, initial substrate concentration (S), initial VSS concentration (X_o, biomass) and the light intensity (I) on photofermentation and their combined effect on hydrogen production by RSM – Box-Behnken Design Method in Set-1. This study also aimed to optimize three operational conditions of the substrate, the VSS and the light intensity leading to the maximization of hydrogen production in a single stage. The optimum S/X_o ratio was also determined via this study. The significant results are as follows;

- These three parameters significantly affected the hydrogen production rate. The interaction between initial biomass and light intensity was also important as each parameter seperately. The hydrogen production rate was more sensitive to changes in light intensity.
- Optimum values, at which the highest hydrogen production rate was achieved, were 35.35 mM HAc initial substrate concentration, 0.27 g VSS/L initial biomass (*Rhodobacter capsulatus*) concentration and 3955 lux (263.6 W/m^2) light intensity.
    - When these values were used, the highest estimated hydrogen production rate to be obtained was 1.04 mmol H_2/L.hour.

- The S/X_o ratio providing the highest hydrogen production rate was 8.3 g COD_{HAc}/g VSS (9.4 g COD/g VSS; 7.7 g acetate/ g VSS).
- Experimentally, the hydrogen production rates were between 0.27-0.91 (mmol H_2/L.h); while the hydrogen yields ranged within 0.02-0.11 g H_2/g acetate (0.6-3.3 mol H_2/mol acetate; 0.019-0.10 g H_2/g COD).

- According to the experimental data, the highest hydrogen production rate was obtained in reactors where the initial substrate concentration, initial biomass concentration and light intensity values were 20 mM acetate, 0.2 g VSS/L and 4500 lux, respectively.
  - The highest hydrogen production rate was 0.91 mmol H_2 L.h (20.4 mL H_2/L.h, STP).
  - The hydrogen yield obtained in these conditions was 0.09 g H_2/g acetate (2.7 mol H_2/mol acetate; 41.5 mmol H_2/g COD_{HAc}).
  - The second highest substrate conversion efficiency was again obtained in this reactor with 68.1%.
- According to the experimental data, the highest hydrogen production yield was obtained in reactors with the initial substrate concentration, initial biomass concentration and light intensity values of 20 mM acetate, 0.35 g VSS/L and 3000 lux, respectively.
  - The highest hydrogen yield obtained was 0.11 g H_2/g Acetate (3.3 mol H_2/mol acetate, 51.6 mmol H_2/g COD_{HAc}).
  - The hydrogen production rate obtained under these conditions was 0.86 mmol H_2/L.h (19.3 mL H_2/L.h, STP).
  - The highest substrate conversion efficiency was achieved in this reactor with 83%.

In Set-2, photofermentation as a second-stage of a two-stage dark fermentation and photofermentation system was studied. The results of Set-2 are as follows;

- Hydrogen production was observed only in the photofermentation reactors conducted with Influent-2.
    - The highest hydrogen production rate obtained with this influent was 0.48±0.08 mmol H_2/L.h.
    - Lower hydrogen production rate (compared to the optimum value, 1.04 mmol H_2/L.h) can be attributed to the different carbon source mixtures formed in the Dark fermentative SBR and their effect on the bacteria.
    - Hydrogen yield was 1.61±0.24 mol H_2/mol acetate or 0.054 g H_2/g acetate (0.050 g H_2/g COD_{HAc}).
    - This yield was lower compared to the highest yield (0.11 g H_2/g acetate, 0.10 g H_2/g COD_{HAc}, 3.3 mole H_2/mole acetate) observed in Set-1 conducted with acetic acid directly. However, it was comparable to two-stage systems.
    - This yield was obtained at 21 mM HAc (30 mM tVFA) substrate concentration, 3955 lux light intensity and 8.3 g COD_{HAc}-acetate/g VSS S/X_o ratio.
- Hydrogen production was not observed in photofermentation reactors conducted with Influent-1.
    - There was no inhibition due to any ammonium ion, pH, bacterial contamination, light intensity, total VFA or butyric acid concentration.
    - Although, Influent-1 and Influent-2 had similar characteristics (TAN, VFA type and concentrations, pH), hydrogen production was not observed in Influent-1. Thus, it was speculated that presence of a substance or substances in Influent-1 might have caused bacterial inhibition effect. This situation was attributed to the operational

conditions, mainly long SRTs of dark fermentative SBR where Influent-1 was produced.

In Set-3, photofermentation as a third-stage of a three-stage system composed of dark fermentation, methanogenesis and photofermentation processes was investigated. The photofermentative hydrogen production yields and total energy yields obtained in this three-stage system, which has not been studied so far, provide a preliminary knowledge for future three-stage systems and comparison with two-stage systems frequently encountered in literature studies. The significant results are as follows;

- The highest hydrogen production rate and hydrogen yield were observed as 0.10±0.005 mmol H_2/L.h and 0.032±0.001 g H_2/g acetate (0.95±0.03 mol H_2/mol acetate) respectively, from Influent-E. These values are nearly one-tenth of the values of the highest estimated hydrogen production rate (1.04 mmol H_2/L.h), experimental hydrogen production rate (0.91 mmol H_2/L.h) and experimental hydrogen yield (0.11 g H_2/g acetate; 3.27 mol H_2/mol acetate) obtained in optimum batch photofermentation conditions in Set-1. Yet, it should be noted that substrate was acetate in Set-1, where, there was no potential inhibitory products for photofermentation and the conditions were optimum operational conditions obtained via the experiment.
- The highest hydrogen production rate and hydrogen yield were observed as 0.07±0.01 mmol H_2/L.h and 0.012±0.001 g H_2/g acetate (0.36±0.02 mol H_2/mol acetate) respectively, from Influent-D. The hydrogen production rate and hydrogen yield observed from Influent-D was lower than that observed from Influent-E. This can be related to the lower concentration of possible inhibitory substance in Influent-E. Influent-E was obtained at 10-day SRT while Influent-D at 20-day SRT of Methanogenesis SBR. Therefore, an additional long SRT effect, this time resultant of methanogenesis SBR, in addition to dark fermentative SBR might have increased the inhibitory effect of Influent-D.

In Set-4, the optimum HRT leading to the highest photofermentative hydrogen production rate in semi-batch reactors was investigated. Photofermentation reactors in Set-4 were also third-stage of a three-stage system. Thus, the effect of operation mode (batch or semi-batch) in photofermentative hydrogen production in a three-stage system could be compared. The significant results are as follows;

- Hydrogen production was observed in lower amounts in Set-4 compared to Set-3.
- The HRT value leading to the highest hydrogen production rate was observed as 4 days for both types of influents (Influent-D and Influent-E).
    - The highest hydrogen production rates observed at 4-day HRT were 0.041 mmol H_2/L.h for Influent-E and 0.025 mmol H_2/L.h for Influent-D.
- The HRT value leading to the highest hydrogen yield was observed as 6 days for both types of influents (Influent-D and Influent-E).
    - The highest hydrogen yields observed at this condition were 0.62 mol H_2/mol acetate for Influent-E and 0.35 mol H_2/mol acetate for Influent-D.
- The hydrogen production rates and yields observed in the reactors conducted with Influent-E were higher than those in the reactors conducted with Influent-D.
- The formation of granules and low bacterial growth were observed in the reactors conducted with both Influent-D and Influent-E. It was thought that a substance/chemical or substances/chemicals produced during the operation of dark fermentative SBR and/or methanogenesis SBR might have caused an inhibitory effect or might have been the source of the stressfull condition. This explains the lower hydrogen production rates and yields observed in Set-4 than those observed at optimum conditions in batch reactors (Set-1).

This thesis study revealed that it is possible to produce photofermentative hydrogen in three-stage systems, composed of dark fermentation, methanogenesis and photofermentation in sequence. In three-stage systems, photofermentative hydrogen production yields and rates decreased, despite the similar influent VFA concentrations. This was attributed to the potential inhibitory substances likely to be produced in dark fermentation and/or methanogenesis stages due to long SRTs. Granules were developed at early stages of photofermentation studies of three-stage systems. This was also attributed to the inhibitory substances/factors resulting in stress for *Rhodobacter capsulatus*. The result of this thesis study might be useful to supply a basis for three-stage systems in future studies.

To better understand the reason of lower hydrogen production rates and yields in a third-stage photofermentation of a three-stage system, more detailed photofermentation sets may be conducted in the light of this thesis study. Moreover, inhibitory factor(s) and granulation phenomenon observed in three-stage photofermentation systems should be searched in detail. Considering the results of TUBITAK Project (112M252), it should be noted that, three-stage system configurations were found to provide higher energy and yields than two-stage dark fermentation and photofermentation system. In other words, addition of the methanogenesis process as an intermediate stage between the two-stage dark fermentation and photofermentation system significantly increased the total (gross) energy and yield obtained per unit substrate by 27-50%. Three-stage systems were also compared with two-stage dark fermentation and methanogenesis systems' efficiencies. The results revealed that energy and yield obtained were very close (89-96%) to the theoretical values of the latter. Configuration of a three-stage system composed of dark fermentative SBR, methanogenesis SBR and batch photofermentation reactor, where the photofermentation stage is Set-3 of this thesis study, even provided the highest energy and yield compared to all possible system combinations and theoretical values. Therefore, three-stage systems seem to be promising. It is believed that optimization of initial COD concentration of the three-stage system might improve the photofermentation stage's efficiency and, in turn,

that of the three-stage system. Such a system, when optimized, might lead to higher total energy yields/rates per unit substrate, because the substrate would be used in full extent, especially compared to two-stage dark fermentation-methanogenesis systems. Yet, the need for TAN removal should be taken into consideration. The result of this thesis study might be useful to achieve higher hydrogen production rates and yields in three-stage systems in future studies.

REFERENCES

Abd-Alla M. H., Morsy F. H., El-Enany A. E., (2011), Hydrogen production from rotten dates by sequential three stages fermentation, *International Journal of Hydrogen Energy, 36,*13518-13527.

Abo-Hashesh M., Ghosh D., Tourigny A., Taous A., Hallenbeck P. C., (2011), Single stage photofermentative hydrogen production from glucose: An attractive alternative to two stage photofermentation or co-culture approaches, *International Journal of Hydrogen Energy, 36,*13889-13895.

Adessi A., Philippis R. D., (2014), Photobioreactor design and illumination systems for H_2 production with anoxygenic photosynthetic bacteria: A review, *International Journal of Hydrogen Energy, 39,* 3127-3141.

Afsar N., Özgür E., Gürgan M., Akköse S., Yüzel M., Gündüz U., Eroglu I., (2011), Hydrogen productivity of photosynthetic bacteria on dark fermenter effluent of potato steam peels hydrolysate, *International Journal of Hydrogen Energy, 36,*432-438.

Akköse S., Gündüz U., Yücel M., Eroğlu I., (2009), Effect of ammonium ion, acetate and aerobic conditions on hydrogen production and expression levels of nitrogenase genes in Rhodobacter sphaeroides O.U.001, *International Journal of Hydrogen Energy, 24,* 8818-8827.

Akman M. C., Erguder T. H., Gündüz U., Eroğlu İ., (2015), Investigation of the effects of initial substrate and biomass concentrations and light intensity on photofermentative hydrogen gas production by Response Surface Methodology, *International Journal of Hydrogen Energy, 40,* 5042-5049.

Androga D. D., Ozgur E., Eroglu I., Gunduz U., Yucel M., (2011), Factors affecting the long term stability of biomass and hydrogen productivity in outdoor

photofermentation, *International Journal of Hydrogen Energy, 36,* 11369-11378.

Androga D. D., Sevinç P., Koku H., Yücel M., Gündüz U., Eroğlu I., (2014), Optimization of temperature and light intensity for improved photofermentative hydrogen production using Rhodobacter capsulatus DSM 1710, *International Journal of Hydrogen Energy, 39*, 2472-2480.

Argun H., Kargi F., Kapdan I. K., (2008), Light fermentation of dark fermentation effluent for bio-hydrogen production by different Rhodobacter species at different initial volatile fatty acid (VFA) concentrations, *International Journal of Hydrogen Energy, 33,* 7405-7412.

Argun H., Kargı F., Kapdan İ. K., Öztekin R., (2008), Batch dark fermentation of powdered wheat starch to hydrogen gas: Effects of the initial substrate and biomass concentrations, *International Journal of Hydrogen Energy, 33,* 6109-6115.

Argun H., Kargi F., (2011), Bio-hydrogen production by different operational modes of dark and photo-fermentation: An overview, *International Journal of Hydrogen Energy, 36*, 7443-7459.

Asada Y., Oshawa M., Nagai Y., Ishimi K., Fukatsu M., Hideno A., Wakayama T., Miyake J., (2008), Re-evaluation of hydrogen productivity from acetate by some photosynthetic bacteria, *International Journal of Hydrogen Energy, 33 (19),* 5147-5150.

Avcıoğlu S. G., Androga D. D., Uyar B., Özgür E., Gündüz U., Yücel M., Eroğlu İ., 2009, "Continuous hydrogen production by R.capsulatus on acetate in panel photobioreactors", HYPOTHESIS VIII, Lisbon, Portugal, April 1-3.

Avcioglu S. G., Ozgur E., Eroglu I., Yucel M., Gunduz U., (2011), Biohydrogen production in an outdoor panel photobioreactor on dark fermentation effluent of molasses, *International Journal of Hydrogen Energy, 36,* 11360-11368.

Azwar M. Y., Hussain M. A., Abdul-Wahab A. K., (2014), Development of biohydrogen production by photobiological, fermentation and electrochemical processes: A review, *Renewable and Sustainable Energy Reviews, 31,* 158-173.

BACAS Report, "Hydrogen as an Energy Carrier", Royal Belgian Academy Council of applied Science (2006).

Barbosa M.J., Rocha J. M. S., Tramper J., Wijffels R. H., (2001), Acetate as a carbon source for hydrogen production by photosynthetic bacteria, *Journal of Biotechnology, 85,* 25-33.

Basak N., Jana A. K., Das D., Saikia D., (2014), Photofermentative molecular biohydrogen production by purple-non-sulfur (PNS) bacteria in various modes: The present progress and future perspective, *International Journal of Hydrogen Energy, 39,* 6853-6871.

Basak N., Das D., (2007), The prospect of purple non-sulfur (PNS) photosynthetic bacteria for hydrogen production: the present state of art, *World Journal of Microbiology and Biotechnology, 23,* 31-42.

Bergey D. H., Holt J. G., (1994), Bergey's Manual of Determinative Bacteriology (9^{th} Ed.) Philedelphia: Lippincott Williams &Wilkins.

Bharathiraja B., Sudharsanaa T., Bharghavi A., Jayamuthunagai J., Praveenkumar R., (2016), Biohydrogen and Biogas – An overview on feedstocks and enhancement process, *Fuel, 185,* 810-828.

Bicakova O., Straka P., (2012), Production of hydrogen from renewable resources and its effectiveness, *International Journal of Hydrogen Energy, 37,*11563-11578.

Boodhun B. S. F., Mudhoo A., Kumar G., Kim S., Lin C., (2017), Research perspectives on constraints, prospects and opportunities in biohydrogen production, *International Journal of Hydrogen Energy, 42,* 27471-27481.

Boran E., Ozgur E., Burg J. V. D., Yucel M., Gunduz U., Eroglu I., (2010) Biological hydrogen production by Rhodobacter capsulatus in solar tubular photo bioreactor, *Journal of Cleaner Production, 18,* 29-35.

Boran E., Özgür E., Yücel M., Gündüz U., Eroglu I., (2012), Biohydrogen production by Rhodobacter capsulatus Hup^- mutant in pilot solar tubular photobioreactor, *International Journal of Hydrogen Energy, 37,* 16437-16445.

Castillo P., Magnin J. P. Velasquez M., Willison J., (2012), Modeling and optimization of hydrogen production by the photosynthetic bacterium Rhodobacter capsulatus by the methodology of design of experiments (DOE): interaction between lactate concentration and light luminosity, *Energy Procedia, 29,* 357-366.

Dalena F., Basile A., Rossi C., 2017, Bioenergy systems for the future: Prospects for biofuels and biohydrogen. Elsevier, New York.

Das D., Veziroglu T. N., (2008), Advances in biological hydrogen production processes, *International Journal of Hydrogen Energy, 33,*6046-6057.

Dincer İ., Acar C., (2015), Review and evaluation of hydrogen production methods for better sustainability, *International Journal of Hydrogen Energy, 40,* 11094-11111.

Dinçer İ., Zamfirescu C., 2016, Sustainable hydrogen production. Elsevier, New York.

Doğan M.G., (2011), Microarray analysis of the effects of heat and cold stress on hydrogen productionmetabolism of Rhodobacter capsulatus, M.S. Thesis, Middle East Technical University.

Dutta S. A., (2014), Review on production, storage of hydrogen and its utilization as an energy resource, *Journal of Industrial and Engineering Chemistry, 20,* 1148-1156.

Elkahlout K., Alipour S., eroglu I., Gunduz U., Yucal M., (2016), Long-term biological hydrogen production by agar immobilized Rhodobacter capsulatus in a sequential batch photobioreactor, *Bioprocess and Biosystems Engineering, 40,* 589-599.

Ergüder T. H., Demirer G. N., (2005), Investigation of granulation of a mixture of suspended anaerobic and aerobic cultures under alternating anaerobic/microaerobic/aerobic conditions, *Process Biochemistry, 40,* 3732-3741.

Eroglu I., Aslan K., Gunduz U., Yucel M., Turker L., (1998), Continuous hydrogen production by Rhobacter sphaeroides O.U.001, *Biohydrogen*, 143-149.

Eroglu I., Sevinc P., Gündüz U., Yücel M., (2010), The effect of temperature and light intensity on hydrogen production by Rhodobacter capsulatus, *Proceedings of World Hydrogen Energy Conference, Germany, 18,* 26-31.

Eroğlu İ., Tabanoğlu A., Gündüz U., Eroğlu E., Yücel M., (2008), Hydrogen production by Rhodobacter sphaeroides O.U.001 in a flat plate solar bioreactor, *International Journal of Hydrogen Energy, 33,* 531-541.

Gandia L. M., Arzamendi G., Dieguez P. M., 2013, Renewable Hydrogen Technologies: Production, Purification, Storage, Applications and Safety. Elsevier, Poland.

Gebicki J., Modigell M., Schumacher M., van der Burg J., Roebroeck E., (2010), Comparison of two reactor concepts for anoxygenic H_2 production by Rhodobacter capsulatus, *Journal of Cleaner Production, 18,* 36-42.

Gustin S., Marinsek-Logar R., (2011), Effect of pH, temperature and air flowrate on the continuous ammonia stripping of the anaerobic digestion effluent, *Process Safety and Environmental Protection, 89,* 61-66.

Hillmer P., Gest H., (1977), H_2 Metabolism in the photosynthetic bacterium Rhodopseudomonas capsulate: H_2 production by growing cultures, *Journal of Bacteriology*, 724-731.

Imhoff J. F., (1995), Taxonomy and physiology of phototropic purple bacteria and green sulfur bacteria, *Anoxygenic Photosynthetic Bacteria, 2,* 1-15.

Jouanneau Y., Wong B., Vignais P. M., (1985), Stimulation by light of nitrogenase synthesis in cells of Rhodopseudomonas capsulate growing in N-limited continuous cultures, *Biochim Biophys Acta, 808,* 149-155.

Kars G., Gunduz U., Yucel M., Turker L., Eroglu I., (2006) Hydrogen production and transcriptional analysis of nifD, nifK and hupS genes in Rhodobacter sphaeroides O.U.001 gron in media with different concentration of molybdenum and iron, *International Journal of Hydrogen Energy, 31,* 1536-1544.

Kirby C. S., Cravotta III C. A., (2005), Net alkalinity and net acidity 1: Theoretical considerations, *Applied Geochemistry, 20,* 1920-1940.

Koku H., Eroglu I., Gündüz U., Yücel M., Türker L., (2002), Aspects of the metabolism of hydrogen production by Rhodobacter sphaeroides, *International Journal of Hydrogen Energy, 27,* 1315-1329.

Kothari R., Tyagi V. V., Pathak A. E., (2010), Waste-to-energy: a way from renewable energy sources to sustainable development, *Renewable and Sustainable Energy Reviews, 14,* 3164-3170.

Laurinavichene T. V., Laurinavichius K. S., Belokopytov B. F., Laurinavichyute D. K., Tsygankov A. A., (2013), Influence of sulfatereducing bacteria, sulfide and molybdate on hydrogen photoproduction by purple nonsulfur bacteria, *International Journal of Hydrogen Energy, 38,* 5545-5554.

Lei X., Sugiura N., Feng C., Maekawa T., (2007), Pretreatment of anaerobic digestion effluent with ammonia stripping and biogas purification, *Journal of Hazardous Materials, 145,* 391-397.

Lin C., Wilson K., 2016, Handbook of Biofuels Production: Process and Technologies. Elsevier, UK.

Liu Q., Zhang X., Zhou Y., Zhao A., Chen S., qian G., Xu Z. P., (2011), Optimization of fermentative biohydrogen production by response surface methodology using fresh leachate as nutrient supplement, *Bioresource Technology, 102,* 8661-8668.

Ljunggren M., Wallberg O., Zacchi G., (2011), Techno-economic comparison of a biological hydrogen process and a 2nd generation ethanol process using barley straw as feedstock, *Bioresource Technology, 102,* 9524-9531.

Lo Y., Chen C., Lee C., chang J., (2011), Photofermentative hydrogen production using dominant components (acetate, lactate, and butyrate) in dark fermentation effluents, *International Journal of Hydrogen Energy, 36,* 14059-14068.

Mars A. E., Özgür E., Peksel B., Louwerse A., Yucel M., Gunduz U., Claassen P. A. M., Eroğlu İ., (2010), Biohydrogen production from beet molasses by sequentiak dark and photofermentation, *International Journal of Hydrogen Energy, 35,* 511-517.

Mathews J., Wang G., (2009), Metabolic pathway engineering for enhanced biohydrogen production, *International Journal of Hydrogen Energy, 34,* 7404-7416.

Mazloomi K., Gomes C., (2012), Adar E., Karatop B., İnce M., Bilgili M. S., (2016), Hydrogen as an energy carrier: Prospects and challenges, *Renewable and Sustainable Energy Reviews, 16,* 3024-3033.

Montgomery D. C., 2009, Design and analysis of experiments. Wiley Hoboken, New Jersey.

Nikolaidis P., Poullikkas A., (2017), A comparative overview of hydrogen production processes, *Renewable and Sustainable Energy Reviews, 67,* 597-611.

Ozkan E., Uyar B., Ozgur E., Yucel M., Eroglu I., Gunduz U., (2012), Photofermentative hydrogen production using dark fermentation effluent of sugar beet thick juice in outdoor conditions, *International Journal of Hydrogen Energy, 37,* 2044-2049.

Özgür E., Mars A. E., Peksel B., Louwerse A., Yücel M., Gündüz U., Claassen P. A., Eroglu I., (2010), Biohydrogen production from beet molasses by sequential dark and photofermentation, *International Journal of Hydrogen Energy, 35,* 511-517.

Özgür E., Peksel B., (2013), Biohydrogen production from barley straw hydrolysate through sequential dark and photofermentation, *Journal of Cleaner Production, 52,* 14-20.

Özgür E., Uyar B., Öztürk Y., Yücel M., Gündüz U., Eroglu I., (2010), Biohydrogen production by Rhodobacter capsulatus on acetate at fluctuating temperatures, *Resources, Conservation and Recycling, 54,* 310-314.

Öztürk Y., Gökçe A., (2012), Characterization of hydrogen production by an ammonium insensitive pseudo-revertant of a CBB deficient Rhodobacter capsulatus strain, *International Journal of Hydrogen Energy, 37,*8811-8819.

Pandey A., Ghang J., Hallenbeck P. C., Larroche C., 2013, Biohydrogen. Elsevier, Polland.

Rezania S., Din M. F. M., Taib S. M., Sohaili J., Chelliapan S., Kamyab H., Saha B. B., (2017), Review on fermentative biohydrogen production from water

hyacinth, wheat straw and rice straw with focus on recent perspectives, *International Journal of Hydrogen Energy, 42,* 20955-20969.

Sagir, E., Alipour S., Elkahlout K., Koku H., Gunduz U., Eroglu I., Yucel M., (2017), Scale-up studies for stable, long-term indoor and outdoor production of hydrogen by immobilized Rhodobacter capsulatus, *International Journal of Hydrogen Energy, 42,* 22743-22755.

Sasikala K., Ramana C. V., Rao P. R., (1991), Environmental regulation for optimal biomass yield and photoproduction of hydrogen by Rhodobacter sphaeroides O.U.001, *International Journal of Hydrogen Energy, 16,* 597-601.

Savasturk D., Kayahan E., Koku H., (2018), Photofermentative hydrogen production from molasses: Scale-up and outdoor operation at low carbon-to-nitrogen ratio, *International Journal of Hydrogen Energy,* 1-12.

Sevinc P., Gündüz U., Eroglu I., Yücel M., (2012), Kinetic analysis of photosynthetic growth, hydrogen production and dual substrate utilization by Rhodobacter capsulatus, *International Journal of Hydrogen Energy, 37,* 16430-16436.

Shi X. Y., Yu H. Q., (2005a), Response surface analysşs on the effect of cell concentration and light intensity on hydrogen production by Rhodopseudomonas capsulata, *Process Biochemistry, 40,* 2475-2481.

Shi X. Y., Yu H. Q., (2005b), Optimization of glutamate concentration and pH for H_2 production from volatile fatty acids by Rhodopseudomonas capsulata, *Letters in Applied Microbiology, 40,* 401-406.

Su H., Cheng J., Zhou J., Song W., Cen K., (2009), Improving hydrogen production from cassava starch by combination of dark and photofermentation, *International Journal of Hydrogen Energy, 34,* 1780-1786.

URL-2, https://microbewiki.kenyon.edu/index.php/Rhodobacter, last access date: May 01, 2018.

URL-1, http://lgem.nl/gemtube-tubular-photobioreactors, last access date: May 01, 2018.

Uyar B., Eroglu I., Yücel M., Gündüz U., Türker L., (2007), Effect of light intensity, wavelength and illumination protocol on hydrogen production in photobioreactors, *International Journal of Hydrogen Energy, 32,* 4670-4677.

Uyar B., Eroglu I. Yücel M., Gündüz U., (2009), Photofermentative hydrogen production from volatile fatty acids present in dark fermentation effluents, *International Journal of Hydrogen Energy, 34,*4517-4523.

Uyar B., Gurgan M., Ozgur E., Gunduz U., Yucel M., Eroglu I., (2015), Hydrogen production by hup (-) mutant and wild-type strains of Rhodobacter capsulatus from dark fermentation effluent of sugar beet thick juice in batch and continuous photobioreactors, *Bioprocess and Biosystems Engineering, 38,* 1935-1942.

Veras T. S., Mozer T. S., Santos D. C. R. M., Cesar A. S., (2017), Hydrogen: Trends, production and characterization of the main process worldwide, *International Journal of Hydrogen Energy, 42,* 2018-2033.

Wang J., Wan W., (2008), Optimization of fermentative hydrogen production process by response surface methodology, *International Journal of Hydrogen Energy, 33,* 6976-6984.

Wang J., Wan W., (2009), Experimental design methods for fermentative hydrogen production: A review, *International Journal of Hydrogen Energy, 34,* 235-244.

Weaver P. F., Wall J. D., Gest H., (1975), Characterization of Rhodopseudomonas capsulata, *Archives of Microbiology, 105,* 207-216.

World Energy Council, (2013), World Energy Resources Research.

Wu T. Y., Hay J. X. W., Kong L. B., Juan J. C., Jahim J. M., (2012), Recent advances in reuse of waste material as substrate to produce biohydrogen by purple non-sulfur (PNS) bacteria, *Renewable and Sustainable Energy Reviews, 16,* 3117-3122.

Wu T.Y., Hay J. X. W., Kong L. B., Juan J. C., Jahim J. M., (2012), Recent advances in reuse of waste material as substrate to produce biohydrogen, *Renewable and Sustainable Energy Reviews, 16,* 3117-3122.

Xing Y., Fan S. Q., Zhang J. N., Fan Y. T., Hou H. W., (2011), Enhanced bio-hydrogen production from corn stalk by anaerobic fermentation using response surface methodology, *International Journal of Hydrogen Energy, 36,* 12770-12779.

Yetis M., Gunduz U., Eroglu I., Yucel M., Turker L., (2000), Photoproduction of hydrogen from sugar refinery wastewater by Rhodobacter sphaeroides OU001, *International Journal of Hydrogen Energy, 25,* 1035-1041.

Zannoni D., Philippis R., 2014, Microbial BioEnergy: Hydrogen Production. Springer, New York.

Zhu H., Fang H. H. P., Zhang T., Beaudette L.A., (2007), Effect of ferrous ion on photo heterotrophic hydrogen production by Rhodobacter sphaeroides, *International Journal of Hydrogen Energy, 32,* 4112-4118.

APPENDIX A

OD – VSS CALIBRATION CURVE

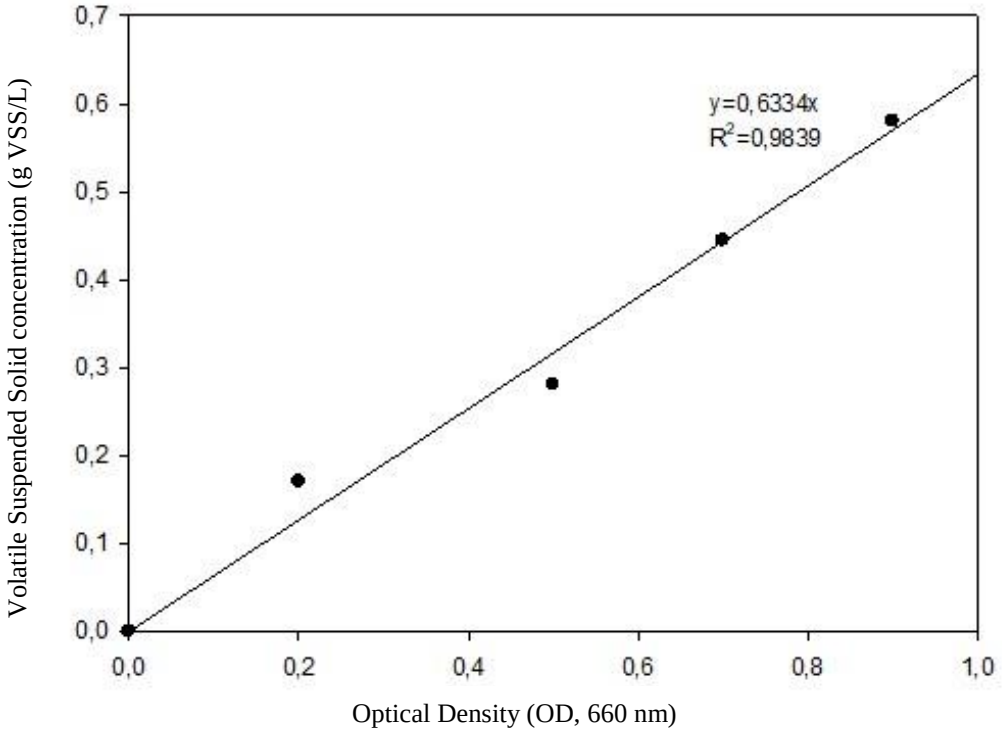

Figure A.1 OD – VSS calibration curve used for dry cell weight for *Rhodobacter capsulatus*

APPENDIX B

HPLC CALIBRATION CURVES FOR THE VFA ANALYSES

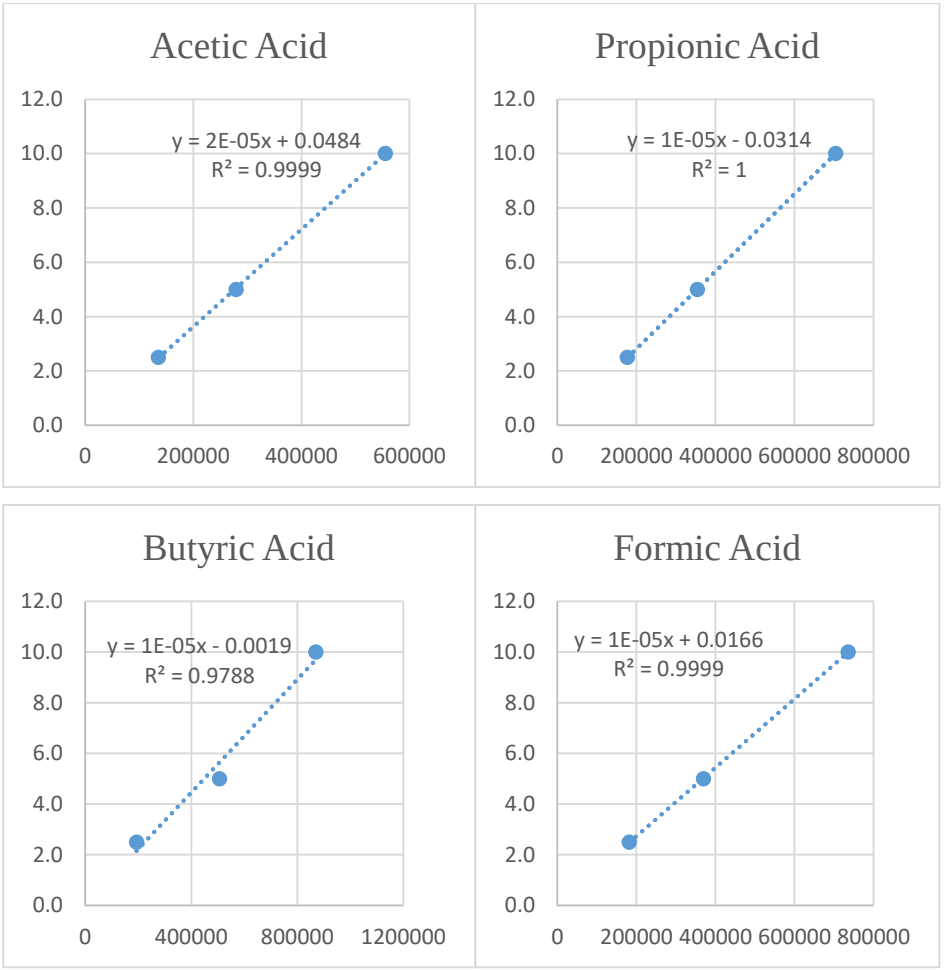

Figure B.1 HPLC Calibration curves used for VFAs (In all the graphs, x-axis is the peak area calculated by the HPLC and y-axis is the concentration, in mM of the related acid.)

APPENDIX C

EQUATIONS AND EXAMPLES USED IN PHOTOFERMENTATION SETS

The formulas used for calculations of yields, rates and efficiencies in photofermentation experiments are presented below with example solutions for Reactor 27 in Set-2. Similar calculations have been done for all photofermentation reactors.

Example calculations for Reactor 27 in Set-2

Hydrogen Production Rate (H_2 productivity)

$$Hydrogen\ Production\ Rate\ (HPR)(mg\ H2/Lc.hour) = y(L/Lc.hour) \times 0.082(g/Lc) \times 1000(mg/g)$$

2 = Density of Hydrogen (g/L at 30°C)

L = Volume of hydrogen produced (mL)

L_c = Effective volume of the reactor = 50 mL

y = slope of L/L_c vs. time graph

Table C.1 Volume of Hydrogen gas produced with respect to time for Reactor 27 (mL, 30^{o}C)

Time (hour)	0	24	48	72	96	120	144	168
Cumulative Hydrogen Production(mL)	0	24.84	52.44	59.8	62.1	66.7	67.62	67.62

L/L_c ratio at 24th hour;

L/L_c = 24.84 mL / 50 mL = **0.497**

Table C.2 L/Lc ratio variations with time

Time (hour)	0	24	48	72	96	120	144	168
L/Lc	0	0.497	1.049	1.196	1.242	1.334	1.352	1.352

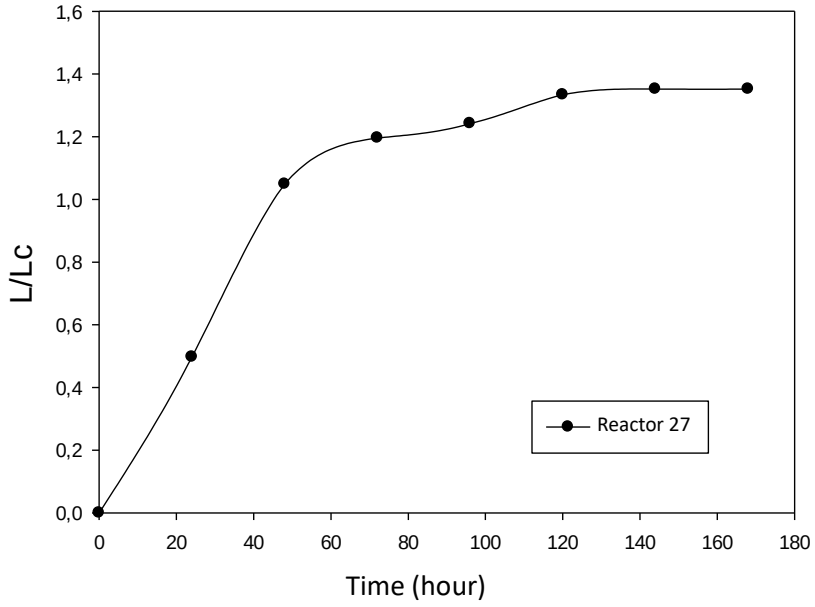

Figure C.1 L/Lc ratio variation with time

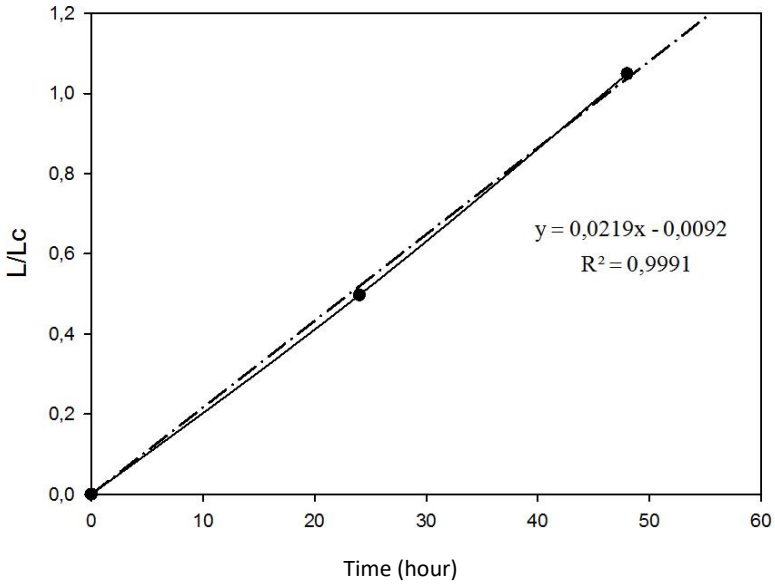

Figure C.2 The slope of linear part of L/Lc ratio variation with time

y value was calculated using Figure C.1 and Figure C.2;

y= 0.0219

$$HPR\ (mg\ H2/Lc.hour) = \ 0.0219x0.082x1000 = 1.8\ mg\frac{H2}{Lc.hour}$$

Hydrogen Yield

$$Hydrogen\ Yield\ (g\ H2/g\ acetate) = \frac{mass\ of\ hydrogen\ produced}{mass\ of\ acetate\ used}$$

$$mass\ of\ acetate\ used\ (g) = acetate\ conc.\ (M)\ x\ liquid\ volume\ (L)$$

$$x\ molecular\ weight\ (\frac{g}{mol})$$

$$mass\ of\ hydrogen\ produced = 0.0676\ (L)x0.082\left(\frac{g}{L}\right) = 0.0055\ g$$

$$mass\ of\ acetate\ used = 0.02\ (M)x0.05\ (L)x60.05\ \left(\frac{g}{mol}\right) = 0.06\ g$$

$$Hydrogen\ Yield\ (g\ H2/g\ acetate) = \frac{0.0055\ g\ H2}{0.06\ g\ acetate}$$

$$= 0.092\ g\ H2/g\ acetate$$

Substrate Conversion Efficiency

$$Substrate\ conv.eff. = \frac{hydrogen\ produced\ (mol)}{hydrogen\ that\ should\ be\ produced\ theoretically\ (mol)} x100$$

$CH_3COOH + 2H_2O \rightarrow 4H_2 + 2CO_2$

Hydrogen that should be produced theoretically from 20 mM (0.001 mol) of acetate is calculated as 0.004 mol.

MW $_{H2}$ = 2 g/mol

Volume of total hydrogen produced (mL, 30°C) = 67.6

Moles of hydrogen produced (g)= 0.0055

$$Substrate\ conversion\ efficiency = \frac{0.00555\ g\ H2\ /\ 2g/mol}{0.004\ mol}\ x100 = 69.3\%$$

Light Conversion Efficiency

$$Light\ conversion\ efficiency = \frac{33{,}6 \times \rho\ H2 \times volume\ of\ hydrogen\ produced}{I \times A \times t}\ x100$$

$33{,}6 = energy\ density\ of\ hydrogen\ (\ Watt.h/g)$

$I = \ Light\ intensity$ = 4500 lux = 300 Watt/m^2

$A =$ 0.002 m^2 (for 55 mL glass reactors)

$t = hydrogen\ production\ period$ =144 hours

$$Light\ conversion\ efficiency = \frac{(33{,}6 \times 0.082 \times 67.62)/1000}{300 \times 0.002 \times 144}\ x100$$

$$= 0.22\%$$

APPENDIX D

EXPERIMENTS PERFORMED FOR AMMONIA REMOVAL AS A PRETREATMENT STEP FOR PHOTOFERMENTATION

Among ammonia removal methods, two methods were initially selected to investigate the ammonium removal from the effluents, namely, ammonia stripping and zeolite (clinoptilolite) adsorption. Preliminary experiments were performed for both methods.

D.1 Materials and Methods

D.1.1 Ammonia Removal with Air Stripping Method

One of the most common treatment methods for reducing the ammonia concentration below the limit values (<36 mg/L NH_4) is air stripping. The most important step in the air stripping method is the pH increase (Lei et al., 2007). Gustin et al. (2011) has reported that the increase in pH value up to 10 provides increase in ammonia removal. Another factor influencing the air stripping method is temperature (Gustin et al., 2011). In the same study conducted from Gustin et al. (2011), it was observed that the ammonia removal did not show a significant change in the working temperature range of 30°C-70°C. The air stripping method also depends on the ventilation rate (Lei et al., 2007). Lei et al. (2007) stated that the optimum air flow rate was 5 L/min for 1 L of wastewater. According to these information, pH, temperature and air flow rate values to be applied in air stripping experiments were determined as 10, 35°C and 5 L/min.L, respectively. The effluents withdrawn from methanogenesis SBR was used as samples. Two samples were withdrawn in two consecutive days and ammonia concentrations were measured as

148.4 mg/L NH_4-N and 170.8 mg/L NH_4-N. It might be possible to observe much higher ammonia concentrations from these values in methanogenesis SBR, in turn, in influents of photofermentation studies. Therefore, in order to investigate the stripping potential of higher ammonia concentrations, two new samples were developed by adding synthetic ammonia to the samples withdrawn from methanogenesis SBR in two consecutive days. Ammonia concentrations of 4 samples used in experiments are given in Table D.1. Experiments were conducted in 250 mL erlenmeyer flask with 200 mL of effective volume.

Table D.1 Ammonia concentrations of influents applied in air stripping experiments

	NH_4-N (mg/L)
Sample 1	170.8
Sample 2	246.4
Sample 3	148.4
Sample 4	215.6

D.1.2 Ammonia Removal with Zeolite Adsorption

The other method applied commonly for reducing the ammonia concentration below the limit values is zeolite adsorption. This method is based on the substitution of cations such as Na^+, K^+, Ca^{+2}, Mg^{+2} on the zeolite surface with ammonia ion (Karadağ et al.,2007). Karadağ et al. (2008) reported that pretreatment of zeolite with NaCI solution increased the removal efficiency. Initial ammonia concentration, zeolite dosage, mixing speed, particle size and temperature are important parameters affecting this method (Erdoğan et al., 2011). Erdoğan et al. (2011) stated that high ammonia concentration and high mixing speed increased the adsorption rate. In the same study, it was also stated that increasing the temperature in the range of 25°C-40°C reduced the adsorption rate. If the zeolite particle size is below 1 mm, the adsorption rate increases. In the light of these information, the mixing speed and temperature were set as 170 rpm and 25°C in the zeolite adsorption experiments, respectively. The particle size was determined to be less than 1 mm. The effluents

withdrawn from methanogenesis SBR was used as samples. It might be possible to observe much higher ammonia concentrations from these values in methanogenesis SBR, in turn, in influents of photofermentation studies. Therefore, in order to investigate the adsorption potential of higher ammonia concentrations, one new sample was developed by adding synthetic ammonia to the sample withdrawn from methanogenesis SBR. The other sample was used directly after withdrawn from methanogenesis SBR. Ammonia concentrations of these two samples were measured as 207.2 mg/L NH_4-N and 74.2 mg/L NH_4-N. The sample, which was used directly, was not withdrawn from methanogenesis SBR concurrently with air stripping experiments. It was aimed to determine the appropriate dose of zeolite by working with 4 different zeolite dosage for two samples. Thus, 0.5, 1, 1.5 and 2 mg zeolite/50 mL sample was applied for each concentration of ammonia studied. Experiments were conducted in 250 mL erlenmeyer flask with 100 mL of effective volume. Zeolite obtained from Manisa-Gördes region was used in the study. Zeolite particle size was first reduced below 1 mm, then pretreated with 1 M NaCI solution.

D.2 Results and Discussion

D.2.1 Results of Ammonia Removal via Air Stripping

In this study, significant ammonia removal was observed with air stripping method. The removal efficiencies obtained after 10 hours are presented in Table D.2. The change in ammonia concentrations in four different samples with different initial ammonia concentrations over time are shown in Figure D.1, Figure D.2, Figure D.3 and Figure D.4.

Table D.2 Removal efficiencies obtained via air stripping

Sample No.	Removal efficiency (%)
1	95
2	94
3	93
4	85

As seen in Figure D.1, Figure D.2, Figure D.3 and Figure D.4 the removal of ammonia does not resemble a zero-order reaction. In order to determine the reaction kinetics, the changes in the logarithm (lnC) of the ammonia concentrations over time were calculated and are presented in Figure D.5, Figure D.6, Figure D.7 and Figure D.8.

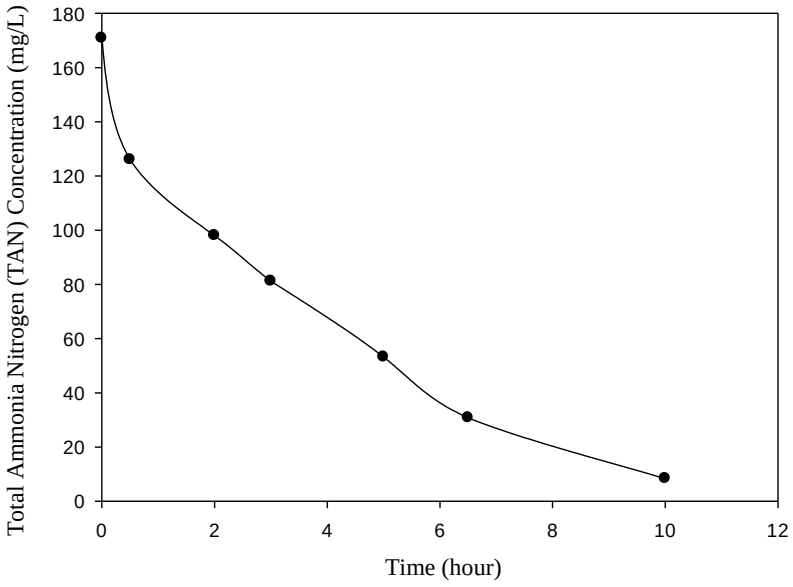

Figure D.1 The change in ammonia concentration in Sample 1

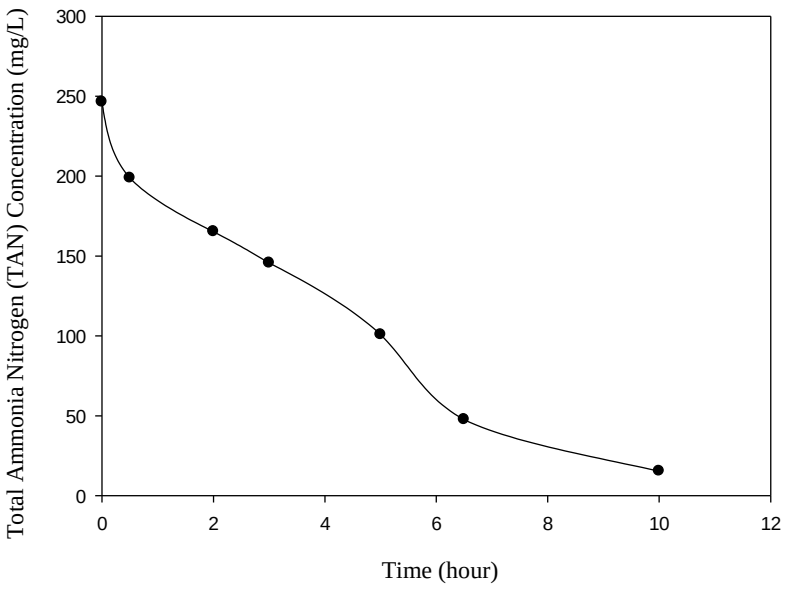

Figure D.2 The change in ammonia concentration in Sample 2

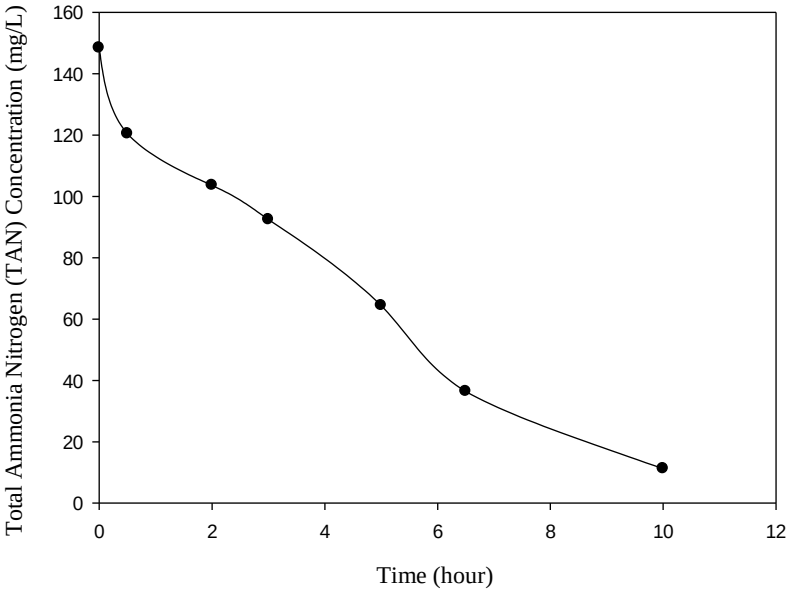

Figure D.3 The change in ammonia concentration in Sample 3

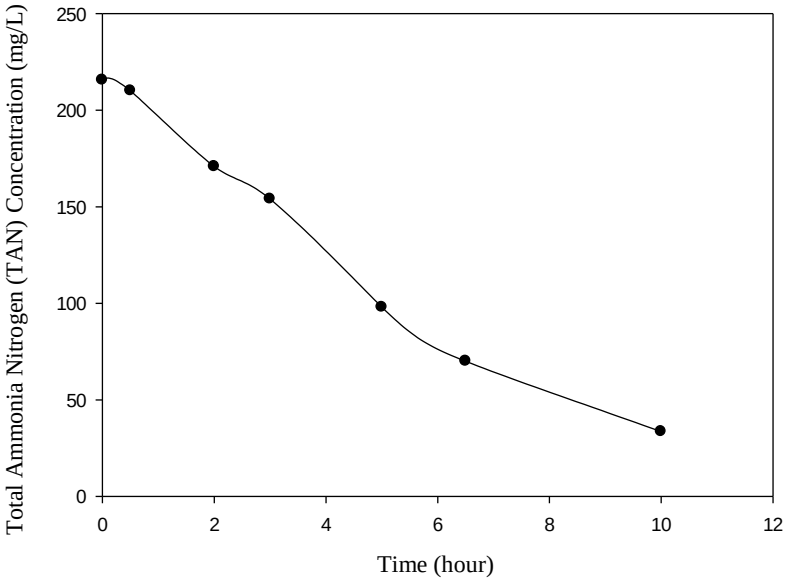

Figure D.4 The change in ammonia concentration in Sample 4

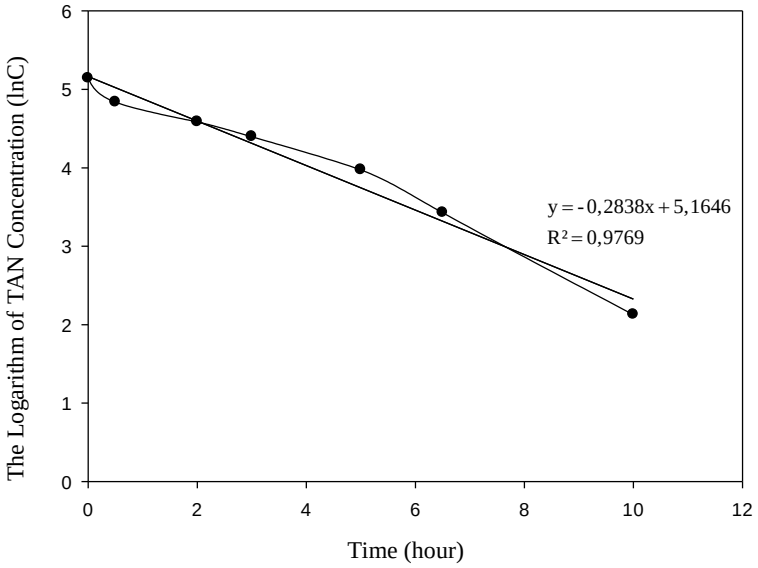

Figure D.5 The change in the logarithm of ammonia concentration in Sample 1

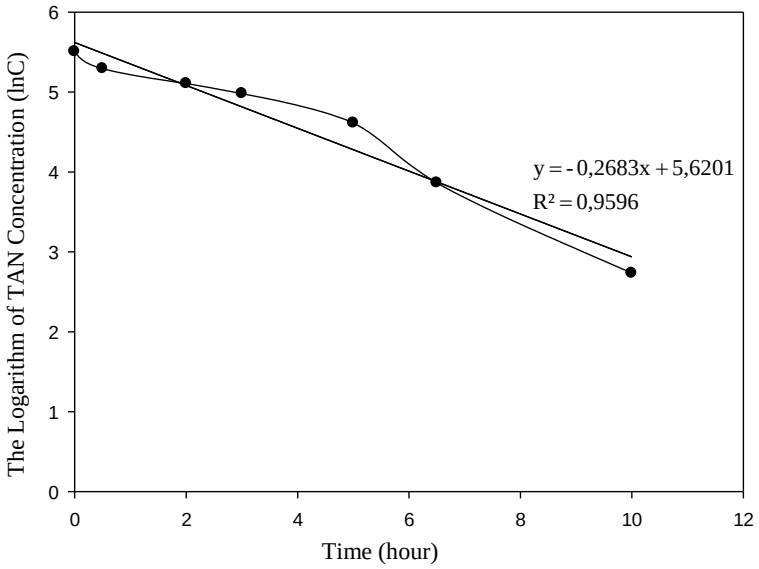

Figure D.6 The change in the logarithm of ammonia concentration in Sample 2

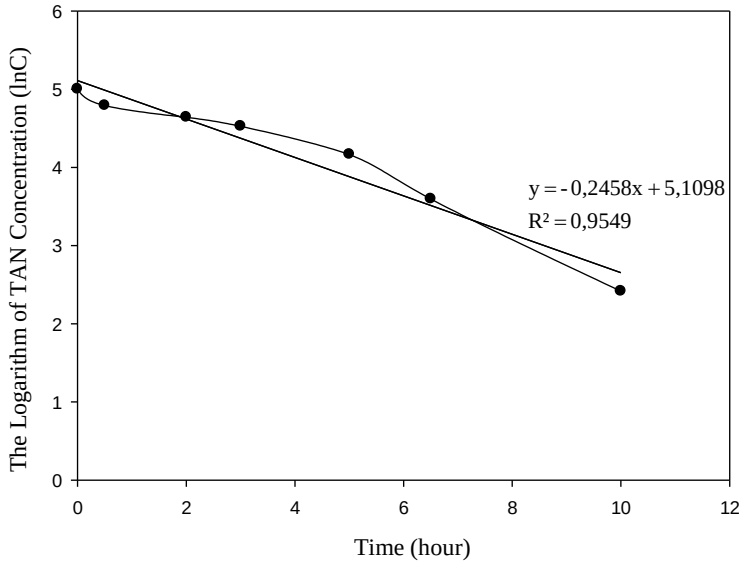

Figure D.7 The change in the logarithm of ammonia concentration in Sample 3

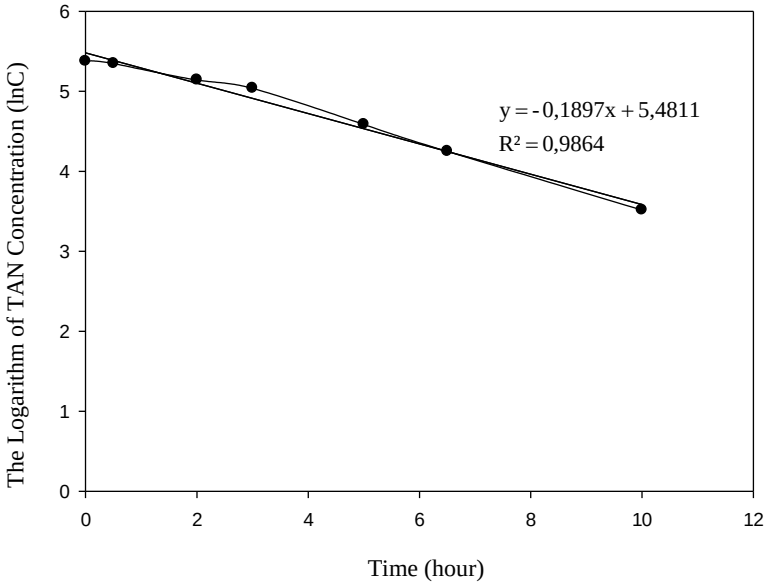

Figure D.8 The change in the logarithm of ammonia concentration in Sample 4

The equations obtained from the regression calculations are seen in Figure D.5, Figure D.6, Figure D.7 and Figure D.8. It is shown that the reaction kinetic is a first-order reaction. Thus, the reaction rate (the change in ammonia concentration over time) is presented in Equation D.1, where the reaction rate constant is 0.2838/hour (the slope of the line in Figure D.5).

$$\ln C_t = 5.1646 - 0.2838t \qquad \text{(Eq. D.1)}$$

It can be seen from Figure D.1, Figure D.2, Figure D.3, Figure D.4 and Table D.2, air stripping method reduced the ammonia concentrations (8.5-32.3 mg/L) below the limit value of 36 mg/L for photofermentation.

D.2.2 Results of Ammonia Removal via Zeolite Adsorption

Sufficient ammonia removal was not observed via zeolite adsorption sufficiently. As seen in Figure D.9-D.12, the ammonia concentrations obtained at the end of the 24-hour removal period were above the limit value for photofermentation. The change in ammonia concentrations in the samples over time for 4 different zeolite dosage are presented in Figure D.9, Figure D.10, Figure D.11 and Figure D.12. There are many parameters affecting zeolite adsorption and, it was not clear which parameter or parameters caused these low removal efficiencies observed (9.5-23.8%). However, it has been foreseen that there might be also a problem due to the storage conditions of Manisa-Gördes zeolite used over the period of time since its first supply. As a result, appropriate zeolite dosage was not observed.

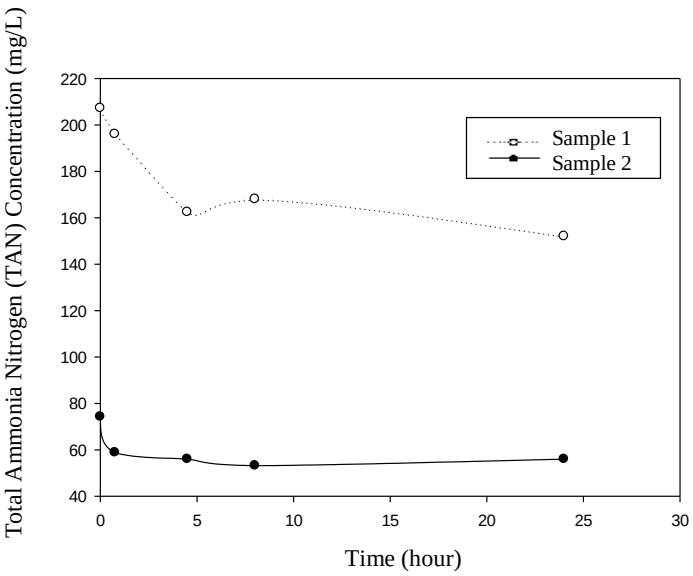

Figure D.9 The change in ammonia concentrations in 0.5 g zeolite/50 mL sample over time

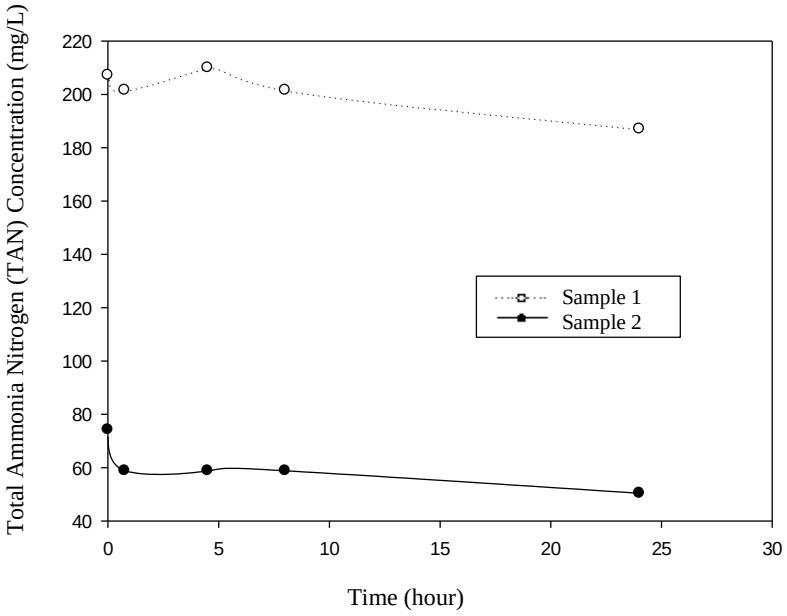

Figure D.10 The change in ammonia concentrations in 1 g zeolite/50 mL sample over time

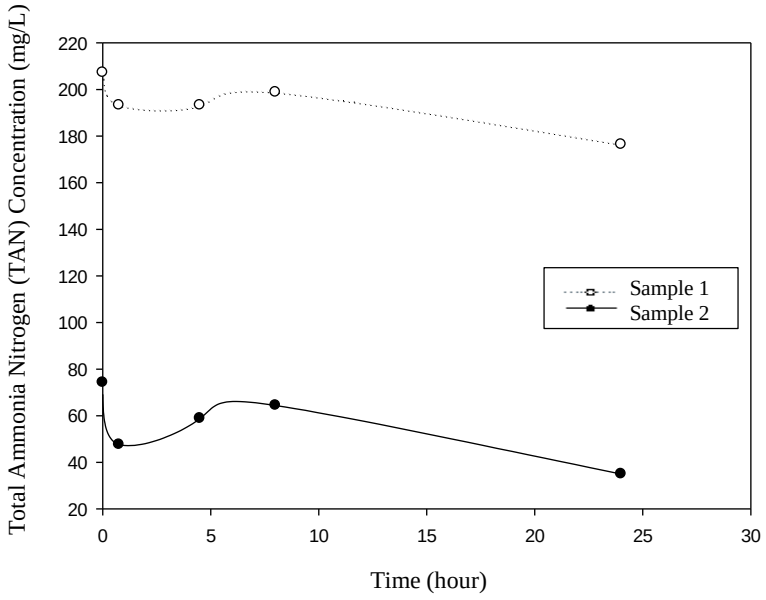

Figure D.11 The change in ammonia concentrations in 1.5 g zeolite/50 mL sample over time

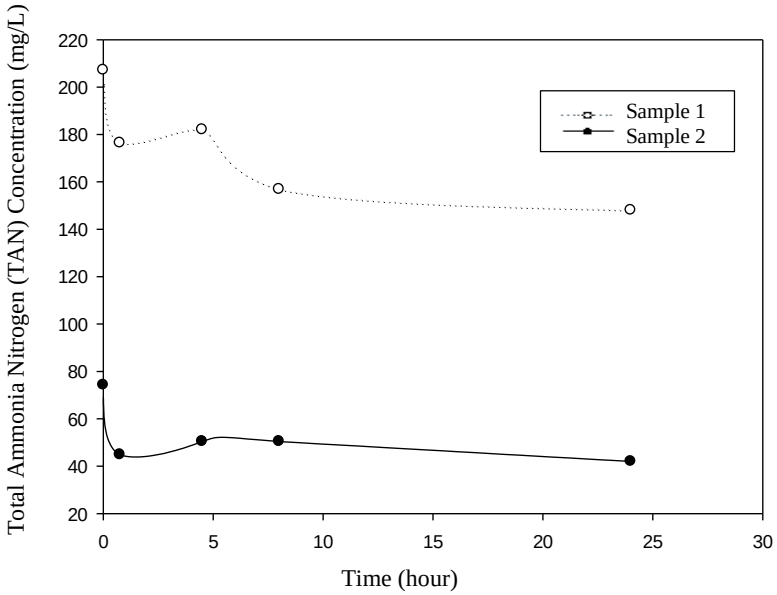

Figure D.12 The change in ammonia concentrations in 2 g zeolite/50 mL sample over time

D.3 Comparison of Air Stripping and Zeolite Adsorption

If sufficient ammonia removal had been observed in the zeolite adsorption method, it was planned to compare these two methods in terms of costs in order to decide which one should be chosen for use as pretreatment method. However, because the removal efficiencies obtained with zeolite adsorption method were very low than expected, any cost comparison was not made. It should be noted that these preliminary studies were performed in order to screen out the method which would decrease the ammonia concentration in influent to non-inhibitory levels for photofermentation. The aim was not to perform detailed study investigating the isotherm kinetics, potential factors or conditions affecting the processes and their optimization. In this respect, as a result, it has been determined with simple analyses that air stripping process was an efficient method to reduce the ammonia concentration in the influents to lower values that would not cause any inhibition for photofermentation.

APPENDIX E

THE HYDROGEN PRODUCTION PERFORMANCE OF EACH PHOTOBIOREACTOR IN SET-1

Table E.1 The hydrogen production performance of each photobioreactor in Set-1

Reactor No	Hydrogen Production Rate (mg H_2/L.h)	Hydrogen Production Rate (mmol H_2/L.h)	Substrate Conversion Efficiency (%)
1	0.52	0.26	35.1
2	0.57	0.28	34.7
3	0.64	0.32	37.0
4	0.64	0.32	37.7
5	0.72	0.36	50.9
8	0.75	0.38	55.6
6	0.63	0.32	30.8
7	0.65	0.32	29.2
9	0.91	0.46	46.2
14	0.75	0.38	39.6
10	1.32	0.89	53.0
13	1.40	0.70	51.4
16	1.87	0.93	57.3
18	1.77	0.89	58.7
19	2.14	1.07	63.7
21	1.94	0.97	58.2
11	1.38	0.69	40.7
20	1.56	0.78	58.0
12	0.48	0.24	13.2
17	0.64	0.32	23.1
15	1.65	0.82	81.1
22	1.79	0.89	84.9
23	1.44	0.72	35.7
29	1.29	0.64	37.6
24	1.76	0.88	54.1
28	1.77	0.89	58.9
25	1.32	0.66	35.8

Reactor No	Hydrogen Production Rate (mg H_2/L.h)	Hydrogen Production Rate (mmol H_2/L.h)	Substrate Conversion Efficiency (%)
30	1.09	0.55	32.8
26	1.84	0.92	67.0
27	1.80	0.90	69.3

Table E.2 The hydrogen production performance of each photobioreactor in Set-1

Reactor No	Hydrogen Yield (g H_2/g acetate)	Light Conversion Efficiency (%)	Total Hydrogen Produced (mmol)
1	0.05	0.39	2.8
2	0.05	0.43	2.8
3	0.05	0.41	3.0
4	0.05	0.38	3.0
5	0.07	0.41	2.0
8	0.07	0.45	2.2
6	0.04	0.37	3.7
7	0.04	0.35	3.5
9	0.06	0.16	1.8
14	0.05	0.16	1.6
10	0.07	0.30	4.2
13	0.07	0.32	4.1
16	0.08	0.40	4.6
18	0.08	0.41	4.7
19	0.08	0.45	5.1
21	0.08	0.41	4.7
11	0.05	0.26	4.9
20	0.08	0.44	7.0
12	0.02	0.07	1.6
17	0.03	0.14	2.8
15	0.11	0.38	3.2
22	0.11	0.40	3.4
23	0.05	0.14	4.3
29	0.05	0.19	4.5
24	0.07	0.29	4.3
28	0.08	0.24	4.7
25	0.05	0.13	2.9
30	0.04	0.14	2.6
26	0.09	0.21	2.7
27	0.09	0.22	2.8